Bulletin of the Geological Survey of Japan, vol. 71 (4), p. 331–353, 2020

Article

SIMS analysis of Si isotope for radiolarian test in Mesozoic bedded chert, Inuyama, central Japan

Maximilien BÔLE[1, 2, 3*], IKEDA Masayuki[2, 3], Peter O. BAUMGARTNER[1], HORI S. Rie[4] and Anne-Sophie BOUVIER[1]

Maximilien BÔLE, IKEDA Masayuki, Peter O. BAUMGARTNER, HORI S. Rie and Anne-Sophie BOUVIER (2020) SIMS analysis of Si isotope for radiolarian test in Mesozoic bedded chert, Inuyama, central Japan. *Bulletin of the Geological Survey of Japan*, vol. 71(4), p. 331–353, 5 figs, 2 tables, 2 appendicies.

Abstract: The global silica cycle is an important component of the long-term climate system, yet its controlling factors are largely uncertain due to poorly constrained proxy records. Because radiolarians and other organisms preferentially extract lighter ^{28}Si from the ocean, the δ^{30}Si of biosiliceous tests can thus be used for a potential proxy of productivity. Additionally, δ^{30}Si of oceanic silica could have reflected changes in the isotopic ratio of sources and sinks.

Here we show δ^{30}Si records measured by secondary ion mass spectrometer (SIMS) in radiolarian silica, precipitated inside radiolarian molds in early Mesozoic bedded chert of the Inuyama section, central Japan. Range of measured δ^{30}Si between -0.3 and 2 ‰ is consistent with that of modern and Cenozoic radiolarian tests. Relatively large intra-chert bed variability up to ~ 0.8 ‰ (1SD) support that δ^{30}Si of the Mesozoic radiolarian molds are not perfectly homogenized in a chert bed during diagenesis. We found an overall inverse correlation between 10-Myr scale δ^{30}Si and biogenic silica (BSi) burial flux, which contradicts with a conventional interpretation of δ^{30}Si as paleoproductivity proxy, despite the low-resolution and scattered our δ^{30}Si records. Although most of the factors controlling oceanic δ^{30}Si are difficult to be constrained, this inverse relation might be explained by changes in δ^{30}Si of mafic/felsic rock weathering ratio, which inferred from paleogeography. Further high-resolution δ^{30}Si records will allow a better understanding of the past silica cycle.

Keywords: Silicon isotopes, δ^{30}Si, Radiolarites, Mesozoic oceanic silica cycle, SIMS

1. Introduction

The global silica cycle is linked to long-term changes in Earth's climate through feedback mechanisms between atmospheric CO_2, climate and the rate of silicate weathering, followed by carbonate and biogenic silica (BSi) deposition. Changes in Si and C cycle dynamics are linked to global climate changes throughout Earth's history, a relationship, which in turn, allows numerical models to reconstruct past atmospheric pCO_2 (Berner, 1991). Understanding the global silica cycle is therefore crucial to elucidate the response of Earth's surface system to changes in external (astronomical) and internal (tectonic and volcanic) forcings.

Silicate weathering and BSi burial are important to constrain the silica cycle as major source and sink, respectively, but are difficult to quantify, and poorly understood their dynamic relation due to large uncertainties in the proxy records. Radiolarians dominated as producers of BSi during much of the Phanerozoic (Hein *et al.*, 1987), whereas siliceous sponges are largely restricted to marginal settings, and diatoms became quantitatively important only in the Cenozoic (Racki and Cordey, 2000; Kidder and Erwin, 2001). Radiolarites were deposited in a broad low-latitude belt, while radiolarian-bearing siliceous mudstones dominated in mid-latitudes (Baumgartner, 2013).

The volume of Paleozoic and Mesozoic Radiolarian-rich deposits is largely underestimated, because much of the ocean floor has been subducted. Plate tectonic reconstructions of Panthalassa and Tethys, based on accreted remnants preserved in Circum-Caribbean,

[1] Institute of Earth Sciences (ISTE), Faculty of Geoscience, Geopolis, University of Lausanne, 1015 Lausanne, Switzerland
[2] Department of Geosciences, Faculty of Sciences, Shizuoka University, 836 Ohya Suruga, Shizuoka 422-8529, Japan.
[3] Department of Earth and Planetary Science, Graduate School of Science, The University of Tokyo, 7-3-1 Hongo, Bunkyo-ku, Tokyo 113-0033 Japan
[4] Department of Earth Sciences, Faculty of Science, Ehime University, Bunkyo-cho 2-5, Matsuyama, Ehime 790-8577, Japan
[*] Corresponding author: M, BÔLE., Rue des Envers 13, 2400 Le Locle, Switzerland

Circum-Pacific and Himalayan terranes, suggest that radiolarian-rich sediments covered more than 80 % of the area of the Mesozoic ocean (Baumgartner *et al.*, 2018).

The modern oceanic silica cycle is relatively well-known, and is considered to be close to steady state (Tréguer and De La Rocha, 2013). Rivers are the main suppliers of silicic acid to oceans followed by seafloor weathering, groundwater, hydrothermal and aeolian inputs. The surface BSi production of diatoms overpasses by two orders of magnitude of the total silicon input to the ocean resulting in high dissolved silica (DSi) undersaturation and strong recycling. With depth, the undersaturation becomes weaker due to silicon recycling, but never reaches the saturation of any silica phases. Only about 3 % of BSi produced in the photic zone is trapped in sediments (Tréguer and De La Rocha, 2013). If steady state is assumed, the total BSi burial has to be proportional to the total input from all sources on timescales longer than the residence time of oceanic DSi (Treguer and De La Rocha, 2013).

BSi of radiolarian silica in bedded cherts is potentially a unique proxy for past Si cycle, because the estimated radiolarian BSi burial flux in the low-latitude pelagic Panthalassa was comparable with the modern global BSi flux, and was the possible major sink of DSi (Ikeda *et al.*, 2017). This hypothesis is consistent with overall in-phase relation between radiolarian BSi flux and global silicate weathering flux calculated by GEOCARBSULFvolc model (Ikeda *et al.*, 2017), implying that the estimated BSi burial flux can be proportional to silicate weathering flux over timescales longer than residence time of oceanic Si (<100 kyr; Ritterbush *et al.*, 2015).

However, controlling factors for the BSi burial are still controversial. Although changes in oceanic upwelling intensity and consequent BSi productivity are proposed as potential controlling factors (Hori *et al.*, 1993; De Wever *et al.*, 2014), their temporal variations are also difficult to be understood due to large uncertainty in their proxy records, such as Al/Ti ratio (Murray *et al.*, 1993; Murray and Leinen, 1996; Dymond *et al.*, 1997). On the other hand, controlling factors for siliceous weathering are also still debated. Today, more than 70 % of silicate weathering occurs only in <10 % land area with highly-weatherable volcanic rock region under humid monsoonal climate (Hartmann *et al.*, 2014). Considering the Mesozoic paleogeography, wide distribution of the volcanic islands and large igneous provinces under intensified mega-monsoonal climate could have further modulate the global silicate weathering (Ikeda *et al.*, 2017), despite of lack of quantitative constraints.

Si isotope of BSi is a potential proxy to understand past Si cycle. Glacial-Interglacial scale δ^{30}Si variations have been documented (e.g. Brzezinski *et al.*, 2002), potentially due to an increase of the diatom productivity and extraction of light silicon by diatoms during interglacial periods (De La Rocha *et al.*, 1998).

Only few scattered data of δ^{30}Si from radiolaria are published. (Wu *et al.*, 1997; Egan *et al.* 2012; Ding *et al.*, 1996; Hendry *et al.* 2014; Abelmann *et al.*, 2015; Fontorbe *et al.*, 2016). Silicon fractionation by modern radiolarians varies between -0.8 ‰ and -2.1 ‰ (Egan *et al.*, 2012; Abelmann *et al.*, 2015), which is similar to that by diatom (Frings *et al.*, 2016). Although factors controlling of δ^{30}Si records of radiolarian test are still debated, even for Cenozoic (e.g. Fontorbe *et al.*, 2016), early Mesozoic Si cycle seems to be a simpler system due to lack of diatom in continent and ocean. In this paper, we investigated the past oceanic silica cycle through in situ δ^{30}Si in radiolarian molds of Mesozoic bedded cherts. Then we compared our δ^{30}Si records with BSi burial flux (Ikeda *et al.*, 2017), to constrain the early Mesozoic Si cycle.

2. Material

We sampled material from bedded cherts from the Inuyama area, central Japan (Fig. 1). These cherts are part of an accretionary prism and are incorporated into several tectonic imbricates (Matsuda and Isozaki, 1991; Kimura and Hori, 1993). High-resolution radiolarian and conodont biostratigraphy, chemo-cyclostratigraphy in this succession have allowed to reconstruct the best studied Early Triassic to Early Jurassic bedded chert sequence (Yao *et al.*, 1980, Hori, 1990; Sugiyama, 1997; Ikeda *et al.*, 2010; Ikeda and Tada, 2013, 2014). Based on biostratigraphic age constraints, average duration of a chert-shale couplet are ~20 kyr throughout the early Mesozoic (Ikeda *et al.*, 2010; Ikeda and Tada, 2014), which is consistent with the precession-scale changes in the accumulation rate of BSi under the extremely slow accumulation of shale mostly composed of aeolian dust (e.g. Hori *et al.*, 1993). Estimated BSi fluctuations should be proportional to DSi input from chemical weathering paced with the monsoon dynamics, over timescales longer than the residence time of oceanic DSi (20 kyr; Tréguer and De La Rocha, 2013; <~100 kyr; Ritterbush *et al.*, 2015), because low-mid-latitude BSi burial flux (Ikeda *et al.*, 2017) is ~90 % of the modern global ocean (Tréguer and De La Rocha, 2013) and was a major sink for oceanic DSi.

Bedded cherts are rocks composed of chert layers (Si-rich), interbedded with clay-rich shale partings (Si-poor), produced by differential compaction and diagenetic reactions of dissolution-precipitation usually forming opal-CT and later quartz (Isaacs, 1981; Tada, 1991). Radiolarian molds filled with nearly pure microquartz and/or chalcedony are found in the silica-rich matrix of cherts. The radiolarian molds that we measured are commonly spherical. Therefore, they could result from Spumellaria, which have regularly a spherical morphology, dwelling in a photic zone due to their symbiotic relation with photosynthetic algae (e.g. Swanberg and Anderson, 1985; Takahashi *et al.*, 2003).

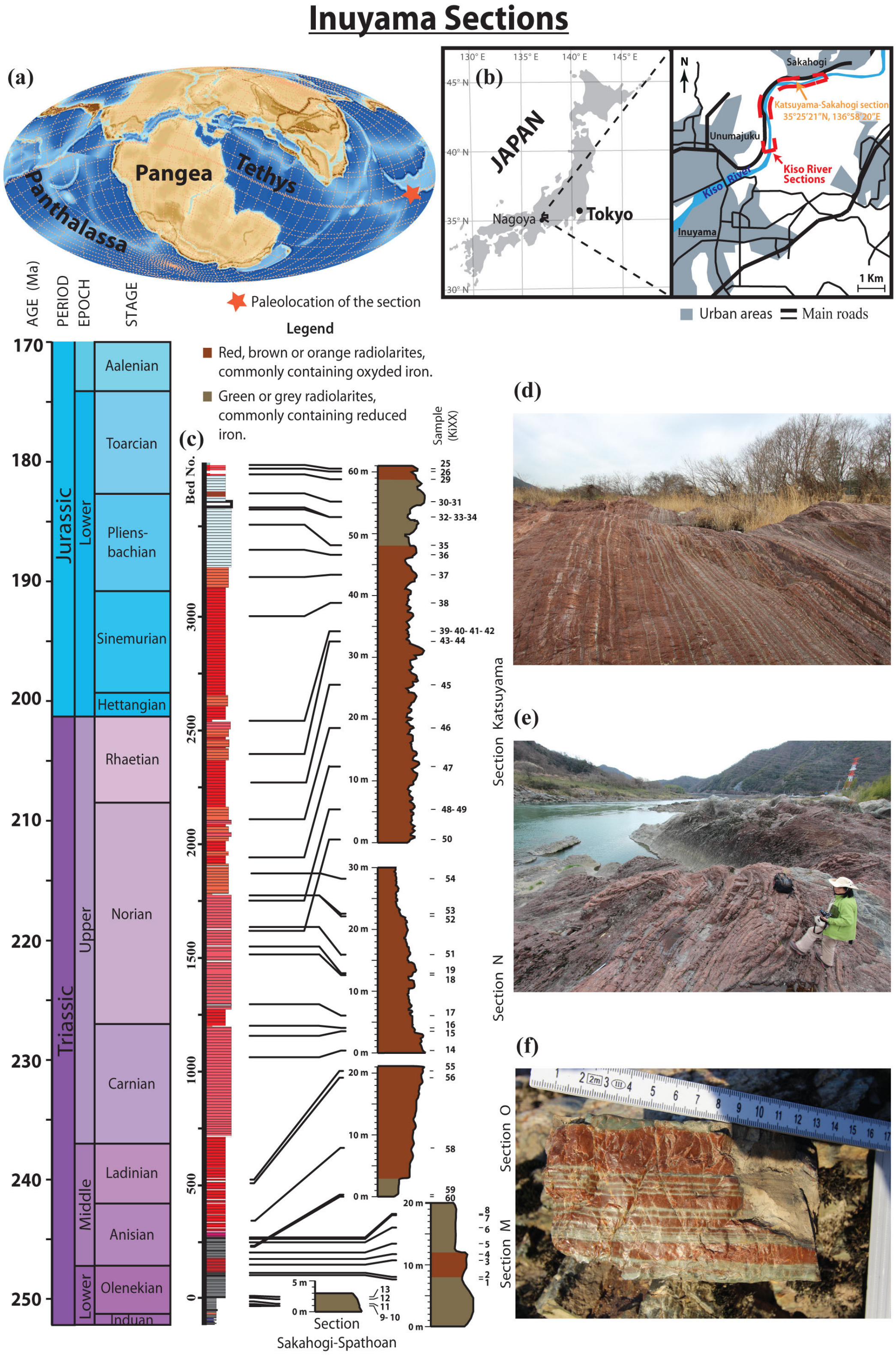

Fig. 1 Log of the Inuyama sections with their Triassic-Early Jurassic paleogeography on a map of Middle Jurassic (a) and their current location (b). The Paleomap (a) is from the Stampfli model developed at the University of Lausanne (Stampfli and Borel, 2002). The bed number log (c) is from Ikeda and Tada (2014). Additional information on the Kiso River sections can be found in Sugiyama (1997). These radiolarites are illustrated through (d) the nice parallel bedding for Late Triassic bedded chert (35°23'57" N, 136°57'34" E), (e) outcropping of Rhatian bedded chert along the Kiso River (35°25'21" N, 136°58'16" E) and (f) millimetric laminations inside single Norian bed (Ki18).

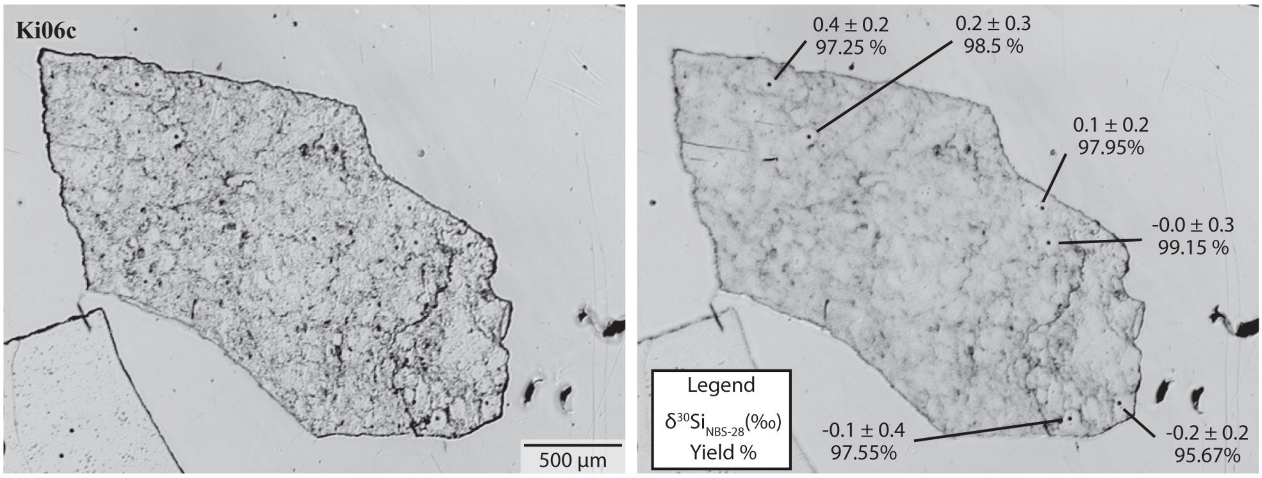

Fig. 2 $\delta^{30}Si_{NBS\text{-}28}$ measurements on sample Ki06c with analytical yield percent relative to the yield of the Paine Quartz Standard (UNIL_Q1). Image on the right are out of focus to better distinguish the analytical spots.

3. Methods

In total, 34 cherts were analysed for the Inuyama section. Sample holders consists of ten fragments of different samples mounted into epoxide around an internal standard. These fragments were previously polished into trapezoidal shapes and the presence of radiolarian molds was checked by optical methods.

The δ^{30}Si of micro-crystalline quartz precipitated inside radiolarian molds was measured by SIMS at University of Lausanne with a primary Cs^{+} ion beam intensity of 2 nA, resulting in a ~10 µm spot (cf. Seitz *et al.*, 2017), to avoid contamination from other sources of silicon in radiolarites (detrital/aeolian minerals). Secondary ions ^{30}Si and ^{28}Si were analyzed at 3000 MRP and collected on Faraday cups (FC) multi-collection mode. The resistances of the L'2 and H'2 FC were 10^{11} Ω for the detection of ^{28}Si and ^{30}Si, respectively. FCs were calibrated in the beginning of each session, using the calibration routine. Mass calibration was performed at the beginning of each session and every 12 h. Samples were gold coated to dissipated charges. Each analysis consists of 20 cycles of 5 sec, and starts with a presputtering time of 30 sec to remove gold and stabilize the secondary ion emission. The standard deviation of each analysis is expressed as analytical standard deviation. The data have been obtained in 7 different sessions for δ^{30}Si measurements, over 7 months.

For each chert sample, we made 4-10 measurements within about 0.5 cm stratigraphic interval (Fig. 2). A quartz internal standard (UNIL_Q1; Paine Quartz; Seitz *et al.*, 2017 for δ^{18}O and method; $\delta^{30}Si_{NBS\text{-}28}$ = -0.13 ± 0.02 ‰ (2SD)) was analysed every 6-10 measurements for instrumental drift correction and calibration.

We subsequently controlled by optical methods that the ion beam actually hit the radiolarian molds for each measurement. In addition, data were postprocessed using the analytical yield and the analytical deviation of each measurement. The analytical yield depends on the nature of the analysed material (mineral species and matrix effect) and on the topography of the analysed surface which modifies the incident angle of the primary ion beam. In addition to instrumental instabilities, the high analytical deviation can also indicate heterogeneity and the analyse of a mixture of silica, clays minerals and/or oxides. Regarding these considerations, the analytical yield and deviation are objective parameters to decide if a measurement must be rejected.

The drift correction was realized using a least square regression line weighted for incertitude (σ_i^2). For the calibration, we calculated the least square δ^{30}Si-mean ($\dot{x}$) and standard deviation (σ_i) for the internal standard also weighted for incertitude (Equation 1 and 2) to keep consistent data processing with the least square drift correction. The calibrated δ^{30}Si for samples ($\delta^{30}\ Si_{NBS\text{-}28}\ Spl$) depend on each sample measurement ($\delta^{30}\ Si\ Spl_{measured}$) and are proportional to the measured least square δ^{30}Si-mean and the true $\delta^{30}Si_{NBS\text{-}28}$ from the internal standard ($\delta^{30}\ Si\ Std_{measured}$ and $\delta^{30}\ Si_{NBS\text{-}28}\ Std$, respectively) (Equation 3). The errors on the calibrated δ^{30}Si ($\sigma(\delta^{30}\ Si_{NBS\text{-}28}\ Spl)$) were obtained by error propagation (Equation 4). The weighted means and standard deviations (Table 2 and Appendix Tables A1 and A2) were then calculated for each sample following equation 1 and 2. Raw, drift corrected and calibrated data are indicated in appendix tables. The δ^{30}Si-data were then filtered with a 10 Ma moving windows average with a step of 5 Ma and compared with estimation of the BSi burial rates in the Inuyama area (Ikeda *et al.*, 2017).

Equation 1

$$\dot{x} = \sum \left(\frac{1}{\sigma_i^2} \times x_i\right) / \left(\frac{1}{\sigma_i^2}\right)$$

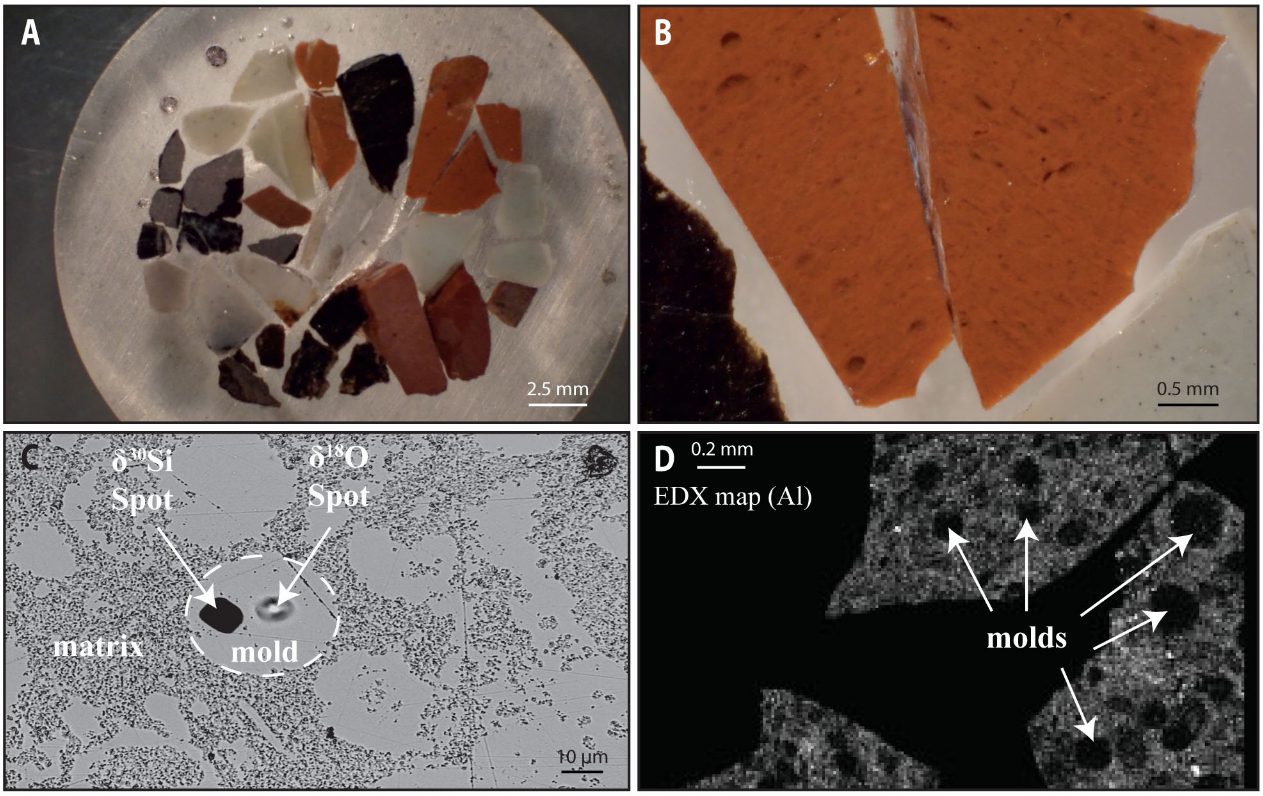

Fig. 3 Illustration of the analyzed materials. A) epoxy sample mount (Br7) including several fragments of about 10 samples. B) Zoom on a sample in this mount with binocular. C) Image of two spots left by a SIMS analysis (δ^{18}O and δ^{30}Si) in radiolarian silica (radiolarian molds) on a gold coated sample mount. The δ^{18}O-spot on the right is covered by a new gold coating. The difference of polishing between the radiolarian molds of nearly pure microcrystalline quartz and the matrix is well illustrated on this image. D) SEM imaging of the aluminium distribution in the sample Ki08c (EDX map). Radiolarian molds are aluminium-free on this image.

Equation 2

$$\dot{\sigma}_{\iota} = \sqrt{\sum \left(\frac{1}{\sigma_i^2} \times (x_i - \dot{x})^2\right) / \sum \left(\frac{1}{\sigma_i^2}\right) \times \frac{N}{N-1}}$$

Equation 3

$$\delta^{30}Si_{NBS-28}\,Spl = \left(\left(\left(1 + \frac{\delta^{30}Si\,Spl_{measured}}{1000}\right) / \frac{(1 + \delta^{30}Si\,Std_{measured} / 1000)}{(1 + \delta^{30}Si_{NBS-28}\,Std / 1000)}\right) - 1\right) \times 1000$$

Equation 4

$$\sigma(\delta^{30}Si_{NBS-28}\,Spl) = \sqrt{(\frac{\partial F}{\partial V_1} \times dV_1)^2 + (\frac{\partial F}{\partial V_2} \times dV_2)^2 + (\frac{\partial F}{\partial V_3} \times dV_3)^2}$$

With $F = \delta^{30}Si_{NBS-28}\,Spl$, $V_1 = \delta^{30}Si\,Spl_{measured}$, $V_2 = \delta^{30}Si\,Std_{measured}$ and $V_3 = \delta^{30}Si_{NBS-28}\,Std$

For the SIMS analyses, it is common to use 2SD, which make sense considering the high accuracy of the method or when measuring very homogenous samples. 2SD was thus also used to discuss the UNIL-Q1 δ^{30}Si. We used 1SD for the LS-mean of samples and for their moving average, following usage in palaeoceanography, such as δ^{13}C and δ^{18}O in low magnesium calcium shells through time (e.g. Veizer *et al.*, 1999).

We also use scanning electron microscopy-energy dispersive X-ray spectrometry (SEM-EDS) in Lausanne University to map the elemental distribution in chert (Fig. 3).

4. Results

All the analytical dataset of our samples and a standard is presented in Appendix Tables, and is summarised in Tables 1 and 2. The means and standard deviations (2SD) of the raw δ^{30}Si from UNIL-Q1 range from -41.77 ‰ to -45.6 ‰ and from 0.33 ‰ to 0.69 ‰, respectively (Table 1). The drift correction only slightly reduced the standard deviations (0.29 ‰ to 0.68 ‰; 2SD). Calibrating data using the LS-means of standard, the arithmetic means and standard deviation (2SD) of the $\delta^{30}Si_{NBS\text{-}28}$ values

Table 1 Raw, drift corrected and calibrated $\delta^{30}Si$ means and standard deviations (2 SD) for the UNIL-Q1 standard (in ‰) between our different sessions. Instrumental fractionation is calculated based on the least square mean and standard deviation of the drift corrected $\delta^{30}Si$. The $\delta^{30}Si_{NBS-28}$ mean and standard deviation (2 SD) of calibrated data are given for all standard measured through a session and for the average $\delta^{30}Si_{NBS-28}$ of the different standard clusters. Reproducibility of the $\delta^{30}Si_{NBS-28}$ based on the average $\delta^{30}Si_{NBS-28}$ of the different standard clusters is much better than on all standard measured (< 0.37 ‰, 2SD vs < 0.71 ‰).

Session	Number of bracketing standard	Raw $\delta^{30}Si$ (‰)		drift corrected $\delta^{30}Si$ (‰)				Fractionation based on LS-mean	Calibrated $\delta^{30}Si_{NBS-28}$ (‰)				Reproducibility of $\delta^{30}Si_{NBS-28}$ (‰)	
		All standard		All standard					All standard		Standard clusters		All standard	Standard clusters
		mean	2 SD	mean	2 SD	LS-mean	LS-STD (1SD)		mean	2SD	mean	2SD	2SD	2SD
Br2	36	-42.67	0.38	-42.67	0.38	-42.65	0.19	1.0444	-0.15	0.40	-0.15	0.21	0.40	0.21
Br3	28	-42.84	0.33	-42.84	0.31	-42.84	0.16	1.0446	-0.13	0.33	-0.13	0.15	0.33	0.15
Br4	16	-45.60	0.49	-45.60	0.39	-45.61	0.19	1.0477	-0.12	0.40	-0.12	0.36	0.40	0.36
Br4v2	18	-43.08	0.69	-43.08	0.68	-43.12	0.37	1.0449	-0.09	0.71	-0.09	0.02	0.71	0.03
Br6	40	-45.36	0.67	-45.38	0.66	-45.36	0.31	1.0474	-0.15	0.69	-0.15	0.20	0.69	0.21
Br7	40	-42.44	0.35	-42.44	0.33	-42.44	0.17	1.0442	-0.13	0.35	-0.13	0.25	0.35	0.25
Br1	24	-41.77	0.37	-41.77	0.29	-41.76	0.12	1.0434	-0.14	0.30	-0.14	0.13	0.30	0.13
Br5	44	-41.79	0.39	-41.79	0.39	-41.80	0.19	1.0435	-0.12	0.41	-0.12	0.17	0.41	0.17
mean		-43.19		-43.20		-43.20			-0.13		-0.13			
2SD		2.97		2.98		2.98			0.04		0.04			

from our standards vary from -0.09 ‰ to -0.15 ‰ and from 0.30 ‰ to 0.71 ‰, respectively. The average of the arithmetic $\delta^{30}Si_{NBS-28}$ means obtained during different sessions is thus -0.13 ± 0.04 ‰ (2SD) which is relatively similar to the bulk UNIL-Q1 $\delta^{30}Si_{NBS-28}$ (-0.13 ± 0.02 ‰; 2SD) and bellow the reproducibility of all $\delta^{30}Si_{NBS-28}$ from standard during a single session. We removed 6 on 189 measurements of samples which had yield deviating more than 10 % from the yield of the quartz standard or their analytical deviation (2SD) exceeding 0.37 ‰.

LS-mean $\delta^{30}Si$ of measured radiolarian molds ranges from -0.3 ‰ to 2 ‰ (Table 2). $\delta^{30}Si$-means have an inter-sample range of up to 2.3 ‰, which is higher than their standard deviation (Table 2). The intra-sample standard deviations (1SD) of the $\delta^{30}Si$-means varies between 0.1 ‰ and 0.75 ‰. The $\delta^{30}Si$-means from our samples range from -0.3 ‰ to 0.8 ‰ during the Early Triassic, from -0.3 ‰ to 1 ‰ during the Middle Triassic, from -0.3 ‰ to 1.5 ‰ during the Late Triassic, and from 0.5 ‰ to 2 ‰ during the Early Jurassic (Fig. 4). The low $\delta^{30}Si$-values from 10-Myr moving windows average are overall associated with high BSi burial rates (Ikeda *et al.*, 2017). A mapping of the aluminium content by SEM-EDS shows that clay minerals are concentrated in the matrix (Fig. 3).

5. Discussion

5. 1 $\delta^{30}Si$ of radiolarian molds and diagenesis

SIMS-measured $\delta^{30}Si$ for Mesozoic radiolarian molds ranges from -0.3 ‰ to 2 ‰ (Fig. 4), which overlap with the range of Cenozoic radiolarian tests (e.g. Fontorbe *et al.*, 2016; Fig. 5), potentially supporting that the Mesozoic radiolarian molds preserve the original values to some extent.

Radiolarian skeletons are originally composed of biogenic opal (opal-A), which is the most soluble silica phase (Walther and Helgeson 1977; Fournier and Rowe, 1977; Gunnarsson and Arnórsson, 2000). During the phase transitions from opal-A to opal-CT and quartz, silicon isotope of radiolarian molds might have changed by contamination of pore water DSi. However, migration of Si from the layers with low Si content (shale bed) to layers with high Si content (chert bed) allows us to ignore interbed migration of Si (Tada, 1991). The lower solubility of quartz (<1000 ppm) than opal-A (<2000 ppm) and opal-CT (<1500 ppm) (e.g. Gunnarsson and Arnórsson, 2000) further implicates the negligible effect of aeolian/detrital quartz dissolution on DSi of pore water. Additionally, clay mineral diagenesis occurs at higher temperature (80 °C; Chamley, 1989; Fagel 2007) than opal-CT transition (65 °C; Matheney and Knauth, 1993), which segregated biosiliceous sediments (Tada, 1991). Considering mass balance in the chert-dominant bedded chert succession with minor-clay component in the Inuyama area (Sugiyama, 1997), we can thus assume that the bulk $\delta^{30}Si$ of radiolarian molds in cherts would be equal to that of former opal-A.

Table 2 List of samples with their age, their $\delta^{30}Si_{NBS-28}$ Least square mean (LS-mean) and their $\delta^{30}Si$ least square standard deviation (LS-std; 1SD). The $\delta^{30}Si_{NBS-28}$ was averaged with a 10 Ma windows moving average (5 Ma step) and compared with BSi.

Sample	Age (Ma)	Number of measurements	Results		Curves	
			$\delta^{30}Si_{NBS-28}$ (‰)		$\delta^{30}Si_{NBS-28}$ (‰)	Biosilica burial rate (g cm^{-2} Kyr^{-1})
			This study		This study	Ikeda *et al.*, 2017
			LS-mean	LS-std (1SD)	10 Ma moving average	10 Ma smooth
Ki20	174.00	5	2.0	0.7	1.42	
Ki22c1	178.00	8	1.1	0.1	1.24	
Ki22c2	178.00	3	0.8	0.2	1.24	
Ki21	178.00	9	1.2	0.3	1.24	
Ki27	180.99	6	0.5	0.6	1.26	0.26
Ki24	182.00	6	1.9	0.2	1.31	0.26
Ki32	184.20	10	2.0	0.4	1.43	0.26
Ki34	184.37	10	1.0	0.3	1.43	0.26
Ki35	185.62	9	2.0	0.2	1.45	0.25
Ki38	193.31	10	0.8	0.4	0.96	0.19
Ki40	201.50	5	0.8	0.5	1.22	0.23
Ki39	201.50	5	1.4	0.3	1.22	0.23
Ki41	201.50	1	1.1		1.22	0.23
Ki42	201.50	10	1.4	0.3	1.22	0.23
Ki44	204.82	9	1.4	0.1	1.22	0.25
ki43	204.82	6	1.2	0.3	1.22	0.25
Ki46	210.27	10	-0.3	0.6	-0.09	0.27
Ki54	214.40	6	0.0	0.5	0.40	0.26
ki48	217.09	4	1.0	0.4	0.71	0.25
Ki51	219.00	6	1.1	0.3	0.94	0.25
Ki15	228.00	10	1.1	0.3	1.10	0.21
Ki57	241.00	9	1.0	0.4	0.52	0.36
Ki58	243.48	6	0.6	0.5	0.39	0.36
Ki08	244.90	10	-0.2	0.3	0.32	0.35
Ki07	245.00	6	0.9	0.2	0.32	0.35
Ki06	245.25	6	0.0	0.3	0.31	0.35
Ki06s	245.25	14	-0.1	0.4	0.31	0.35
Ki05	246.20	6	-0.3	0.2	0.30	0.33
Ki04	246.60	9	0.7	0.3	0.30	0.33
Ki03	247.20	10	0.2	0.6	0.29	0.32
Ki02	247.80	7	0.4	0.4	0.28	0.31
Ki01	248.00	10	0.3	0.5	0.28	0.31
Ki10	250.20	6	-0.2	0.3	0.25	
Ki09	250.30	9	0.7	0.3	0.25	

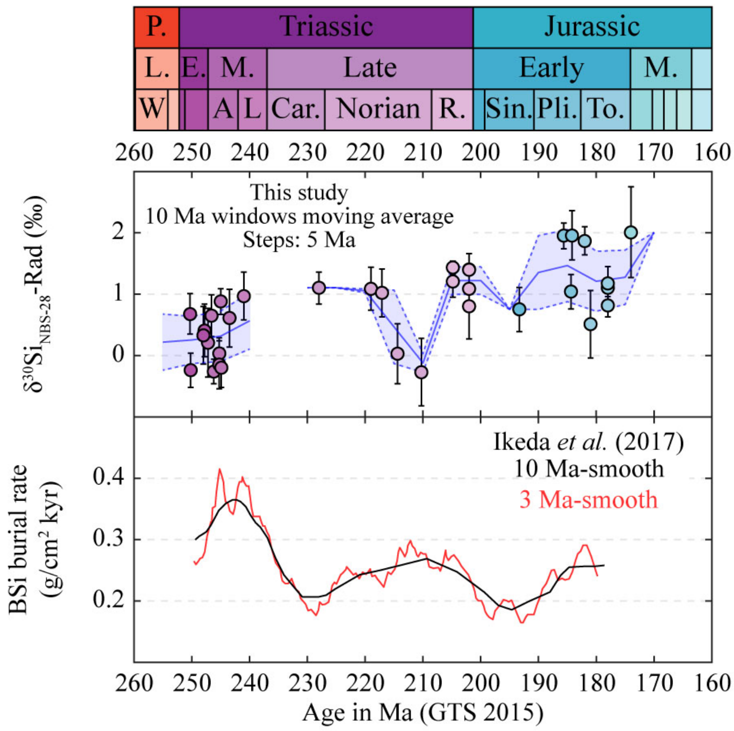

Fig. 4 Evolution of $\delta^{30}Si_{NBS-28}$ through time from radiolarian silica in the Inuyama Area (this study). Our results are compared with estimations of the BSi burial rate (Ikeda *et al.*, 2017). The trend and variation of $\delta^{30}Si$ can be correlated (R= -0.73) with the trend and/or variations observed in the BSi burial rate. The geological timescale (GTS 2015) used for this figure is the timescale of the international commission of stratigraphy (Cohen *et al.* 2013). The color filling inside markers corresponds to the color of the geological stage. The boundaries of curves, when plotted, are equivalent to 1SD. The moving average for radiolarian silica is realized using a 10 Ma windows and 5 Ma steps. The $\delta^{30}Si_{NBS-28}$ error bars correspond to the least square standard deviation of samples presented in Table 2.

The relatively large internal $\delta^{30}Si$-scattering up to 0.8 ‰ (1SD) for each sample suggests that kyr-scale $\delta^{30}Si$ heterogeneity within each chert sample still exist after the diagenesis. Micrometric isotopic variations have been previously observed even in Precambrian cherts, supporting that the $\delta^{30}Si$ is not homogenised through time in cherts (Marin-Carbonne *et al.*, 2011, 2012). Even fragments of cherts included as enclave in tonalitic intrusions (>700 °C) or metamorphosed in amphibolite facies seem to preserve their $\delta^{30}Si$ (André *et al.*, 2006). Therefore, it is reasonable to assess $\delta^{30}Si$ records of radiolarian molds in Mesozoic bedded chert as those in Mesozoic radiolarian tests, despite of diagenetic homogenization to some extent.

5. 2 Evolution of radiolarian $\delta^{30}Si$

The increasing trend of radiolarian $\delta^{30}Si$ through the Triassic might be interpreted as an increase of the radiolarian productivity resulting in a higher biogenic fractionation (e.g. De La Rocha *et al.* 1998), despite of large scattering and complex fractionation of $\delta^{30}Si$ (Fig. 4). However, this conventional interpretation contradicts with low $\delta^{30}Si$ mainly associated with higher BSi burial rates (Ikeda *et al.*, 2017) (Fig. 5). Upwelling of isotopically-light DSi might have affected the observed negative correlation between $\delta^{30}Si$ and BSi flux in equatorial Panthalassa. Regarding the radiolarian BSi as major sink of DSi in the Mesozoic ocean before the post-Cretaceous rise of diatoms (Ikeda *et al.*, 2017), however, radiolarian $\delta^{30}Si$ could have reflected $\delta^{30}Si$ of oceanic DSi on timescale longer than residence time of oceanic DSi (~100 kyr: Ritterbush *et al.*, 2015).

$\delta^{30}Si$ of oceanic DSi is controlled by changes in $\delta^{30}Si$ values of sources and sinks (e.g. Frings *et al.*, 2016). Major source of oceanic DSi is river input, which $\delta^{30}Si$ currently varies from 0 ‰ to 4 ‰, mainly depending on diatom uptake and rock types of provenance (e.g. Frings *et al.*, 2016). However, before the rise of diatom, biogenic uptake in continent can be negligible. Small difference exists between continental felsic rocks ($\delta^{30}Si$ = -0.5 to 0.5 ‰) and mantle-origin mafic rocks ($\delta^{30}Si$ = -1 to 0 ‰) (Opfergelt and Delmelle, 2012). Up to 1 ‰ amplitudes of 10-Myr scale $\delta^{30}Si$ data can be explained by changes in felsic/mafic ratios, although our $\delta^{30}Si$ data is too low-resolution to discuss its <10-Myr scale dynamics.

On another hand, $\delta^{30}Si$ of siliceous sponges varies from -6 ‰ to -1 ‰ (Frings *et al.*, 2016), whereas that of radiolarias and diatoms varies from -1.1 ‰ to 1.7‰ (Abelmann *et al.*, 2015; Fontorbe *et al.*, 2016) and from -1 ‰ to 3 ‰ (e.g. Frings *et al.*, 2016), respectively. Changes in the relative contribution of sponge BSi deposition might be a candidate to explain $\delta^{30}Si$ variations, despite of lack of evidence of massive sponge deposition, except for some biotic events after Carnian Pluvial Event, Norian Manicouagan impact, and the end-Triassic extinction (Thibodeau *et al.*, 2016; Onoue *et al.*, 2016; Shi *et al.*, 2017). However, there are no significant $\delta^{30}Si$ variations across the end-Triassic extinction, implying negligible effect of sponge deposition on Si cycle at this event (Fig. 4).

On the other hand, 10-Myr scale BSi burial flux also correlates with calculated global silicate weathering rate, which potentially linked with changes in weathering of highly-weatherable volcanic rocks with lighter silicon isotope (Ikeda *et al.*, 2017). This idea is consistent with

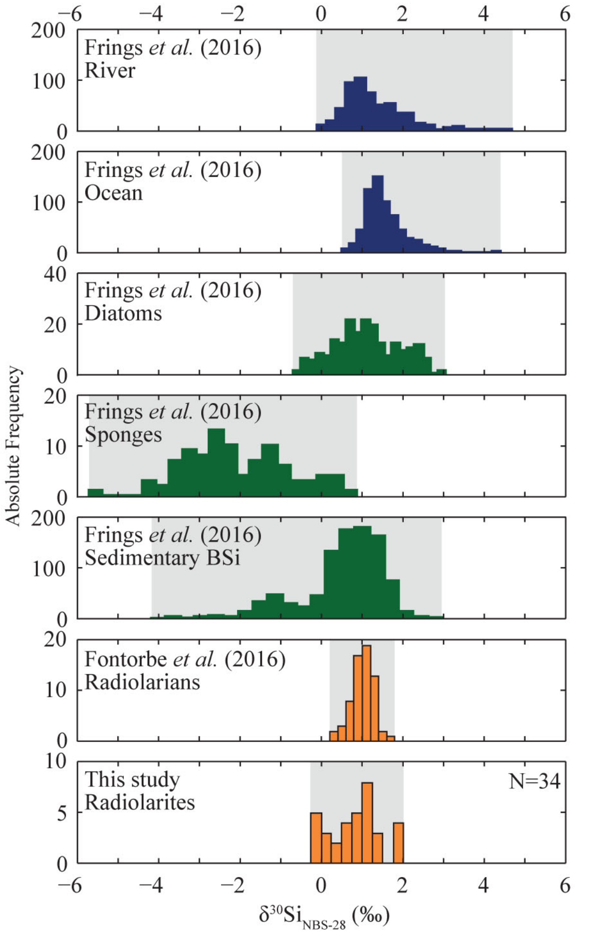

Fig. 5 $\delta^{30}Si_{NBS-28}$-distribution in rivers, oceans, diatoms, sponges and sedimentary biogenic silica from Frings *et al.* (2016) compared with $\delta^{30}Si_{NBS-28}$-distribution for Cenozoic radiolarians (Fontorbe *et al.*, 2016) and for the Triassic to Jurassic radiolarites from the Inuyama Area (this study). The relative similar range between Cenozoic radiolarians and Mesozoic radiolarites supports that the Mesozoic radiolarian molds preserve the original values.

the overall negative correlation between radiolarian δ^{30}Si and the BSi burial flux in the Inuyama area, despite of large scattering and low-resolution δ^{30}Si records (Fig. 4). Further high-resolution works are necessary to improve our understanding of δ^{30}Si cycle of radiolarian molds and unravelling some radiolarian crisis through geologic events, in response to bolide impact, massive volcanism, oceanic acidification, and oceanic anoxic events.

6. Conclusion and perspective

We measured δ^{30}Si of the Mesozoic radiolarian molds in Inuyama chert by SIMS. Range of δ^{30}Si between -0.3 and 2 ‰ is consistent with that of modern and Cenozoic radiolarian tests. Relatively large δ^{30}Si up to 0.8 ‰ (1SD) in intra-chert bed supports that δ^{30}Si of the Mesozoic radiolarian molds is not perfectly homogenized in a chert bed during the diagenesis, and potentially record of kyr-scale changes in radiolarian δ^{30}Si . 10-Myr scale trend of δ^{30}Si of the Mesozoic radiolarian molds from 250 Ma to 180 Ma is overall out-of-phase relation with BSi burial flux. This relation contradicts with interpretation of δ^{30}Si as a productivity proxy, despite of low-resolution and scattered δ^{30}Si records. Further high-resolution analysis will allow a better understanding of the past silica cycle, opening the possibility of accurate estimations of the past oceanic silica cycle and the contribution of past radiolarian productivity.

Acknowledgements:We thank the Swiss National Science Foundation (Project Numbers 200021_185067 and 200020_162670) and the University of Lausanne for their financial support. We acknowledge Nakae, S. and Okazaki, Y. and an anonymous reviewer for fruitful comments on our manuscript.

References

Abelmann, A., Gersonde, R., Knorr, G., Zhang, X., Chapligin, B., Maier, E., Esper, O., Friedrichsen, H., Lohmann, G., Meyer, H. and Tiedemann, R. (2015) The seasonal sea-ice zone in the glacial Southern Ocean as a carbon sink. *Nature Communications*, **6**, 1–13p.

André, L., Cardinal, D., Alleman, L. Y. and Moorbath, S. (2006) Silicon isotopes in ~3.8 Ga West Greenland rocks as clues to the Eoarchaean supracrustal Si cycle. *Earth and Planetary Science Letters*, **245**, 162–173.

Baumgartner, P. O. (2013) Mesozoic radiolarites– accumulation as a function of sea surface fertility on Tethyan margins and in ocean basins. *Sedimentology*, **60**, 292–318.

Baumgartner, P. O., Andjic, G., Sandoval-Gutierrez, M., Bandini-Maeder, A., Diserens, M-C., Baumgartner-Mora, C. and Kukoc, C. (2018) Radiolarian biochronology and paleoceanography of Pacific Terranes in Central America and the Caribbean. *Abstracts of AAPG Hedberg Conference*, 10–16, https://www.researchgate.net/publication/329196576 (Accessed:2018-12-23).

Berner, R. A. (1991) A model for atmospheric CO_2 over phanerozoic time. *American Journal of Science*, **291**, 339–376.

Brzezinski, M. A., Pride, C. J., Franck, V. M., Sigman, D. M., Sarmiento, J. L., Matsumoto, K., Gruber, N., Rau, G. H. and Coale, K. H. (2002). A switch from $Si(OH)_4$ to NO_3^- depletion in the glacial Southern Ocean. *Geophysical Research Letters*, **29**, 1–4.

Chamley, H. (1989) *Clay Sedimentology*, Springer - Verlag, Berlin Heidelberg, 623p.

Cohen, K. M., Finney, S. C., Gibbard, P. L. and Fan, J.-X. (2013; updated) The ICS International Chronostratigraphic Chart. *Episodes*, **36**, 199–204.

De La Rocha, C. L, Brzezinski, M. A., DeNiro M. J. and Shemesh A. (1998) Silicon-isotope composition of diatoms as an indicator of past oceanic change. *Nature*, **395**, 680–683.

De Wever P., O'Dogherty L. and Gorican S. (2014) Monsoon as a cause of radiolarite in the Tethyan realm. *Comptes Rendus Geoscience*, **346**, 287–297.

Ding, T., Jiang, S., Wan, D., Li, Y., Song, H., Liu, Z., Yao, X. (1996) *Silicon isotope Geochemistry*, Geological Publishing House, Beijing, China, 125p.

Dymond, J., Collier, R., McManus, J., Honjo, S. and Manganini, S. (1997) Can the aluminum and titanium contents of ocean sediments be used to determine the paleoproductivity of the oceans? *Paleoceanography*, **12**, 586–593.

Egan, K. E., Rickaby, R. E. M, Leng, M. J., Hendry, K. R., Hermoso, M., Sloane, H. J., Bostock, H. and Halliday, A. N. (2012) Diatom silicon isotopes as proxy for silicic acid utilisation. A Southern Ocean core top calibration. *Geochimica et Cosmochimica Acta*, **96**, 174–192.

Fagel, N. (2007) Clay minerals, deep circulation and climate. *Development in Marin Geology*, **1**, 139–184.

Fontorbe, G., Frings, P. J., De La Rocha, C. L., Hendry, J. R. and Conley, D. J. (2016) A silicon depleted North Atlantic since the Palaeogene: Evidence from sponge and radiolarian silicon isotopes. *Earth and Planetary Science Letters*, **453**, 67–77.

Fournier, R. O. and Rowe J. J. (1997) The solubility of amorphous silica in water at high temperatures and high pressures. *American Mineralogist*, **62**, 1052–1056.

Frings, P. J., Clymans, W., Fontorbe, G., De La Rocha, C. L. and Conley, D. J. (2016) The continental Si cycle and its impact on the ocean Si isotope budget. *Chemical Geology*, **425**, 12–36.

Gunnarsson, I. and Arnórsson, S. (2000) Amorphous silica solubility and the thermodynamic properties of H_4SiO_4 in the range of 0 °C to 350 °C at Psat. *Geochimica et Cosmochimica Acta*, **64**, 2295–2307.

Hartmann, J., Moosdorf, N., Lauerwald, R., Hinderer, M. and West, A. J. (2014) Global chemical weathering and associated P-release – The role of lithology, temperature and soil properties. *Chemical Geology*, **363**, 145–163.

Hein, J. R., Park, M. and Parrish, J. T. (1987) Distribution of siliceous deposits in space and time. *In* Hein, J. R., ed., *Siliceous sedimentary rock-hosted ores and petroleum*, Van Nostrand Reinhold Company, Inc., New York, 10–57.

Hendry, K.R., Robinson, L.F., McManus, J.F. and Hays, J.D. (2014) Silicon isotopes indicate enhanced carbon export efficiency in the North Atlantic during deglaciation. *Nature Communications*, **5** (3107), 1–9.

Hori, R. (1990) Lower Jurassic radiolarian zones of SW Japan. *Transactions and proceedings of the Paleontological Society of Japan. New Series.*, no. 159, 562–586.

Hori, R. S., Cho, C. and Umeda, H. (1993) Origin of cyclicity in Triassic-Jurassic radiolarian bedded cherts of the Mino accretionary complex from Japan. *Island Arc*, **2**, 170–180.

Ikeda, M. and Tada, R. (2014) A 70 million year astronomical time scale for the deep-sea bedded chert sequence (Inuyama, Japan): Implications for Triassic–Jurassic geochronology. *Earth and Planetary Science Letters*, **399**, 30–43.

Ikeda, M. and Tada, R. (2013) Long period astronomical cycles from the Triassic to Jurassic bedded chert sequence (Inuyama, Japan); Geologic evidences for the chaotic behavior of solar planets. *Earth, Planets and Space*, **65**, 351–360.

Ikeda, M., Tada, R. and Ozaki, K. (2017) Astronomical pacing of the global silica cycle recorded in Mesozoic bedded cherts. *Nature Communications*, **8**, 1–9.

Ikeda, M., Tada, R. and Sakuma, H. (2010) Astronomical cycle origin of bedded chert: A middle Triassic bedded chert sequence, Inuyama, Japan. *Earth and Planetary Science Letters*, **297**, 369–378.

Isaacs, C. M. (1981) Porosity reduction during diagenesis of the Monterey Formation, Santa Barbara coastal area, California. *In* Garrison, R. E. and Douglas, R. G., eds., *The Monterey Formation and related siliceous rocks of California*, Los Angeles, Pacific Section, SEPM, 257–271.

Kimura, K. and Hori, R. (1993) Offscraping accretionary process of Jurassic chert-clastic complexes in the Mino-Tamba belt, central Japan. *Journal of Structural Geology*, **15**, 145–161.

Kidder, D. L. and Erwin, D. H. (2001) Secular Distribution of Biogenic Silica through the Phanerozoic: Comparison of Silica-Replaced Fossils and Bedded Cherts at the Series Level. *Journal of Geology*, **109**, 509–522.

Marin-Carbonne, J., Chaussidon, M., Boiron, M. C. and Robert, F. (2011) A combined in situ oxygen, silicon isotopic and fluid inclusion study of a chert sample from Onverwacht Group (3.35 Ga, South Africa): New constraints on fluid circulation. *Chemical Geology*, **286**, 59–71.

Marin-Carbonne, J., Chaussidon, M. and Robert, F. (2012) Micrometer-scale chemical and isotopic criteria (O and Si) on the origin and history of Precambrian cherts: Implications for paleo-temperature reconstructions. *Geochimica et Cosmochimica Acta*, **92**, 129–147.

Matheney, R.K. and Knauth, L.P. (1993) New isotopic temperature estimates for early silica diagenesis in bedded cherts. *Geology*, **21**, 519–522.

Matsuda, T. and Isozaki, Y. (1991) Well-documented travel history of Mesozoic pelagic chert in Japan: from remote ocean to subduction zone. *Tectonics*, **10**, 475–499.

Murray, R. W., Leinen, M. and Isern, A. (1993) Biogenic flux of Al to sediment in the central equatorial Pacific Ocean: Evidence for increased productivity during glacial periods. *Paleoceanography*, **8**, 651–670.

Murray, R. W. and Leinen, M. (1996) Scavenged excess aluminum and its relationship to bulk titanium in biogenic sediment from the central equatorial Pacific Ocean. *Geochimica et Cosmochimica Acta*, **60**, 3869–3878.

Onoue, T., Sato, H., Yamashita, D., Ikehara, M., Yasukawa, K., Fujinaga, K., Kato, Y. and Matsuoka, A. (2016) Bolide impact triggered the Late Triassic extinction event in equatorial Panthalassa. *Scientific Reports*, **6**, 29609.

Opfergelt, S. and Delmelle, P. (2012) Silicon isotopes and continental weathering processes: Assessing controls on Si transfer to the ocean. *Comptes Rendus Geoscience*, **344**, 723–738.

Racki, G. and Cordey, F. (2000) Radiolarian palaeoecology and radiolarites: Is the present the key to the past? *Earth-Science Reviews*., **52**, 83–120.

Ritterbush, K. A., Rosas, S., Corsetti, F. A., Bottjer, D. J. and West, A. J. (2015) Andean sponges reveal long-term benthic ecosystem shifts following the end-Triassic mass extinction. *Palaeogeography, Palaeoclimatology, Palaeoecology*, **420**, 193–209.

Seitz, S., Baumgartner, L. P., Bouvier, A. S., Putlitz, B. and Vennemann, T. (2017) Quartz reference materials for oxygen isotope analysis by SIMS. *Geostandards and Geoanalytical Research*, **41**, 69–75.

Shi, Z., Preto, N., Jiang, H., Krystyn, L., Zhang, Y., Ogg, J. G. and Du, Y. (2017) Demise of Late Triassic sponge mounds along the northwestern margin of the Yangtze Block, South China: Related to the Carnian Pluvial Phase? *Palaeogeography, Palaeoclimatology, Palaeoecology*, **474**, 247–263.

Stampfli, G. M. and Borel G. D. (2002). A plate tectonic model for Paleozoic and Mesozoic constrained by daynamic plate boundaries and restored synthetic oceanic isochrons. *Earth and Planetary Science Letters*, **196**, 17–33.

Sugiyama, K. (1997) Triassic and Lower Jurassic radiolarian biostratigraphy in the siliceous claystone and bedded chert units of the southeastern Mino Terrane, Central Japan. *Bulletin of the Mizunami Fossil Museum*, **24**, 79–193.

Swanberg, N. R. and Anderson, O. R. (1985) The nutrition of radiolarians: Tropic activity of some Spumellaria. *Limnology and Oceanography*, **30**, 646–652.

Tada, R. (1991) Origin of rhythmical bedding in middle Miocene siliceous rocks of the Onnagawa Formation, northern Japan. *Journal of Sedimentary Research*, **61**, 1123–1145.

Takahashi O., Mayama S. and Matsuoka A. (2003) Host-symbiont association of polycystine Radiolaria: Epifluorescence microscopic observation of living Radiolaria. *Marine Micropaleontology*, **49**, 187–194.

Thibodeau A.M., Ritterbush K., Yager J.A., West A.J., Ibarra Y., Bottjer D.J. and Corsetti F.A. (2016). Mercury anomalies and the timing of biotic recovery following the end-Triassic mass extinction. *Nature Communications*, **7**, 1–8.

Tréguer P. J. and De La Rocha C. L. (2013) The world ocean silica cycle. *Annual Review of Marine Science*, **5**, 477–501.

Veizer J., Ala D., Azmy K., Bruckschen P., Buhl D., Bruhn F., Carden G. A. F., Diener A., Ebneth S. and Godderis Y. (1999) $^{87}Sr/^{86}Sr$, $\delta^{13}C$ and $\delta^{18}O$ evolution of Phanerozoic seawater. *Chemical Geology*, **161**, 59–88.

Walther, J. V, and Helgeson, H. C. (1977) Calculation of the thermodynamic properties of aqueous silica and the solubility of quartz and its polymorphs at high pressure and temperatures. *American Journal of Science*, **277**, 1315–1351.

Wu, S., Ding, T., Meng, X. and Bai, L. (1997) Determination and geological implication of O-Si isotope of the sediment core in the CC area, the Pacific Ocean. *Chinese Science Bulletin*, **42**, 1462–1465.

Yao, A., Matsuda, T. and Isozaki, Y. (1980) Triassic and Jurassic radiolarians from the Inuyama area, central Japan. *Journal of Geoscience, Osaka City University*, **23**, 135–154.

Recieved January 7, 2019
Accepted March 27, 2020
Published on-line June 5, 2020

Appendix

Table A1 Least square drift corrected and calibrated $\delta^{30}Si$ measurements (‰) for each sample. The LS-mean and standard deviation for each sample is indicated in bold font. All $\delta^{30}Si$ are relative to NBS-28 and all standard deviations are given as 2σ. Analytical standard deviation is sometime higher than 0.37 (2SD) due the use of error propagation during calibration.

Sample	**Ki20**	**Ki22c2**	**Ki22c1**	**Ki21**	**Ki27**	**Ki24**	**Ki32**	**Ki34**	**Ki35**	**Ki38**	**Ki41**	**Ki39**
age	174.00	178.00	178.00	178.00	180.99	182.00	184.20	184.37	185.62	193.31	201.50	201.50
LS-mean ($\delta^{30}Si_{NBS-28}$) and LS-SD (2 SD) (‰)	**2.01 ± 1.47**	**0.82 ± 0.37**	**1.10 ± 0.29**	**1.18 ± 0.54**	**0.51 ± 1.10**	**1.87 ± 0.47**	**1.96 ± 0.79**	**1.04 ± 0.56**	**1.95 ± 0.42**	**0.75 ± 0.72**	**1.09 ± 0.20**	**1.40 ± 0.53**
Number of measurements	5	6	9	9	6	6	10	10	9	10	2	5
Accepted measurements	5	5	8	9	6	6	10	10	9	10	1	4
Rejected measurements	0	1	1	0	0	0	0	0	0	0	1	1
$\delta^{30}Si_{NBS-28}$ and analytical standard deviation (2SD) of all accepted measurements (‰) 1	3.00 ± 0.31	0.79 ± 0.28	0.92 ± 0.28	1.17 ± 0.29	0.37 ± 0.25	2.02 ± 0.26	1.37 ± 0.20	0.58 ± 0.29	1.96 ± 0.26	1.39 ± 0.19	1.09 ± 0.20	1.68 ± 0.27
2	2.13 ± 0.26	0.66 ± 0.27	0.93 ± 0.39	1.08 ± 0.21	1.16 ± 0.24	1.75 ± 0.20	1.92 ± 0.28	1.25 ± 0.21	2.22 ± 0.23	0.73 ± 0.33		1.31 ± 0.22
3	2.52 ± 0.27	1.03 ± 0.33	1.08 ± 0.21	0.67 ± 0.28	0.96 ± 0.21	1.87 ± 0.27	1.74 ± 0.16	1.30 ± 0.25	2.06 ± 0.30	0.84 ± 0.34		1.62 ± 0.15
4	1.16 ± 0.17		1.11 ± 0.28	1.52 ± 0.29	0.19 ± 0.19	2.16 ± 0.21	2.02 ± 0.24	0.85 ± 0.28	1.53 ± 0.19	1.14 ± 0.30		1.03 ± 0.17
5	1.56 ± 0.19		1.18 ± 0.34	1.15 ± 0.24	-0.39 ± 0.33	1.92 ± 0.18	1.82 ± 0.19	1.18 ± 0.22	2.06 ± 0.24	0.64 ± 0.31		1.41 ± 0.24
6			0.97 ± 0.34	1.06 ± 0.27	0.56 ± 0.48	1.49 ± 0.22	2.19 ± 0.33	0.99 ± 0.28	2.08 ± 0.26	0.64 ± 0.17		
7			1.31 ± 0.25	1.44 ± 0.29			2.25 ± 0.24	1.19 ± 0.23	1.93 ± 0.30	0.74 ± 0.25		
8			1.24 ± 0.24	1.03 ± 0.20			2.84 ± 0.24	1.36 ± 0.22	1.81 ± 0.29	0.49 ± 0.22		
9				1.53 ± 0.26			1.73 ± 0.22	0.60 ± 0.25	2.03 ± 0.30	0.05 ± 0.37		
10							1.86 ± 0.22	0.99 ± 0.29		0.63 ± 0.36		
11												
12												
13												
14												
Session	Br6	Br2	Br2	Br2	Br1	Br3	Br7	Br7	Br2	Br5	Br4v2	Br4
Sample order during the session	5	3	2	4	3	5	7	9	9	2	3	5

Sample	**Ki40**	**Ki42**	**Ki43**	**Ki44**	**Ki46**	**Ki54**	**Ki48**	**Ki51**	**Ki15**	**Ki57**	**Ki58**	**Ki08**
age	201.50	201.50	204.82	204.82	210.27	214.4	217.09	219.00	228.00	241.00	243.48	244.90
LS-mean ($\delta^{30}Si_{NBS-28}$) and LS-SD (2 SD) (‰)	**0.80 ± 1.06**	**1.40 ± 0.52**	**1.21 ± 0.52**	**1.43 ± 0.22**	**-0.27 ± 1.10**	**0.03 ± 0.97**	**1.02 ± 0.78**	**1.09 ± 0.69**	**1.10 ± 0.52**	**0.97 ± 0.78**	**0.61 ± 0.93**	**-0.20 ± 0.64**
Number of measurements	5	10	6	9	10	6	5	6	10	10	6	10
Accepted measurements	5	10	6	9	10	6	4	6	10	9	6	10
Rejected measurements	0	0	0	0	0	0	1	0	0	1	0	0
$\delta^{30}Si_{NBS-28}$ and analytical standard deviation (2SD) of all accepted measurements (‰) 1	-0.11 ± 0.18	1.47 ± 0.28	0.82 ± 0.24	1.44 ± 0.24	-0.57 ± 0.21	-0.12 ± 0.23	1.54 ± 0.22	0.51 ± 0.20	1.31 ± 0.35	0.65 ± 0.19	0.85 ± 0.23	0.27 ± 0.23
2	0.88 ± 0.21	1.59 ± 0.29	1.03 ± 0.17	1.41 ± 0.31	0.83 ± 0.25	0.15 ± 0.33	0.63 ± 0.15	1.20 ± 0.19	1.31 ± 0.31	1.46 ± 0.26	0.91 ± 0.28	0.15 ± 0.20
3	1.21 ± 0.20	1.38 ± 0.24	1.17 ± 0.26	1.30 ± 0.29	-1.06 ± 0.22	-0.67 ± 0.24	1.08 ± 0.32	1.36 ± 0.29	0.98 ± 0.29	1.23 ± 0.24	0.92 ± 0.24	-0.03 ± 0.23
4	1.09 ± 0.17	1.37 ± 0.19	1.51 ± 0.23	1.26 ± 0.25	-0.62 ± 0.27	0.75 ± 0.21	0.91 ± 0.16	0.93 ± 0.25	1.14 ± 0.28	0.66 ± 0.25	0.90 ± 0.23	0.00 ± 0.20
5	0.97 ± 0.18	0.76 ± 0.20	1.32 ± 0.27	1.43 ± 0.19	-0.01 ± 0.27	0.25 ± 0.27		1.45 ± 0.18	0.88 ± 0.24	1.54 ± 0.21	0.15 ± 0.26	-0.69 ± 0.18
6		1.38 ± 0.25	1.40 ± 0.20	1.45 ± 0.22	-0.24 ± 0.19	-0.16 ± 0.17		1.09 ± 0.24	1.04 ± 0.24	1.04 ± 0.23	-0.15 ± 0.27	-0.17 ± 0.27
7		1.56 ± 0.25		1.63 ± 0.18	-0.02 ± 0.20				1.55 ± 0.20	0.45 ± 0.27		-0.34 ± 0.28
8		1.56 ± 0.35		1.41 ± 0.26	0.05 ± 0.25				0.99 ± 0.18	0.67 ± 0.23		-0.21 ± 0.32
9		1.67 ± 0.21		1.52 ± 0.21	-0.01 ± 0.26				1.25 ± 0.22	0.98 ± 0.29		-0.29 ± 0.26
10		1.36 ± 0.23			-0.90 ± 0.20				0.67 ± 0.22			-0.64 ± 0.20
11												
12												
13												
14												
Session	Br4	Br7	Br6	Br2	Br7	Br1	Br6	Br3	Br2	Br7	Br3	Br7
Sample order during the session	1	3	4	8	5	5	2	4	5	1	7	4

Sample	**Ki07**	**Ki06**	**Ki06s**	**Ki05**	**Ki04**	**Ki3s**	**Ki03**	**Ki02**	**Ki01**	**Ki10**	**Ki09**	
age	245.00	245.25	245.25	246.20	246.60	247.20	247.20	247.80	248.00	250.2	250.30	
LS-mean ($\delta^{30}Si_{NBS-28}$) and LS-SD (2 SD) (‰)	**0.88 ± 0.42**	**0.03 ± 0.53**	**-0.15 ± 0.78**	**-0.26 ± 0.40**	**0.65 ± 0.67**		**0.21 ± 1.11**	**0.41 ± 0.85**	**0.33 ± 0.94**	**-0.24 ± 0.57**	**0.68 ± 0.65**	**Total**
Number of measurements	6	6	14	6	9	8	10	7	10	6	9	266
Accepted measurements	6	6	14	6	9	0	10	7	10	6	9	252
Rejected measurements	0	0	0	0	0	8	0	0	0	0	0	14
$\delta^{30}Si_{NBS-28}$ and analytical standard deviation (2SD) of all accepted measurements (‰) 1	1.11 ± 0.24	0.43 ± 0.19	-0.03 ± 0.39	-0.09 ± 0.49	0.75 ± 0.29		0.31 ± 0.26	0.86 ± 0.23	0.63 ± 0.27	-0.38 ± 0.26	0.33 ± 0.26	
2	0.96 ± 0.31	0.16 ± 0.28	0.02 ± 0.32	-0.37 ± 0.30	0.83 ± 0.19		0.17 ± 0.28	-0.16 ± 0.30	0.79 ± 0.13	-0.42 ± 0.25	0.80 ± 0.29	
3	0.79 ± 0.16	0.07 ± 0.20	0.16 ± 0.22	-0.46 ± 0.25	1.14 ± 0.23		0.73 ± 0.27	0.77 ± 0.22	0.71 ± 0.19	-0.02 ± 0.25	0.97 ± 0.37	
4	1.14 ± 0.29	-0.10 ± 0.32	-0.19 ± 0.20	0.01 ± 0.25	0.59 ± 0.23		0.84 ± 0.33	0.52 ± 0.29	0.44 ± 0.21	-0.52 ± 0.28	0.26 ± 0.31	
5	0.70 ± 0.25	-0.23 ± 0.18	0.11 ± 0.25	-0.39 ± 0.23	0.26 ± 0.24		0.08 ± 0.17	0.72 ± 0.25	-0.27 ± 0.30	0.34 ± 0.42	1.03 ± 0.26	
6	0.64 ± 0.26	-0.23 ± 0.36	0.24 ± 0.24	-0.14 ± 0.33	0.19 ± 0.16		-0.23 ± 0.18	0.23 ± 0.19	0.77 ± 0.21	-0.20 ± 0.30	0.35 ± 0.26	
7			-0.24 ± 0.40		0.39 ± 0.28		0.73 ± 0.27	-0.16 ± 0.23	0.51 ± 0.19		0.72 ± 0.18	
8			0.22 ± 0.47		0.83 ± 0.25		0.46 ± 0.34		-0.48 ± 0.16		0.52 ± 0.28	
9			-0.23 ± 0.43		1.02 ± 0.34		0.43 ± 0.18		0.12 ± 0.18		1.15 ± 0.27	
10			0.14 ± 0.37				-1.00 ± 0.21		-0.14 ± 0.31			
11			-0.65 ± 0.20									
12			-1.06 ± 0.20									
13			-0.09 ± 0.23									
14			-0.03 ± 0.29									
Session	Br3	Br3	Br5	Br1	Br2	Br2	Br7	Br3	Br7	Br1	Br2	
Sample order during the session	3	6	8	2	7	1	2	8	6	1	6	

Table A2 All the analytical dataset of the samples and a standard.

		SIMS ANALYSES						Mount: BR2	Standard: UNIL-Q1 (Paine)		Analyse: δ^{30}Si			Value= -0.13±0.02 (NBS-28, 2σ)						Date: 03.09.2015	
	Beam	H'2/L'2 (30Si/28Si)		L'2 (30Si/Coeff)		H'2 (28Si/Coeff)		Time	Yield	mean	Measurements		mean	Drift correction			Calibration			Comment	
	nA	*CPS*	*2SD*	*CPS*	*2SD*	*CPS*	*2SD*		CPS/nA	*2SD*	$\delta^{30}Si$	*2SD int*	*2SD*	$\delta^{30}Si$	*2SD*		$\delta^{30}Si_{NBS\text{-}28}$	*2SD*			
d30Si_030915_BR2_Paine_test@1	2.26	3.2687E-02	1.5872E-02	7.0687E+07	1.1240E-01	2.3118E+06	1.0604E-01	16:57	3.1284E+07	3.1148E+07	-42.75	0.32	-42.66							Setting: Standard	
d30Si_030915_BR2_Paine_test@2	2.26	3.2689E-02	1.0757E-02	7.0462E+07	1.1922E-01	2.3047E+06	1.1042E-01	17:01	3.1152E+07	1.5384E+05	-42.68	0.22	0.16							Setting: Standard	
d30Si_030915_BR2_Paine_test@3	2.26	3.2694E-02	1.3079E-02	7.0423E+07	1.1688E-01	2.3039E+06	1.0647E-01	17:04	3.1126E+07		-42.55	0.26								Setting: Standard	
d30Si_030915_BR2_Paine_test@4	2.26	3.2688E-02	1.5435E-02	7.0486E+07	1.1414E-01	2.3042E+06	1.1717E-01	17:07	3.1147E+07		-42.71	0.31								Setting: Standard	
d30Si_030915_BR2_Paine_test@5	2.26	3.2693E-02	1.6394E-02	7.0499E+07	1.3955E-01	2.3048E+06	1.4128E-01	17:10	3.1136E+07		-42.58	0.33								Setting: Standard	
d30Si_030915_BR2_Paine_test@6	2.26	3.2688E-02	1.3543E-02	7.0292E+07	1.1098E-01	2.2976E+06	1.0713E-01	17:14	3.1046E+07		-42.71	0.27								Setting: Standard	
d30Si_030915_BR2_Paine@1	2.26	3.2694E-02	1.5181E-02	6.9683E+07	1.1456E-01	2.2783E+06	1.0862E-01	17:17	3.0782E+07	3.0755E+07	-42.55	0.30	-42.77	-42.57	0.30	-42.79	-0.04	0.25	-0.27	Standard	
d30Si_030915_BR2_Paine@02	2.27	3.2682E-02	1.1378E-02	6.9711E+07	1.2302E-01	2.2785E+06	1.1625E-01	17:21	3.0759E+07	7.4196E+04	-42.89	0.23	0.36	-42.90	0.23	0.31	-0.39	0.23	0.33	Standard	
d30Si_030915_BR2_Paine@03	2.27	3.2680E-02	1.6388E-02	6.9728E+07	1.2192E-01	2.2785E+06	1.2124E-01	17:24	3.0779E+07		-42.95	0.33		-42.96	0.33		-0.46	0.26		Standard	
d30Si_030915_BR2_Paine@04	2.27	3.2688E-02	1.4874E-02	6.9620E+07	1.0511E-01	2.2769E+06	9.4673E-02	17:27	3.0702E+07		-42.71	0.30		-42.72	0.30		-0.21	0.25		Standard	
d30Si_030915_Ki3S_rad@1	2.27	3.2749E-02	1.6859E-02	5.1262E+07	2.4876E-01	1.6786E+06	2.4497E-01	17:30	2.2626E+07	2.2818E+07	-40.93	0.34	-40.88							Ki3S	Yield
d30Si_030915_Ki3S_rad@2	2.26	3.2766E-02	1.3178E-02	4.8409E+07	2.2682E-01	1.5859E+06	2.2852E-01	17:34	2.1376E+07	2.2135E+06	-40.43	0.26	0.89							Ki3S	Yield
d30Si_030915_Ki3S_rad@3	2.27	3.2749E-02	2.0690E-02	4.8957E+07	5.6754E-02	1.6038E+06	5.7820E-02	17:37	2.1605E+07		-40.93	0.41								Ki3S	Yield
d30Si_030915_Ki3S_rad@4	2.27	3.2720E-02	1.6079E-02	5.6224E+07	2.0840E-01	1.8396E+06	2.0247E-01	17:40	2.4820E+07		-41.79	0.32								Ki3S	Yield
d30Si_030915_Ki3S_rad@5	2.27	3.2763E-02	1.7839E-02	5.2504E+07	1.0394E-01	1.7200E+06	1.0313E-01	17:44	2.3169E+07		-40.52	0.36								Ki3S	Yield
d30Si_030915_Ki3S_rad@6	2.27	3.2762E-02	1.6637E-02	5.2583E+07	1.6773E-01	1.7229E+06	1.6217E-01	17:47	2.3173E+07		-40.56	0.33								Ki3S	Yield
d30Si_030915_Ki3S_rad@7	2.27	3.2756E-02	1.5645E-02	5.0516E+07	3.1287E-01	1.6548E+06	3.1276E-01	17:50	2.2285E+07		-40.73	0.31								Ki3S	Yield
d30Si_030915_Ki3S_rad@8	2.27	3.2740E-02	2.0530E-02	5.3220E+07	7.4002E-02	1.7424E+06	7.8460E-02	17:53	2.3487E+07		-41.18	0.41								Ki3S	Yield
d30Si_030915_Ki22c1_rad@1	2.27	3.2748E-02	1.4319E-02	6.2360E+07	2.5919E-02	2.0419E+06	2.6538E-02	17:57	2.7525E+07	2.8729E+07	-40.96	0.29	-41.43							Ki22C1	Yield
d30Si_030915_Ki22c1_rad@2	2.27	3.2724E-02	1.3817E-02	6.5276E+07	1.0292E-01	2.1358E+06	1.0897E-01	18:00	2.8815E+07	1.7030E+06	-41.66	0.28	0.44	-41.67	0.28		0.90	0.24		Ki22C1	
d30Si_030915_BR2_Paine@05	2.27	3.2698E-02	9.9477E-03	6.9788E+07	1.1346E-01	2.2831E+06	1.0870E-01	18:03	3.0781E+07	3.0675E+07	-42.41	0.20	-42.69	-42.42	0.20	-42.70	0.11	0.22	-0.18	Standard	
d30Si_030915_BR2_Paine@06	2.27	3.2683E-02	1.4823E-02	6.9573E+07	1.2514E-01	2.2741E+06	1.2135E-01	18:07	3.0657E+07	2.1453E+05	-42.87	0.30	0.40	-42.88	0.30	0.34	-0.37	0.25	0.36	Standard	
d30Si_030915_BR2_Paine@07	2.29	3.2685E-02	1.2259E-02	6.9774E+07	1.0113E-01	2.2806E+06	9.8226E-02	18:10	3.0533E+07		-42.79	0.25		-42.80	0.25		-0.29	0.23		Standard	
d30Si_030915_BR2_Paine@08	2.27	3.2689E-02	1.0243E-02	6.9756E+07	9.9679E-02	2.2804E+06	1.0233E-01	18:13	3.0729E+07		-42.68	0.20		-42.69	0.20		-0.18	0.22		Standard	
d30Si_030915_Ki22c1_rad@3	2.27	3.2724E-02	1.9482E-02	6.3715E+07	2.2270E-01	2.0850E+06	2.2781E-01	18:17	2.8094E+07		-41.65	0.39		-41.66	0.39		0.90	0.28		Ki22C1	
d30Si_030915_Ki22c1_rad@4	2.27	3.2729E-02	1.0581E-02	6.5590E+07	5.8589E-02	2.1469E+06	5.6218E-02	18:20	2.8907E+07		-41.50	0.21		-41.51	0.21		1.06	0.23		Ki22C1	
d30Si_030915_Ki22c1_rad@5	2.27	3.2730E-02	1.4120E-02	6.3659E+07	1.3707E-01	2.0852E+06	1.2918E-01	18:23	2.8049E+07		-41.48	0.28		-41.49	0.28		1.08	0.25		Ki22C1	
d30Si_030915_Ki22c1_rad@6	2.27	3.2732E-02	1.6827E-02	6.7115E+07	9.6219E-02	2.1968E+06	8.8619E-02	18:26	2.9583E+07		-41.41	0.34		-41.42	0.34		1.15	0.26		Ki22C1	
d30Si_030915_Ki22c1_rad@7	2.27	3.2726E-02	1.6874E-02	6.3738E+07	2.6734E-02	2.0859E+06	3.2168E-02	18:30	2.8062E+07		-41.61	0.34		-41.62	0.34		0.95	0.26		Ki22C1	
d30Si_030915_Ki22c1_rad@8	2.27	3.2737E-02	1.2569E-02	6.8121E+07	1.1726E-01	2.2314E+06	1.0650E-01	18:33	3.0018E+07		-41.28	0.25		-41.29	0.25		1.29	0.24		Ki22C1	
d30Si_030915_Ki22c1_rad@9	2.27	3.2734E-02	1.1850E-02	6.6993E+07	8.3217E-02	2.1928E+06	8.0588E-02	18:36	2.9511E+07		-41.36	0.24		-41.36	0.24		1.21	0.23		Ki22C1	
d30Si_030915_Ki22C2_rad@1	2.27	3.2720E-02	1.4179E-02	6.6657E+07	1.2513E-01	2.1822E+06	1.1069E-01	18:40	2.9368E+07	2.7029E+07	-41.78	0.28	-41.00	-41.79	0.28		0.76	0.25		Ki22C2	
d30Si_030915_Ki22C2_rad@2	2.27	3.2715E-02	1.3497E-02	6.5550E+07	6.6668E-01	2.1445E+06	6.6701E-01	18:43	2.8892E+07	5.3019E+06	-41.91	0.27	1.72	-41.92	0.27		0.63	0.24		Ki22C2	
d30Si_030915_Ki22C2_rad@3	2.27	3.2757E-02	1.5328E-02	6.0644E+07	9.8168E-02	1.9861E+06	9.5456E-02	18:46	2.6714E+07		-40.69	0.31								Ki22C2	Yield
d30Si_030915_Ki22C2_rad@4	2.27	3.2728E-02	1.6302E-02	6.6806E+07	8.3038E-02	2.1864E+06	7.9917E-02	18:49	2.9436E+07		-41.56	0.33		-41.56	0.33		1.01	0.26		Ki22C2	
d30Si_030915_BR2_Paine@09	2.27	3.2692E-02	1.1050E-02	7.0310E+07	1.0519E-01	2.2986E+06	1.0531E-01	18:53	3.0988E+07	3.0837E+07	-42.61	0.22	-42.57	-42.61	0.22	-42.58	-0.09	0.23	-0.05	Standard	
d30Si_030915_BR2_Paine@10	2.27	3.2692E-02	1.2444E-02	6.9922E+07	8.9388E-02	2.2848E+06	9.4032E-02	18:56	3.0792E+07	2.1480E+05	-42.60	0.25	0.08	-42.61	0.25	0.07	-0.09	0.24	0.08	Standard	
d30Si_030915_BR2_Paine@11	2.27	3.2694E-02	1.1138E-02	6.9982E+07	9.7723E-02	2.2882E+06	9.7959E-02	18:59	3.0831E+07		-42.53	0.22		-42.54	0.22		-0.01	0.23		Standard	
d30Si_030915_BR2_Paine@12	2.27	3.2694E-02	1.5243E-02	6.9871E+07	1.0025E-01	2.2842E+06	1.0330E-01	19:03	3.0738E+07		-42.54	0.30		-42.54	0.30		-0.02	0.25		Standard	
d30Si_030915_Ki22C2_rad@5	2.27	3.2775E-02	1.7302E-02	5.5381E+07	7.9738E-02	1.8149E+06	8.6541E-02	19:06	2.4376E+07		-40.17	0.35								Ki22C2	Yield
d30Si_030915_Ki22C2_rad@6	2.27	3.2784E-02	2.2939E-02	5.3142E+07	1.5654E-01	1.7424E+06	1.5735E-01	19:09	2.3387E+07		-39.92	0.46								Ki22C2	Yield
d30Si_030915_Ki21_rad@1	2.27	3.2732E-02	1.4682E-02	6.7028E+07	8.2338E-02	2.1939E+06	8.5387E-02	19:13	2.9512E+07	2.9310E+07	-41.42	0.29	-41.41	-41.43	0.29		1.15	0.25		Ki21	
d30Si_030915_Ki21_rad@2	2.27	3.2729E-02	1.0343E-02	6.8106E+07	8.4599E-02	2.2290E+06	8.2063E-02	19:16	2.9987E+07	2.6665E+06	-41.51	0.21	0.53	-41.51	0.21		1.06	0.23		Ki21	
d30Si_030915_Ki21_rad@3	2.27	3.2716E-02	1.3917E-02	6.9057E+07	1.0325E-01	2.2591E+06	1.0358E-01	19:19	3.0389E+07		-41.90	0.28		-41.91	0.28		0.64	0.24		Ki21	
d30Si_030915_Ki21_rad@4	2.27	3.2744E-02	1.4509E-02	6.1416E+07	2.1616E-01	2.0108E+06	2.1450E-01	19:22	2.7024E+07		-41.09	0.29		-41.09	0.29		1.50	0.25		Ki21	
d30Si_030915_Ki21_rad@5	2.27	3.2732E-02	1.2205E-02	6.8046E+07	8.9280E-02	2.2273E+06	8.4314E-02	19:26	2.9953E+07		-41.44	0.24		-41.44	0.24		1.13	0.23		Ki21	
d30Si_030915_Ki21_rad@6	2.27	3.2728E-02	1.3732E-02	6.6905E+07	6.4271E-02	2.1899E+06	6.0335E-02	19:29	2.9446E+07		-41.53	0.27		-41.54	0.27		1.03	0.24		Ki21	
d30Si_030915_Ki21_rad@7	2.27	3.2741E-02	1.4288E-02	6.1453E+07	5.9736E-02	2.0120E+06	5.6079E-02	19:32	2.7062E+07		-41.16	0.29		-41.17	0.29		1.42	0.25		Ki21	
d30Si_030915_Ki21_rad@8	2.27	3.2727E-02	1.0176E-02	6.7868E+07	1.7685E-01	2.2210E+06	1.7127E-01	19:36	2.9860E+07		-41.56	0.20		-41.56	0.20		1.01	0.22		Ki21	
d30Si_030915_BR2_Paine@13	2.27	3.2699E-02	1.3770E-02	7.0232E+07	1.0871E-01	2.2967E+06	1.0425E-01	19:39	3.0913E+07	3.0838E+07	-42.39	0.28	-42.49	-42.40	0.28	-42.49	0.13	0.24	0.04	Standard	
d30Si_030915_BR2_Paine@14	2.27	3.2709E-02	1.1614E-02	7.0162E+07	1.0142E-01	2.2958E+06	9.1776E-02	19:42	3.0867E+07	1.2775E+05	-42.11	0.23	0.64	-42.11	0.23	0.55	0.43	0.23	0.58	Standard	
d30Si_030915_BR2_Paine@15	2.27	3.2692E-02	8.7517E-03	7.0003E+07	9.8259E-02	2.2884E+06	9.9923E-02	19:45	3.0796E+07		-42.59	0.18		-42.59	0.18		-0.07	0.22		Standard	
d30Si_030915_BR2_Paine@16	2.27	3.2683E-02	1.4489E-02	7.0002E+07	1.0497E-01	2.2881E+06	1.0610E-01	19:49	3.0775E+07		-42.86	0.29		-42.87	0.29		-0.35	0.25		Standard	
d30Si_030915_Ki21_rad@9	2.27	3.2744E-02	1.3202E-02	6.9458E+07	9.2310E-02	2.2743E+06	8.6229E-02	19:52	3.0552E+07		-41.08	0.26		-41.08	0.26		1.51	0.24		Ki21	
d30Si_030915_Ki15_rad@1	2.27	3.2737E-02	1.7317E-02	6.7385E+07	1.2935E-01	2.2062E+06	1.2653E-01	19:55	2.9622E+07	3.0009E+07	-41.29	0.35	-41.48	-41.29	0.35		1.29	0.26		Ki15	
d30Si_030915_Ki15_rad@2	2.27	3.2737E-02	1.5466E-02	6.7060E+07	1.6278E-01	2.1953E+06	1.6678E-01	19:59	2.9496E+07	1.4397E+06	-41.29	0.31	0.49	-41.29	0.31		1.29	0.25		Ki15	
d30Si_030915_Ki15_rad@3	2.27	3.2726E-02	1.4656E-02	6.9494E+07	1.0328E-01	2.2743E+06	1.0459E-01	20:02	3.0549E+07		-41.61	0.29		-41.61	0.29		0.96	0.25		Ki15	
d30Si_030915_Ki15_rad@4	2.27	3.2731E-02	1.3983E-02	6.8310E+07	1.1537E-01	2.2361E+06	1.1834E-01	20:05	3.0046E+07		-41.45	0.28		-41.45	0.28		1.12	0.24		Ki15	
d30Si_030915_Ki15_rad@5	2.28	3.2723E-02	1.1931E-02	7.1562E+07	8.4753E-02	2.3420E+06	8.6113E-02	20:09	3.1452E+07		-41.70	0.24		-41.70	0.24		0.86	0.23		Ki15	
d30Si_030915_Ki15_rad@6	2.28	3.2728E-02	1.1754E-02	6.8359E+07	8.5718E-02	2.2381E+06	7.7042E-02	20:12	3.0030E+07		-41.55	0.24		-41.55	0.24		1.02	0.23		Ki15	
d30Si_030915_Ki15_rad@7	2.28	3.2745E-02	9.7906E-03	6.5598E+07	1.3139E-01	2.1495E+06	1.2014E-01	20:15	2.8828E+07		-41.06	0.20		-41.06	0.20		1.53	0.22		Ki15	
d30Si_030915_Ki15_rad@8	2.28	3.2726E-02	9.2152E-03	6.8204E+07	7.7514E-02	2.2321E+06	8.0069E-02	20:18	2.9964E+07		-41.59	0.18		-41.59	0.18		0.97	0.22		Ki15	
d30Si_030915_Ki15_rad@9	2.28	3.2735E-02	1.1172E-02	6.7281E+07	1.1389E-01	2.2017E+06	1.1129E-01	20:22	2.9563E+07		-41.35	0.22		-41.35	0.22		1.23	0.23		Ki15	

Table A2 Continued.

SIMS ANALYSES						Mount: BR2			Standard: UNIL-Q1 (Paine)		Analyse: δ^{30}Si			Value= -0.13±0.02 (NBS-28, 2σ)						Date: 03.09.2015
	Beam	H'2/L'2 (30Si/28Si)		L'2 (30Si/Coeff)		H'2 (28Si/Coeff)		Time	Yield	mean	Measurements		mean	Drift correction			Calibration			Comment
	nA	CPS	2SD	CPS	2SD	CPS	2SD		CPS/nA	2SD	$\delta^{30}Si$	2SD int	2SD	$\delta^{30}Si$	2SD		$\delta^{30}Si_{NBS-28}$	2SD		
d30Si_030915_BR2_Paine@17	2.27	3.2690E-02	1.4568E-02	7.0136E+07	1.1794E-01	2.2941E+06	1.0669E-01	20:25	3.0836E+07	3.0799E+07	-42.67	0.29	-42.59	-42.67	0.29	-42.59	-0.15	0.25	-0.07	Standard
d30Si_030915_BR2_Paine@18	2.28	3.2688E-02	1.8037E-02	7.0093E+07	1.1699E-01	2.2925E+06	1.0701E-01	20:28	3.0800E+07	1.3591E+05	-42.71	0.36	0.27	-42.71	0.36	0.23	-0.20	0.27	0.24	Standard
d30Si_030915_BR2_Paine@19	2.28	3.2698E-02	1.1392E-02	7.0237E+07	1.0615E-01	2.2967E+06	1.0721E-01	20:32	3.0857E+07		-42.41	0.23		-42.41	0.23		0.12	0.23		Standard
d30Si_030915_BR2_Paine@20	2.28	3.2693E-02	1.5741E-02	6.9948E+07	1.0087E-01	2.2868E+06	9.9959E-02	20:35	3.0703E+07		-42.57	0.31		-42.57	0.31		-0.04	0.25		Standard
d30Si_030915_Ki15_rad@10	2.28	3.2716E-02	1.0776E-02	6.9531E+07	1.0497E-01	2.2759E+06	9.4792E-02	20:38	3.0537E+07		-41.90	0.22		-41.90	0.22		0.65	0.23		Ki15
d30Si_030915_Ki9_rad@1	2.28	3.2705E-02	1.3044E-02	7.0936E+07	1.2251E-01	2.3214E+06	1.0837E-01	20:42	3.1151E+07	3.0274E+07	-42.23	0.26	-41.89	-42.23	0.26		0.31	0.24		Ki09
d30Si_030915_Ki9_rad@2	2.28	3.2720E-02	1.4574E-02	6.7386E+07	7.8828E-02	2.2049E+06	7.7565E-02	20:45	2.9604E+07	1.6946E+06	-41.78	0.29	0.63	-41.78	0.29		0.78	0.25		Ki09
d30Si_030915_Ki9_rad@3	2.28	3.2725E-02	1.8691E-02	6.5120E+07	1.1842E-01	2.1314E+06	1.1876E-01	20:48	2.8592E+07		-41.62	0.37		-41.62	0.37		0.95	0.27		Ki09
d30Si_030915_Ki9_rad@4	2.28	3.2702E-02	1.5312E-02	7.0892E+07	1.2606E-01	2.3185E+06	1.2108E-01	20:51	3.1112E+07		-42.29	0.31		-42.29	0.31		0.25	0.25		Ki09
d30Si_030915_Ki9_rad@5	2.28	3.2727E-02	1.3002E-02	6.7699E+07	1.1528E-01	2.2158E+06	1.1386E-01	20:55	2.9729E+07		-41.56	0.26		-41.56	0.26		1.01	0.24		Ki09
d30Si_030915_Ki9_rad@6	2.28	3.2705E-02	1.2780E-02	7.0346E+07	1.1938E-01	2.3019E+06	1.1071E-01	20:58	3.0867E+07		-42.21	0.26		-42.20	0.26		0.34	0.24		Ki09
d30Si_030915_Ki9_rad@7	2.28	3.2717E-02	9.1153E-03	6.9233E+07	9.0624E-02	2.2649E+06	8.9704E-02	21:01	3.0376E+07		-41.86	0.18		-41.85	0.18		0.70	0.22		Ki09
d30Si_030915_Ki9_rad@8	2.28	3.2711E-02	1.4062E-02	7.0284E+07	8.1807E-02	2.2993E+06	8.1119E-02	21:05	3.0846E+07		-42.04	0.28		-42.04	0.28		0.51	0.24		Ki09
d30Si_030915_Ki9_rad@9	2.28	3.2732E-02	1.3680E-02	6.8839E+07	1.1557E-01	2.2530E+06	1.1352E-01	21:08	3.0184E+07		-41.44	0.27		-41.44	0.27		1.14	0.24		Ki09
d30Si_030915_BR2_Paine@21	2.28	3.2681E-02	1.0822E-02	7.1908E+07	9.6591E-02	2.3502E+06	9.7210E-02	21:11	3.1578E+07	3.1513E+07	-42.92	0.22	-42.79	-42.92	0.22	-42.79	-0.41	0.23	-0.27	Standard
d30Si_030915_BR2_Paine@22	2.28	3.2691E-02	1.4090E-02	7.1814E+07	9.0667E-02	2.3477E+06	9.1274E-02	21:14	3.1505E+07	1.0345E+05	-42.63	0.28	0.24	-42.62	0.28	0.21	-0.10	0.24	0.22	Standard
d30Si_030915_BR2_Paine@23	2.28	3.2686E-02	1.1573E-02	7.1704E+07	1.0805E-01	2.3449E+06	9.7910E-02	21:18	3.1452E+07		-42.78	0.23		-42.78	0.23		-0.26	0.23		Standard
d30Si_030915_BR2_Paine@24	2.28	3.2684E-02	1.3058E-02	7.1842E+07	9.6674E-02	2.3484E+06	9.4787E-02	21:21	3.1517E+07		-42.83	0.26		-42.83	0.26		-0.31	0.24		Standard
d30Si_030915_Ki4C_rad@1	2.28	3.2718E-02	1.4400E-02	6.7128E+07	9.9781E-02	2.1963E+06	9.6489E-02	21:24	2.9444E+07	3.0239E+07	-41.83	0.29	-41.91	-41.82	0.29		0.74	0.25		Ki04C
d30Si_030915_Ki4C_rad@2	2.28	3.2721E-02	9.5208E-03	6.9043E+07	1.3916E-01	2.2605E+06	1.2690E-01	21:28	3.0302E+07	1.1552E+06	-41.75	0.19	0.64	-41.75	0.19		0.81	0.22		Ki04C
d30Si_030915_Ki4C_rad@3	2.28	3.2731E-02	1.1254E-02	6.7751E+07	9.2481E-02	2.2172E+06	8.8627E-02	21:31	2.9706E+07		-41.45	0.23		-41.45	0.23		1.13	0.23		Ki04C
d30Si_030915_Ki4C_rad@4	2.28	3.2713E-02	1.1513E-02	6.8764E+07	1.1598E-01	2.2495E+06	1.1234E-01	21:34	3.0172E+07		-41.98	0.23		-41.97	0.23		0.58	0.23		Ki04C
d30Si_030915_Ki4C_rad@5	2.28	3.2702E-02	1.1848E-02	6.9922E+07	1.6186E-01	2.2870E+06	1.6041E-01	21:38	3.0691E+07		-42.30	0.24		-42.29	0.24		0.24	0.23		Ki04C
d30Si_030915_Ki4C_rad@6	2.28	3.2700E-02	8.0270E-03	7.0885E+07	9.0174E-02	2.3180E+06	8.9241E-02	21:41	3.1081E+07		-42.36	0.16		-42.35	0.16		0.18	0.22		Ki04C
d30Si_030915_Ki4C_rad@7	2.28	3.2706E-02	1.3764E-02	6.9897E+07	9.2811E-02	2.2859E+06	9.5888E-02	21:44	3.0652E+07		-42.17	0.28		-42.17	0.28		0.38	0.24		Ki04C
d30Si_030915_Ki4C_rad@8	2.28	3.2721E-02	1.2281E-02	6.9777E+07	8.4784E-02	2.2829E+06	8.6294E-02	21:47	3.0591E+07		-41.75	0.25		-41.74	0.25		0.82	0.23		Ki04C
d30Si_030915_Ki4C_rad@9	2.28	3.2727E-02	1.6765E-02	6.7343E+07	9.6880E-02	2.2040E+06	9.4344E-02	21:51	2.9507E+07		-41.57	0.34		-41.56	0.34		1.01	0.26		Ki04C
d30Si_030915_Ki44_rad@1	2.28	3.2741E-02	1.1908E-02	6.8848E+07	8.6897E-02	2.2544E+06	8.7865E-02	21:54	3.0182E+07		-41.16	0.24		-41.15	0.24		1.43	0.23		Ki44
d30Si_030915_BR2_Paine@25	2.28	3.2683E-02	1.4298E-02	7.1742E+07	9.6409E-02	2.3450E+06	8.8822E-02	21:57	3.1455E+07	3.1416E+07	-42.87	0.29	-42.69	-42.86	0.29	-42.68	-0.35	0.25	-0.16	Standard
d30Si_030915_BR2_Paine@26	2.28	3.2687E-02	9.2350E-03	7.1687E+07	1.0528E-01	2.3435E+06	1.0246E-01	22:01	3.1438E+07	7.5919E+04	-42.74	0.18	0.37	-42.73	0.18	0.32	-0.21	0.22	0.33	Standard
d30Si_030915_BR2_Paine@27	2.28	3.2698E-02	1.4460E-02	7.1556E+07	1.0853E-01	2.3397E+06	1.0437E-01	22:04	3.1370E+07		-42.43	0.29		-42.42	0.29		0.11	0.25		Standard
d30Si_030915_BR2_Paine@28	2.28	3.2688E-02	7.0230E-03	7.1697E+07	9.2215E-02	2.3435E+06	8.8595E-02	22:07	3.1401E+07		-42.72	0.14		-42.71	0.14		-0.19	0.21		Standard
d30Si_030915_Ki44_rad@2	2.28	3.2740E-02	1.5265E-02	6.9974E+07	1.1253E-01	2.2910E+06	1.1307E-01	22:10	3.0655E+07	3.0551E+07	-41.19	0.31	-41.18	-41.19	0.31		1.40	0.25		Ki44
d30Si_030915_Ki44_rad@3	2.28	3.2736E-02	1.4482E-02	7.1225E+07	8.6454E-02	2.3326E+06	7.7928E-02	22:14	3.1193E+07	8.0769E+05	-41.30	0.29	0.21	-41.29	0.29		1.29	0.25		Ki44
d30Si_030915_Ki44_rad@4	2.28	3.2735E-02	1.2597E-02	7.0045E+07	1.2242E-01	2.2931E+06	1.2202E-01	22:17	3.0685E+07		-41.34	0.25		-41.33	0.25		1.25	0.24		Ki44
d30Si_030915_Ki44_rad@5	2.28	3.2740E-02	9.2657E-03	6.9955E+07	1.2491E-01	2.2906E+06	1.2356E-01	22:20	3.0641E+07		-41.18	0.19		-41.17	0.19		1.42	0.22		Ki44
d30Si_030915_Ki44_rad@6	2.28	3.2741E-02	1.1069E-02	6.8689E+07	1.2902E-01	2.2505E+06	1.1969E-01	22:24	3.0079E+07		-41.15	0.22		-41.14	0.22		1.44	0.23		Ki44
d30Si_030915_Ki44_rad@7	2.28	3.2747E-02	8.9239E-03	7.0431E+07	1.0452E-01	2.3063E+06	1.0159E-01	22:27	3.0847E+07		-40.98	0.18		-40.97	0.18		1.62	0.22		Ki44
d30Si_030915_Ki44_rad@8	2.28	3.2740E-02	1.2774E-02	7.0208E+07	8.7631E-02	2.2976E+06	8.0694E-02	22:30	3.0739E+07		-41.20	0.26		-41.19	0.26		1.40	0.24		Ki44
d30Si_030915_Ki44_rad@9	2.29	3.2743E-02	1.0382E-02	6.8420E+07	1.3881E-01	2.2401E+06	1.3814E-01	22:33	2.9940E+07		-41.09	0.21		-41.08	0.21		1.51	0.23		Ki44
d30Si_030915_Ki35_rad@1	2.28	3.2758E-02	1.2989E-02	6.9064E+07	1.2380E-01	2.2638E+06	1.1696E-01	22:37	3.0249E+07		-40.67	0.26		-40.66	0.26		1.95	0.24		Ki35
d30Si_030915_BR2_Paine@29	2.28	3.2680E-02	1.2319E-02	7.1696E+07	9.8828E-02	2.3444E+06	9.1310E-02	22:40	3.1391E+07	3.1377E+07	-42.94	0.25	-42.76	-42.93	0.25	-42.75	-0.42	0.23	-0.23	Standard
d30Si_030915_BR2_Paine@30	2.28	3.2687E-02	1.3720E-02	7.1770E+07	1.0328E-01	2.3458E+06	1.0042E-01	22:44	3.1429E+07	1.3094E+05	-42.73	0.27	0.26	-42.72	0.27	0.22	-0.20	0.24	0.23	Standard
d30Si_030915_BR2_Paine@31	2.28	3.2687E-02	1.5268E-02	7.1711E+07	9.6995E-02	2.3443E+06	9.6941E-02	22:47	3.1408E+07		-42.75	0.31		-42.74	0.31		-0.22	0.25		Standard
d30Si_030915_BR2_Paine@32	2.28	3.2691E-02	1.0132E-02	7.1428E+07	9.8129E-02	2.3351E+06	9.5767E-02	22:50	3.1282E+07		-42.63	0.20		-42.62	0.20		-0.10	0.22		Standard
d30Si_030915_Ki35_rad@2	2.28	3.2766E-02	1.1402E-02	6.8756E+07	1.0508E-01	2.2527E+06	1.0399E-01	22:53	3.0152E+07	2.9876E+07	-40.42	0.23	-40.67	-40.41	0.23		2.21	0.23		Ki35
d30Si_030915_Ki35_rad@3	2.28	3.2761E-02	1.4989E-02	6.8978E+07	1.6074E-01	2.2596E+06	1.6210E-01	22:57	3.0233E+07	1.0492E+06	-40.58	0.30	0.38	-40.56	0.30		2.05	0.25		Ki35
d30Si_030915_Ki35_rad@4	2.28	3.2744E-02	9.3645E-03	6.8504E+07	1.2516E-01	2.2429E+06	1.2349E-01	23:00	3.0049E+07		-41.08	0.19		-41.07	0.19		1.52	0.22		Ki35
d30Si_030915_Ki35_rad@5	2.28	3.2761E-02	1.2068E-02	6.6329E+07	1.5829E-01	2.1746E+06	1.4430E-01	23:03	2.9096E+07		-40.58	0.24		-40.56	0.24		2.05	0.23		Ki35
d30Si_030915_Ki35_rad@6	2.28	3.2762E-02	1.3199E-02	6.9467E+07	1.1818E-01	2.2759E+06	1.1377E-01	23:07	3.0459E+07		-40.56	0.26		-40.54	0.26		2.07	0.24		Ki35
d30Si_030915_Ki35_rad@7	2.28	3.2757E-02	1.4762E-02	6.6260E+07	1.0846E-01	2.1716E+06	1.0019E-01	23:10	2.9057E+07		-40.70	0.30		-40.69	0.30		1.92	0.25		Ki35
d30Si_030915_Ki35_rad@8	2.28	3.2753E-02	1.4295E-02	6.7238E+07	1.5922E-01	2.2023E+06	1.5517E-01	23:13	2.9482E+07		-40.81	0.29		-40.80	0.29		1.80	0.25		Ki35
d30Si_030915_Ki35_rad@9	2.28	3.2760E-02	1.5032E-02	6.8657E+07	1.3825E-01	2.2507E+06	1.2435E-01	23:16	3.0110E+07		-40.60	0.30		-40.59	0.30		2.02	0.25		Ki35
d30Si_030915_BR2_Paine@33	2.28	3.2690E-02	1.5042E-02	7.1276E+07	8.5477E-02	2.3301E+06	8.8889E-02	23:20	3.1269E+07	3.1133E+07	-42.66	0.30	-42.65	-42.65	0.30	-42.64	-0.13	0.25	-0.12	Standard
d30Si_030915_BR2_Paine@34	2.28	3.2681E-02	1.2069E-02	7.1028E+07	1.0906E-01	2.3212E+06	1.0489E-01	23:23	3.1115E+07	2.0383E+05	-42.93	0.24	0.45	-42.91	0.24	0.39	-0.40	0.23		Standard
d30Si_030915_BR2_Paine@35	2.28	3.2690E-02	1.2324E-02	7.1001E+07	1.3126E-01	2.3212E+06	1.2931E-01	23:27	3.1124E+07		-42.65	0.25		-42.63	0.25		-0.11	0.23		Standard
d30Si_030915_BR2_Paine@36	2.28	3.2700E-02	8.2229E-03	7.0813E+07	1.1254E-01	2.3154E+06	1.0918E-01	23:30	3.1022E+07		-42.37	0.16		-42.36	0.16		0.18	0.22		Standard

Table A2 Continued.

SIMS ANALYSES								Mount: BR3	Standard: UNIL-Q1 (Paine)		Analyse: δ^{30}Si			Value= -0.13±0.02 (NBS-28, 2σ)						Date: 03.09.2015
	Beam	H'2/L'2 (30Si/28Si)		L'2 (30Si/Coeff)		H'2 (28Si/Coeff)		Time	Yield	mean	Measurements		mean	Drift correction			Calibration			Comment
	nA	CPS	2SD	CPS	2SD	CPS	2SD		CPS/nA	2SD	$\delta^{30}Si$	2SD int	2SD	$\delta^{30}Si$	2SD		$\delta^{30}Si_{NBS28}$	2SD		
d30Si_030915_BR3_Paine_test@1	2.95	3.2675E-02	6.2872E-03	1.1213E+08	1.0747E-01	3.6642E+06	1.0556E-01	10:05	3.7981E+07	3.7351E+07	-43.09	0.13	-42.91							Setting: Standard
d30Si_030915_BR3_Paine_test@2	2.96	3.2682E-02	1.2070E-02	1.1171E+08	6.2295E-02	3.6510E+06	6.7105E-02	10:09	3.7698E+07	7.5902E+05	-42.88	0.24	0.30							Setting: Standard
d30Si_030915_BR3_Paine_test@3	2.97	3.2682E-02	1.0184E-02	1.1100E+08	9.7157E-02	3.6278E+06	9.1043E-02	10:12	3.7420E+07		-42.88	0.20								Setting: Standard
d30Si_030915_BR3_Paine_test@4	2.96	3.2686E-02	9.6006E-03	1.1084E+08	1.1302E-01	3.6246E+06	1.0309E-01	10:15	3.7397E+07		-42.76	0.19								Setting: Standard
d30Si_030915_BR3_Paine_test@5	2.97	3.2675E-02	1.1150E-02	1.1050E+08	1.5044E-01	3.6109E+06	1.4508E-01	10:18	3.7217E+07		-43.08	0.22								Setting: Standard
d30Si_030915_BR3_Paine_test@6	2.97	3.2676E-02	7.6194E-03	1.1095E+08	1.0389E-01	3.6256E+06	9.9872E-02	10:22	3.7352E+07		-43.07	0.15								Setting: Standard
d30Si_030915_BR3_Paine_test@7	2.97	3.2685E-02	1.0739E-02	1.0979E+08	1.0918E-01	3.5888E+06	1.0592E-01	10:25	3.6941E+07		-42.79	0.21								Setting: Standard
d30Si_030915_BR3_Paine_test@8	2.97	3.2687E-02	8.3907E-03	1.0939E+08	1.0076E-01	3.5774E+06	9.3054E-02	10:28	3.6806E+07		-42.73	0.17								Setting: Standard
d30Si_030915_BR3_Paine@1	2.24	3.2688E-02	1.5603E-02	7.9842E+07	1.2759E-01	2.6100E+06	1.2215E-01	10:32	3.5719E+07	3.5859E+07	-42.70	0.31	-42.76	-42.79	0.31	-42.83	-0.07	0.23	-0.11	Standard
d30Si_030915_BR3_Paine@02	2.24	3.2685E-02	1.5305E-02	8.0251E+07	1.0616E-01	2.6242E+06	1.0085E-01	10:35	3.5820E+07	2.2364E+05	-42.79	0.31	0.31	-42.87	0.31	0.08	-0.16	0.23	0.09	Standard
d30Si_030915_BR3_Paine@03	2.24	3.2692E-02	1.2761E-02	8.0502E+07	9.5218E-02	2.6318E+06	9.7118E-02	10:39	3.5960E+07		-42.59	0.26		-42.67	0.26		0.05	0.21		Standard
d30Si_030915_BR3_Paine@04	2.24	3.2680E-02	1.0213E-02	8.0475E+07	1.1060E-01	2.6301E+06	1.1363E-01	10:42	3.5937E+07		-42.96	0.20		-43.03	0.20		-0.33	0.20		Standard
d30Si_030915_BR3_Paine@05	2.24	3.2687E-02	1.1033E-02	8.0389E+07	1.1222E-01	2.6277E+06	1.1142E-01	11:21	3.5880E+07	3.5835E+07	-42.74	0.22	-42.77	-42.80	0.22	-42.82	-0.08	0.20	-0.11	Standard
d30Si_030915_BR3_Paine@06	2.24	3.2691E-02	1.6327E-02	8.0645E+07	1.1874E-01	2.6364E+06	1.2532E-01	11:25	3.5958E+07	2.6308E+05	-42.62	0.33	0.36	-42.67	0.33	0.31	0.05	0.24	0.33	Standard
d30Si_030915_BR3_Paine@07	2.24	3.2677E-02	9.0856E-03	7.9925E+07	1.5800E-01	2.6120E+06	1.5538E-01	11:28	3.5649E+07		-43.03	0.18		-43.08	0.18		-0.38	0.19		Standard
d30Si_030915_BR3_Paine@08	2.24	3.2689E-02	7.7881E-03	8.0391E+07	1.0209E-01	2.6293E+06	9.3148E-02	11:31	3.5852E+07		-42.68	0.16		-42.73	0.16		-0.01	0.19		Standard
d30Si_030915_Ki7C_rad@1	2.24	3.2726E-02	1.2216E-02	7.7732E+07	5.8207E-02	2.5441E+06	5.4915E-02	11:38	3.4695E+07	3.4951E+07	-41.61	0.24	-41.83	-41.66	0.24		1.11	0.21		Ki07C
d30Si_030915_Ki7C_rad@2	2.24	3.2721E-02	1.5353E-02	7.7458E+07	1.4446E-01	2.5345E+06	1.4418E-01	11:41	3.4547E+07	7.5457E+05	-41.76	0.31	0.41	-41.80	0.31		0.96	0.23		Ki07C
d30Si_030915_Ki7C_rad@3	2.24	3.2715E-02	8.0328E-03	7.8936E+07	9.3491E-02	2.5827E+06	9.2580E-02	11:45	3.5226E+07		-41.92	0.16		-41.96	0.16		0.79	0.19		Ki07C
d30Si_030915_Ki7C_rad@4	2.24	3.2726E-02	1.4500E-02	7.8267E+07	9.9890E-02	2.5626E+06	9.2018E-02	11:48	3.4901E+07		-41.59	0.29		-41.63	0.29		1.14	0.22		Ki07C
d30Si_030915_Ki7C_rad@5	2.24	3.2712E-02	1.2513E-02	7.8019E+07	2.2485E-01	2.5518E+06	2.2597E-01	11:51	3.4775E+07		-42.02	0.25		-42.05	0.25		0.70	0.21		Ki07C
d30Si_030915_Ki7C_rad@6	2.24	3.2710E-02	1.3116E-02	7.9702E+07	1.1500E-01	2.6070E+06	1.1933E-01	11:54	3.5563E+07		-42.07	0.26		-42.10	0.26		0.64	0.21		Ki07C
d30Si_030915_Ki51_rad@1	2.24	3.2706E-02	1.0172E-02	7.9344E+07	9.1960E-02	2.5949E+06	8.9846E-02	11:58	3.5395E+07	3.4445E+07	-42.20	0.20	-41.65	-42.23	0.20		0.51	0.20		Ki51
d30Si_030915_Ki51_rad@2	2.24	3.2728E-02	9.6286E-03	7.6583E+07	1.4323E-01	2.5063E+06	1.4759E-01	12:01	3.4135E+07	1.0735E+06	-41.54	0.19	0.64	-41.57	0.19		1.20	0.19		Ki51
d30Si_030915_Ki51_rad@3	2.24	3.2733E-02	1.4440E-02	7.7664E+07	1.1995E-01	2.5422E+06	1.1313E-01	12:04	3.4630E+07		-41.39	0.29		-41.42	0.29		1.36	0.22		Ki51
d30Si_030915_BR3_Paine@09	2.24	3.2693E-02	1.0410E-02	8.0844E+07	1.0599E-01	2.6429E+06	1.0371E-01	12:07	3.6022E+07	3.6101E+07	-42.57	0.21	-42.73	-42.60	0.21	-42.75	0.13	0.20	-0.03	Standard
d30Si_030915_BR3_Paine@10	2.24	3.2686E-02	1.1547E-02	8.1105E+07	9.3516E-02	2.6511E+06	9.4209E-02	12:11	3.6137E+07	1.0794E+05	-42.76	0.23	0.23	-42.79	0.23	0.20	-0.07	0.20	0.21	Standard
d30Si_030915_BR3_Paine@11	2.24	3.2687E-02	1.1975E-02	8.1047E+07	1.0351E-01	2.6506E+06	9.9416E-02	12:14	3.6134E+07		-42.73	0.24		-42.75	0.24		-0.04	0.21		Standard
d30Si_030915_BR3_Paine@12	2.24	3.2683E-02	1.2928E-02	8.1028E+07	1.0004E-01	2.6498E+06	9.4833E-02	12:17	3.6112E+07		-42.85	0.26		-42.87	0.26		-0.16	0.21		Standard
d30Si_030915_Ki51_rad@4	2.24	3.2719E-02	1.2741E-02	7.7336E+07	1.3237E-01	2.5303E+06	1.2756E-01	12:21	3.4478E+07		-41.81	0.25		-41.83	0.25		0.93	0.21		Ki51
d30Si_030915_Ki51_rad@5	2.25	3.2736E-02	8.9637E-03	7.6079E+07	1.1530E-01	2.4919E+06	1.1045E-01	12:24	3.3880E+07		-41.31	0.18		-41.33	0.18		1.45	0.19		Ki51
d30Si_030915_Ki51_rad@6	2.24	3.2724E-02	1.2074E-02	7.6651E+07	1.6499E-01	2.5084E+06	1.6341E-01	12:27	3.4151E+07		-41.66	0.24		-41.68	0.24		1.09	0.21		Ki51
d30Si_030915_Ki24_rad@1	2.24	3.2754E-02	1.2907E-02	7.6934E+07	1.1669E-01	2.5197E+06	1.1309E-01	12:30	3.4283E+07	3.3452E+07	-40.77	0.26	-40.92	-40.78	0.26		2.02	0.21		Ki24
d30Si_030915_Ki24_rad@2	2.25	3.2745E-02	9.9085E-03	7.4673E+07	8.7587E-02	2.4440E+06	8.1973E-02	12:34	3.3259E+07	1.3202E+06	-41.04	0.20	0.45	-41.05	0.20		1.75	0.20		Ki24
d30Si_030915_Ki24_rad@3	2.24	3.2749E-02	1.3585E-02	7.4489E+07	1.3498E-01	2.4395E+06	1.3067E-01	12:37	3.3209E+07		-40.92	0.27		-40.93	0.27		1.87	0.22		Ki24
d30Si_030915_Ki24_rad@4	2.24	3.2759E-02	1.0536E-02	7.5011E+07	8.4256E-02	2.4570E+06	7.9608E-02	12:40	3.3439E+07		-40.64	0.21		-40.65	0.21		2.16	0.20		Ki24
d30Si_030915_Ki24_rad@5	2.26	3.2751E-02	8.9260E-03	7.3293E+07	9.4002E-02	2.4002E+06	9.5443E-02	12:43	3.2450E+07		-40.88	0.18		-40.88	0.18		1.92	0.19		Ki24
d30Si_030915_Ki24_rad@6	2.24	3.2737E-02	1.0813E-02	7.6411E+07	8.5403E-02	2.5015E+06	8.3864E-02	12:47	3.4075E+07		-41.29	0.22		-41.29	0.22		1.49	0.20		Ki24
d30Si_030915_Ki6C_rad@1	2.24	3.2702E-02	9.3909E-03	7.7473E+07	7.5322E-02	2.5335E+06	7.3156E-02	12:50	3.4541E+07		-42.31	0.19		-42.31	0.19		0.43	0.19		Ki06C
d30Si_030915_BR3_Paine@13	2.24	3.2676E-02	9.1282E-03	7.9346E+07	1.0639E-01	2.5929E+06	1.0458E-01	12:53	3.5373E+07	3.5520E+07	-43.07	0.18	-42.88	-43.07	0.18	-42.88	-0.37	0.19	-0.17	Standard
d30Si_030915_BR3_Paine@14	2.24	3.2689E-02	8.7227E-03	7.9790E+07	9.5323E-02	2.6068E+06	1.0172E-01	12:57	3.5556E+07	1.9670E+05	-42.70	0.17	0.30	-42.70	0.17	0.27	0.02	0.19	0.28	Standard
d30Si_030915_BR3_Paine@15	2.24	3.2682E-02	1.3738E-02	7.9844E+07	9.7867E-02	2.6107E+06	9.1314E-02	13:00	3.5576E+07		-42.89	0.27		-42.89	0.27		-0.18	0.22		Standard
d30Si_030915_BR3_Paine@16	2.24	3.2683E-02	9.0427E-03	7.9789E+07	1.0031E-01	2.6075E+06	9.8651E-02	13:03	3.5574E+07		-42.87	0.18		-42.86	0.18		-0.15	0.19		Standard
d30Si_030915_Ki6C_rad@2	2.24	3.2693E-02	1.4200E-02	7.8499E+07	1.0089E-01	2.5676E+06	8.9339E-02	13:06	3.4985E+07	3.4695E+07	-42.57	0.28	-42.71	-42.56	0.28		0.16	0.22		Ki06C
d30Si_030915_Ki6C_rad@3	2.24	3.2690E-02	1.0032E-02	7.8042E+07	1.1918E-01	2.5512E+06	1.1967E-01	13:10	3.4788E+07	8.4980E+05	-42.66	0.20	0.50	-42.66	0.20		0.07	0.20		Ki06C
d30Si_030915_Ki6C_rad@4	2.25	3.2684E-02	1.5786E-02	7.9072E+07	1.0154E-01	2.5856E+06	8.9306E-02	13:13	3.5219E+07		-42.82	0.32		-42.81	0.32		-0.10	0.23		Ki06C
d30Si_030915_Ki6C_rad@5	2.25	3.2680E-02	8.8349E-03	7.6306E+07	1.2811E-01	2.4938E+06	1.2812E-01	13:16	3.3980E+07		-42.95	0.18		-42.94	0.18		-0.23	0.19		Ki06C
d30Si_030915_Ki6C_rad@6	2.25	3.2680E-02	1.7941E-02	7.7819E+07	1.1470E-01	2.5429E+06	1.2079E-01	13:20	3.4654E+07		-42.95	0.36		-42.94	0.36		-0.23	0.25		Ki06C
d30Si_030915_Ki56_rad@1	2.24	3.2715E-02	1.1438E-02	7.6875E+07	7.1230E-02	2.5149E+06	6.6858E-02	13:23	3.4250E+07	3.3596E+07	-41.92	0.23	-42.17	-41.90	0.23		0.85	0.20		Ki58
d30Si_030915_Ki56_rad@2	2.24	3.2717E-02	1.3821E-02	7.4950E+07	1.3737E-01	2.4525E+06	1.3439E-01	13:26	3.3398E+07	1.4770E+06	-41.86	0.28	0.92	-41.84	0.28		0.91	0.22		Ki58
d30Si_030915_Ki56_rad@3	2.24	3.2717E-02	1.1866E-02	7.3754E+07	1.1540E-01	2.4132E+06	1.1335E-01	13:29	3.2866E+07		-41.86	0.24		-41.84	0.24		0.92	0.21		Ki58
d30Si_030915_Ki56_rad@4	2.25	3.2716E-02	1.1655E-02	7.3258E+07	8.1070E-02	2.3967E+06	7.6710E-02	13:33	3.2630E+07		-41.88	0.23		-41.86	0.23		0.90	0.21		Ki58
d30Si_030915_Ki56_rad@5	2.24	3.2692E-02	1.3222E-02	7.6566E+07	1.2848E-01	2.5031E+06	1.2903E-01	13:36	3.4110E+07		-42.60	0.26		-42.57	0.26		0.15	0.21		Ki58
d30Si_030915_BR3_Paine@17	2.24	3.2687E-02	1.1110E-02	8.0028E+07	9.0278E-02	2.6159E+06	8.8983E-02	13:39	3.5658E+07	3.5626E+07	-42.75	0.22	-43.00	-42.73	0.22	-42.97	-0.01	0.20	-0.27	Standard
d30Si_030915_BR3_Paine@18	2.25	3.2672E-02	1.1292E-02	7.9880E+07	1.0023E-01	2.6100E+06	9.8988E-02	13:42	3.5556E+07	1.0604E+05	-43.19	0.23	0.37	-43.16	0.23	0.32	-0.46	0.20	0.33	Standard
d30Si_030915_BR3_Paine@19	2.25	3.2679E-02	1.5750E-02	7.9964E+07	9.2994E-02	2.6131E+06	1.0240E-01	13:46	3.5616E+07		-42.99	0.31		-42.96	0.31		-0.25	0.23		Standard
d30Si_030915_BR3_Paine@20	2.25	3.2676E-02	1.2143E-02	8.0111E+07	9.3055E-02	2.6177E+06	9.0982E-02	13:49	3.5675E+07		-43.08	0.24		-43.05	0.24		-0.34	0.21		Standard
d30Si_030915_Ki56_rad@6	2.24	3.2682E-02	1.3729E-02	7.7046E+07	1.2286E-01	2.5182E+06	1.1980E-01	13:52	3.4324E+07		-42.90	0.27		-42.87	0.27		-0.15	0.22		Ki58
d30Si_030915_Ki2C_rad@1	2.24	3.2715E-02	1.1563E-02	7.7323E+07	1.5357E-01	2.5296E+06	1.5306E-01	13:56	3.4454E+07	3.4314E+07	-41.93	0.23	-42.38	-41.90	0.23		0.86	0.21		Ki02C
d30Si_030915_Ki2C_rad@2	2.25	3.2682E-02	1.4893E-02	8.0727E+07	9.4518E-02	2.6383E+06	9.3060E-02	13:59	3.5942E+07	2.1155E+06	-42.90	0.30	0.83	-42.87	0.30		-0.16	0.23		Ki02C
d30Si_030915_Ki2C_rad@3	2.25	3.2712E-02	1.0820E-02	7.3531E+07	6.8995E-02	2.4060E+06	7.2550E-02	14:02	3.2727E+07		-42.02	0.22		-41.98	0.22		0.77	0.20		Ki02C
d30Si_030915_Ki2C_rad@4	2.25	3.2703E-02	1.4432E-02	7.5308E+07	1.9525E-01	2.4630E+06	1.9113E-01	14:05	3.3532E+07		-42.26	0.29		-42.22	0.29		0.52	0.22		Ki02C
d30Si_030915_Ki2C_rad@5	2.25	3.2710E-02	1.2445E-02	7.6289E+07	1.0249E-01	2.4955E+06	1.0129E-01	14:09	3.3968E+07		-42.07	0.25		-42.03	0.25		0.72	0.21		Ki02C
d30Si_030915_Ki2C_rad@6	2.25	3.2694E-02	9.5069E-03	7.7190E+07	1.2376E-01	2.5238E+06	1.2561E-01	14:12	3.4374E+07		-42.54	0.19		-42.50	0.19		0.23	0.19		Ki02C
d30Si_030915_Ki2C_rad@7	2.25	3.2681E-02	1.1661E-02	7.9063E+07	1.0516E-01	2.5837E+06	1.0263E-01	14:15	3.5202E+07		-42.91	0.23		-42.87	0.23		-0.16	0.21		Ki02C
d30Si_030915_BR3_Paine@21	2.25	3.2689E-02	1.2409E-02	7.9822E+07	1.0844E-01	2.6092E+06	1.0585E-01	14:25	3.5529E+07	3.5461E+07	-42.69	0.25	-42.86	-42.64	0.25	-42.81	0.08	0.21	-0.09	Standard
d30Si_030915_BR3_Paine@22	2.25	3.2680E-02	1.1089E-02	7.9602E+07	1.0520E-01	2.6029E+06	9.9791E-02	14:29	3.5394E+07	1.1169E+05	-42.94	0.22	0.25	-42.88	0.22	0.21	-0.17	0.20	0.22	Standard
d30Si_030915_BR3_Paine@23	2.25	3.2679E-02	1.2876E-02	7.9646E+07	1.1004E-01	2.6030E+06	1.1131E-01	14:32	3.5448E+07		-42.97	0.26		-42.91	0.26		-0.20	0.21		Standard
d30Si_030915_BR3_Paine@24	2.25	3.2683E-02	1.3000E-02	7.9762E+07	1.0126E-01	2.6068E+06	9.8114E-02	14:35	3.5472E+07		-42.86	0.26		-42.80	0.26		-0.08	0.21		Standard
d30Si_030915_BR3_Paine@25	2.25	3.2691E-02	9.2987E-03	7.9703E+07	1.3082E-01	2.6055E+06	1.2737E-01	15:11	3.5441E+07	3.5550E+07	-42.64	0.19	-42.91	-42.56	0.19	-42.83	0.17	0.19	-0.09	Standard
d30Si_030915_BR3_Paine@26	2.25	3.2678E-02	9.6762E-03	7.9991E+07	1.1212E-01	2.6141E+06	1.1492E-01	15:15	3.5546E+07	1.6123E+05	-43.02	0.19	0.36	-42.94	0.19	0.31	-0.23	0.19	0.36	Standard
d30Si_030915_BR3_Paine@27	2.25	3.2679E-02	1.0628E-02	8.0073E+07	9.0828E-02	2.6179E+06	8.1637E-02	15:18	3.5582E+07		-42.98	0.21		-42.90	0.21			0.20		Standard
d30Si_030915_BR3_Paine@28	2.25	3.2678E-02	1.2869E-02	8.0209E+07	8.7631E-02	2.6212E+06	8.9838E-02	15:21	3.5632E+07		-43.00	0.26		-42.92	0.26		-0.21	0.21		Standard

Table A2 Continued.

	SIMS ANALYSES							Mount: BR4		Standard: UNIL-Q1 (Paine)		Analyse: δ^{30}Si			Value= -0.13±0.02 (NBS-28, 2σ)					Date: 03.09.2015	
	Beam	H'2/L'2 (30Si/28Si)		L'2 (30Si/Coeff)		H'2 (28Si/Coeff)		Time	Yield	mean	Measurements		mean	Drift correction			Calibration			*Comment*	
	nA	*CPS*	*2SD*	*CPS*	*2SD*	*CPS*	*2SD*		CPS/nA	*2SD*	$\delta^{30}Si$	*2SD int*	*2SD*	$\delta^{30}Si$	*2SD*		$\delta^{30}Si_{NBS-28}$	*2SD*			
d30Si_020915_Paine@1	2.82	3.2523E-02	9.9294E-03	7.4151E+07	2.1783E-01	2.4112E+06	2.1018E-01	10:02	2.6325E+07	3.0863E+07	-47.54	0.20	-46.82							Setting: Standard	
d30Si_020915_Paine@2	2.82	3.2528E-02	1.0860E-02	7.3971E+07	2.3800E-01	2.4060E+06	2.3489E-01	10:05	2.6188E+07	8.7974E+06	-47.40	0.22	0.84							Setting: Standard	
d30Si_020915_Paine@3	2.82	3.2544E-02	1.7757E-02	7.4083E+07	1.8241E-01	2.4107E+06	1.7446E-01	10:09	2.6229E+07		-46.94	0.36								Setting: Standard	
d30Si_020915_Paine@4	2.83	3.2535E-02	1.3506E-02	7.4297E+07	2.2129E-01	2.4177E+06	2.1739E-01	10:12	2.6295E+07		-47.20	0.27								Setting: Standard	
d30Si_020915_Paine@5	2.83	3.2546E-02	1.2153E-02	7.4337E+07	2.2347E-01	2.4195E+06	2.1606E-01	10:15	2.6308E+07		-46.88	0.24								Setting: Standard	
d30Si_020915_Paine@6	2.82	3.2552E-02	1.0820E-02	9.8091E+07	1.2170E-01	3.1949E+06	1.1625E-01	10:23	3.4741E+07		-46.71	0.22								Setting: Standard	
d30Si_020915_Paine@7	2.83	3.2551E-02	9.7748E-03	9.7926E+07	9.5872E-02	3.1892E+06	8.5702E-02	10:26	3.4611E+07		-46.73	0.20								Setting: Standard	
d30Si_020915_Paine@8	2.83	3.2561E-02	1.2064E-02	9.8059E+07	9.5963E-02	3.1943E+06	8.4903E-02	10:29	3.4689E+07		-46.45	0.24								Setting: Standard	
d30Si_020915_Paine@9	2.83	3.2558E-02	8.7009E-03	9.8186E+07	9.7307E-02	3.1983E+06	8.7008E-02	10:32	3.4729E+07		-46.51	0.17								Setting: Standard	
d30Si_020915_Paine@10	2.83	3.2568E-02	9.8810E-03	9.8148E+07	8.3126E-02	3.1948E+06	8.6428E-02	10:36	3.4674E+07		-46.22	0.20								Setting: Standard	
d30Si_020915_Paine@11	2.83	3.2560E-02	8.2523E-03	9.8191E+07	9.1561E-02	3.1971E+06	8.8840E-02	10:39	3.4705E+07		-46.47	0.17								Setting: Standard	
d30Si_020915_Paine@12	2.82	3.2582E-02	9.3217E-03	9.7986E+07	8.6879E-02	3.1940E+06	7.8282E-02	11:13	3.4772E+07	3.4669E+07	-45.81	0.19	-45.85	-45.63	0.19	-45.68	-0.15	0.22	-0.20	Standard	
d30Si_020915_Paine@13	2.83	3.2581E-02	1.0729E-02	9.4161E+07	1.1472E-01	3.0658E+06	1.0770E-01	11:16	3.3318E+07	1.9675E+06	-45.85	0.21	0.14	-45.67	0.21	0.13	-0.19	0.23	0.14	Standard	
d30Si_020915_Paine@14	2.83	3.2583E-02	1.1800E-02	9.8710E+07	1.1136E-01	3.2164E+06	1.1121E-01	11:19	3.4912E+07		-45.80	0.24		-45.63	0.24		-0.15	0.23		Standard	
d30Si_020915_Paine@15	2.83	3.2577E-02	1.2392E-02	1.0100E+08	3.3931E-02	3.2902E+06	3.0999E-02	11:22	3.5673E+07		-45.95	0.25		-45.79	0.25		-0.32	0.23		Standard	
d30Si_020915_Ki40C_rad@1	2.83	3.2584E-02	8.7786E-03	9.4593E+07	1.2279E-01	3.0822E+06	1.2206E-01	11:26	3.3434E+07	3.2967E+07	-45.74	0.18	-44.86	-45.59	0.18		-0.11	0.22		Ki40	
d30Si_020915_Ki40C_rad@2	2.83	3.2617E-02	1.0446E-02	9.4750E+07	7.9341E-02	3.0916E+06	6.9655E-02	11:29	3.3468E+07	9.9949E+05	-44.79	0.21	1.02	-44.65	0.21		0.88	0.23		Ki40	
d30Si_020915_Ki40C_rad@3	2.83	3.2628E-02	9.7511E-03	9.3534E+07	1.4252E-01	3.0516E+06	1.3927E-01	11:32	3.3012E+07		-44.47	0.20		-44.33	0.20		1.21	0.22		Ki40	
d30Si_020915_Ki40C_rad@4	2.83	3.2624E-02	8.3011E-03	9.1656E+07	6.7558E-02	2.9904E+06	6.2500E-02	11:35	3.2376E+07		-44.58	0.17		-44.45	0.17		1.09	0.22		Ki40	
d30Si_020915_Ki40C_rad@5	2.83	3.2621E-02	9.2252E-03	9.2147E+07	1.2059E-01	3.0057E+06	1.2020E-01	11:39	3.2544E+07		-44.69	0.18		-44.56	0.18		0.97	0.22		Ki40	
d30Si_020915_Ki40C_mat@1	2.83	3.2614E-02	1.2897E-02	9.0044E+07	1.3905E-01	2.9367E+06	1.3680E-01	11:42	3.1794E+07	2.9199E+07	-44.87	0.26	-44.35	-44.75	0.26		0.77	0.24		Ki40 matrix	
d30Si_020915_Ki40C_mat@2	2.83	3.2636E-02	1.0807E-02	7.8346E+07	7.9853E-02	2.5568E+06	8.0175E-02	11:45	2.7665E+07	3.9851E+06	-44.22	0.22	0.89	-44.11	0.22		1.44	0.23		Ki40 matrix	Yield
d30Si_020915_Ki40C_mat@3	2.83	3.2627E-02	1.5059E-02	8.4163E+07	2.1239E-01	2.7463E+06	2.1605E-01	11:48	2.9732E+07		-44.49	0.30		-44.38	0.30		1.16	0.25		Ki40 matrix	
d30Si_020915_Ki40C_mat@4	2.83	3.2651E-02	1.2098E-02	7.8254E+07	8.0917E-02	2.5548E+06	8.3633E-02	11:52	2.7605E+07		-43.81	0.24		-43.72	0.24		1.85	0.23		Ki40 matrix	Yield
d30Si_020915_Paine@16	2.83	3.2588E-02	1.0207E-02	1.0062E+08	9.4110E-02	3.2789E+06	9.6070E-02	12:08	3.5502E+07	3.5259E+07	-45.63	0.20	-45.69	-45.57	0.20	-45.72	-0.09	0.22	-0.24	Standard	
d30Si_020915_Paine@17	2.84	3.2580E-02	9.9793E-03	1.0088E+08	1.5463E-01	3.2869E+06	1.5225E-01	12:11	3.5575E+07	8.2022E+05	-45.87	0.20	0.37	-45.82	0.20	0.21	-0.34	0.22	0.22	Standard	
d30Si_020915_Paine@18	2.84	3.2582E-02	8.9222E-03	1.0008E+08	6.8048E-02	3.2607E+06	6.5209E-02	12:14	3.5287E+07		-45.82	0.18		-45.77	0.18		-0.30	0.22		Standard	
d30Si_020915_Paine@20	2.84	3.2597E-02	1.2129E-02	9.9828E+07	1.4368E-01	3.2562E+06	1.3573E-01	12:57	3.5204E+07	3.4480E+07	-45.37	0.24	-45.29	-45.43	0.24	-45.35	0.06	0.23	0.14	Standard	
d30Si_020915_Paine@21	2.84	3.2600E-02	1.3150E-02	9.5795E+07	1.7153E-01	3.1230E+06	1.6685E-01	13:00	3.3759E+07	1.2667E+06	-45.28	0.26	0.18	-45.34	0.26	0.15	0.16	0.24	0.16	Standard	
d30Si_020915_Paine@22	2.84	3.2604E-02	1.0883E-02	9.7063E+07	1.0209E-01	3.1647E+06	1.0152E-01	13:03	3.4197E+07		-45.17	0.22		-45.23	0.22		0.27	0.23		Standard	
d30Si_020915_Paine@23	2.84	3.2598E-02	1.1110E-02	9.8760E+07	1.0897E-01	3.2210E+06	1.0148E-01	13:07	3.4760E+07		-45.33	0.22		-45.41	0.22		0.08	0.23		Standard	
d30Si_020915_Ki39C_rad@1	2.84	3.2652E-02	1.3611E-02	9.3237E+07	1.7241E-01	3.0444E+06	1.7475E-01	13:29	3.2797E+07	3.2782E+07	-43.76	0.27	-44.00	-43.89	0.27		1.68	0.24		Ki39	
d30Si_020915_Ki39C_rad@2	2.84	3.2641E-02	1.0819E-02	9.2177E+07	1.2077E-01	3.0086E+06	1.1730E-01	13:33	3.2415E+07	1.2128E+06	-44.10	0.22	0.49	-44.23	0.22		1.31	0.23		Ki39	
d30Si_020915_Ki39C_rad@3	2.84	3.2651E-02	7.4558E-03	9.1870E+07	9.1450E-02	2.9996E+06	9.2586E-02	13:36	3.2327E+07		-43.80	0.15		-43.94	0.15		1.62	0.21		Ki39	
d30Si_020915_Ki39C_rad@4	2.84	3.2632E-02	8.6803E-03	9.6095E+07	1.1948E-01	3.1375E+06	1.0888E-01	13:39	3.3820E+07		-44.36	0.17		-44.51	0.17		1.03	0.22		Ki39	
d30Si_020915_Ki39C_rad@5	2.84	3.2644E-02	1.1935E-02	9.2526E+07	1.5894E-01	3.0205E+06	1.5687E-01	13:42	3.2553E+07		-43.99	0.24		-44.14	0.24		1.41	0.23		Ki39	
d30Si_020915_Paine@24	2.84	3.2598E-02	1.0019E-02	9.9604E+07	1.0829E-01	3.2469E+06	1.0848E-01	13:46	3.5060E+07	3.4594E+07	-45.36	0.20	-45.56	-45.52	0.20	-45.73	-0.04	0.22	-0.26	Standard	
d30Si_020915_Paine@25	2.84	3.2588E-02	1.0454E-02	9.9646E+07	1.7489E-01	3.2474E+06	1.7248E-01	13:49	3.5030E+07	1.1051E+06	-45.65	0.21	0.29	-45.82	0.21	0.26	-0.35	0.22	0.27	Standard	
d30Si_020915_Paine@26	2.85	3.2587E-02	8.8288E-03	9.6531E+07	1.6169E-01	3.1456E+06	1.5969E-01	13:52	3.3917E+07		-45.68	0.18		-45.85	0.18		-0.38	0.22		Standard	
d30Si_020915_Paine@27	2.85	3.2591E-02	1.1541E-02	9.7847E+07	9.1926E-02	3.1903E+06	8.7533E-02	13:55	3.4368E+07		-45.55	0.23		-45.73	0.23		-0.26	0.23		Standard	

Table A2 Continued.

	SIMS ANALYSES							Mount: BR4v2	Standard: UNIL-Q1 (Paine)		Analyse: $\delta^{30}Si$			Value= -0.13±0.02 (NBS-28, 2σ)						Date: 03.09.2015
	Beam	H'2/L'2 (30Si/28Si)		L'2 (30Si/Coeff)		H'2 (28Si/Coeff)		Time	Yield	mean	Measurements		mean	Drift correction		Calibration				Comment
	nA	*CPS*	*2SD*	*CPS*	*2SD*	*CPS*	*2SD*		CPS/nA	*2SD*	$\delta^{30}Si$	*2SD int*	*2SD*	$\delta^{30}Si$	*2SD*		$\delta^{30}Si_{NBS-28}$	*2SD*		
d30Si_040915_BR4_Paine@1	2.33	3.2677E-02	1.1111E-02	8.4303E+07	1.4469E-01	2.7567E+06	1.3319E-01	0	3.6219E+07	3.5641E+07	-43.04	0.22	-43.01							Setting: Standard
d30Si_040915_BR4_Paine@2	2.34	3.2691E-02	7.3868E-03	8.1704E+07	1.1866E-01	2.6711E+06	1.1937E-01	1	3.4961E+07	2.6970E+06	-42.63	0.15	0.78							Setting: Standard
d30Si_040915_BR4_Paine@3	2.34	3.2677E-02	9.2090E-03	8.2091E+07	1.5683E-01	2.6826E+06	1.5533E-01	2	3.5121E+07		-43.04	0.18								Setting: Standard
d30Si_040915_BR4_Paine@4	2.34	3.2693E-02	1.1562E-02	8.1632E+07	1.1860E-01	2.6690E+06	1.1802E-01	3	3.4904E+07		-42.56	0.23								Setting: Standard
d30Si_040915_BR4_Paine@5	2.34	3.2676E-02	1.4900E-02	7.4776E+07	1.6760E-01	2.4436E+06	1.6393E-01	4	3.1937E+07		-43.07	0.30								Setting: Standard
d30Si_040915_BR4_Paine@6	2.34	3.2659E-02	1.2601E-02	8.7057E+07	1.1632E-01	2.8433E+06	1.1725E-01	5	3.7203E+07		-43.56	0.25								Setting: Standard
d30Si_040915_BR4_Paine@7	2.34	3.2679E-02	7.0994E-03	8.3225E+07	1.5934E-01	2.7219E+06	1.4642E-01	6	3.5509E+07		-42.99	0.14								Setting: Standard
d30Si_040915_BR4_Paine@8	2.34	3.2680E-02	7.7632E-03	8.0416E+07	2.1591E-01	2.6282E+06	2.1209E-01	7	3.4298E+07		-42.95	0.16								Setting: Standard
d30Si_040915_BR4_Paine@9	2.34	3.2679E-02	1.2674E-02	8.3395E+07	1.2314E-01	2.7236E+06	1.3337E-01	8	3.5578E+07		-42.97	0.25								Setting: Standard
d30Si_040915_BR4_Paine@10	2.34	3.2644E-02	1.3700E-02	8.6099E+07	1.9825E-01	2.8106E+06	1.9444E-01	9	3.6740E+07		-43.99	0.27								Setting: Standard
d30Si_040915_BR4_Paine@11	2.35	3.2679E-02	7.9642E-03	8.5974E+07	1.6549E-01	2.8095E+06	1.6395E-01	10	3.6659E+07		-42.96	0.16								Setting: Standard
d30Si_040915_BR4_Paine@12	2.34	3.2657E-02	1.4912E-02	8.8997E+07	1.9070E-01	2.9089E+06	1.7753E-01	11	3.8079E+07		-43.62	0.30								Setting: Standard
d30Si_040915_BR4_Paine@13	2.35	3.2684E-02	9.0542E-03	8.2865E+07	1.2373E-01	2.7085E+06	1.2587E-01	12	3.5333E+07		-42.83	0.18								Setting: Standard
d30Si_040915_BR4_Paine@14	2.35	3.2686E-02	8.3286E-03	8.4266E+07	9.1881E-02	2.7544E+06	9.0038E-02	13	3.5931E+07		-42.78	0.17								Setting: Standard
d30Si_040915_BR4_Paine@15	2.35	3.2694E-02	9.2168E-03	8.3456E+07	1.3326E-01	2.7285E+06	1.3149E-01	14	3.5589E+07		-42.53	0.18								Setting: Standard
d30Si_040915_BR4_Paine@16	2.35	3.2677E-02	1.5127E-02	8.5898E+07	1.3879E-01	2.8047E+06	1.5102E-01	15	3.6618E+07		-43.03	0.30								Setting: Standard
d30Si_040915_BR4_Paine@17	2.35	3.2689E-02	9.5313E-03	8.2581E+07	1.1661E-01	2.6993E+06	1.1507E-01	16	3.5216E+07		-42.69	0.19								Setting: Standard
d30Si_040915_BR4_Paine@18	2.34	3.2679E-02	9.5366E-03	8.5453E+07	1.4558E-01	2.7923E+06	1.4702E-01	17	3.6583E+07	3.6642E+07	-42.98	0.19	-43.12	-42.93	0.19	-43.07	0.07	0.40	-0.08	Standard
d30Si_040915_BR4_Paine@19	2.35	3.2661E-02	1.0937E-02	8.6477E+07	1.5850E-01	2.8244E+06	1.5749E-01	18	3.6868E+07	1.3429E+06	-43.52	0.22	0.82	-43.47	0.22	0.71	-0.49	0.40	0.74	Standard
d30Si_040915_BR4_Paine@20	2.35	3.2665E-02	8.3444E-03	8.7634E+07	1.7846E-01	2.8648E+06	1.6951E-01	19	3.7359E+07		-43.38	0.17		-43.33	0.17		-0.35	0.40		Standard
d30Si_040915_BR4_Paine@21	2.35	3.2692E-02	1.0079E-02	8.3962E+07	8.1061E-02	2.7449E+06	7.9766E-02	20	3.5757E+07		-42.61	0.20		-42.56	0.20		0.45	0.40		Standard
d30Si_040915_BR4_Paine@22	2.35	3.2678E-02	9.5927E-03	8.4321E+07	1.5606E-01	2.7554E+06	1.5549E-01	31	3.5888E+07	3.6211E+07	-43.02	0.19	-43.08	-43.00	0.19	-43.08	-0.01	0.40	-0.09	Standard
d30Si_040915_BR4_Paine@23	2.35	3.2684E-02	8.4275E-03	8.4676E+07	1.1396E-01	2.7693E+06	1.0541E-01	32	3.6004E+07	1.8631E+06	-42.84	0.17	0.80	-42.83	0.17	0.76	0.17	0.40	0.79	Standard
d30Si_040915_BR4_Paine@24	2.35	3.2687E-02	1.0581E-02	8.5300E+07	1.6291E-01	2.7880E+06	1.6437E-01	33	3.6262E+07		-42.74	0.21	0.80	-42.73	0.21		0.28	0.40		Standard
d30Si_040915_BR4_Paine@25	2.35	3.2659E-02	1.1782E-02	8.9236E+07	1.2595E-01	2.9145E+06	1.2747E-01	34	3.7931E+07		-43.56	0.24		-43.55	0.24		-0.58	0.41		Standard
d30Si_040915_BR4_Paine@26	2.35	3.2651E-02	7.1539E-03	8.8410E+07	1.8994E-01	2.8868E+06	1.9097E-01	35	3.7664E+07		-43.81	0.14		-43.81	0.14		-0.85	0.39		Standard
d30Si_040915_BR4_Paine@27	2.35	3.2683E-02	1.7097E-02	8.3575E+07	1.3612E-01	2.7317E+06	1.3510E-01	36	3.5514E+07		-42.86	0.34		-42.86	0.34		0.15	0.42		Standard
d30Si_040915_BR4_Paine@28	2.35	3.2659E-02	1.1533E-02	8.6054E+07	1.5429E-01	2.8105E+06	1.5585E-01	37	3.6589E+07		-43.55	0.23		-43.56	0.23		-0.59	0.40		Standard
d30Si_040915_BR4_Paine@29	2.35	3.2686E-02	1.3047E-02	8.3492E+07	1.0558E-01	2.7291E+06	1.0150E-01	38	3.5498E+07		-42.76	0.26		-42.77	0.26		0.24	0.41		Standard
d30Si_040915_BR4_Paine@30	2.35	3.2682E-02	1.1241E-02	8.2751E+07	1.2243E-01	2.7060E+06	1.1355E-01	39	3.5183E+07		-42.89	0.22		-42.90	0.22		0.10	0.40		Standard
d30Si_040915_BR4_Paine@31	2.35	3.2686E-02	1.0208E-02	8.3726E+07	1.3262E-01	2.7367E+06	1.3139E-01	40	3.5581E+07		-42.78	0.20		-42.79	0.20		0.22	0.40		Standard
d30Si_040915_Ki41_rad@1	2.36	3.2720E-02	1.0150E-02	7.7345E+07	1.3637E-01	2.5306E+06	1.3666E-01	49	3.2841E+07	3.3730E+07	-41.76	0.20	-42.01	-41.80	0.20		1.25	0.40		Ki41
d30Si_040915_Ki41_rad@2	2.35	3.2729E-02	1.8727E-02	7.7343E+07	6.1451E-02	2.5317E+06	6.4292E-02	50	3.2853E+07	3.0611E+06	-41.51	0.37	1.32		1.64			1.72		Ki41 intenal error
d30Si_040915_BR4_Paine@32	2.35	3.2681E-02	9.9304E-03	8.2620E+07	1.4261E-01	2.7002E+06	1.4438E-01	51	3.5093E+07	3.5617E+07	-42.90	0.20	-43.04	-42.95	0.20	-43.09	0.05	0.40	-0.10	Standard
d30Si_040915_BR4_Paine@33	2.36	3.2673E-02	1.0927E-02	8.4653E+07	1.0648E-01	2.7661E+06	1.0690E-01	52	3.5935E+07	7.4899E+05	-43.16	0.22	0.22	-43.20	0.22	0.19	-0.21	0.40	0.20	Standard
d30Si_040915_BR4_Paine@34	2.36	3.2678E-02	1.1001E-02	8.3915E+07	1.2060E-01	2.7420E+06	1.2043E-01	53	3.5610E+07		-43.01	0.22		-43.06	0.22		-0.07	0.40		Standard
d30Si_040915_BR4_Paine@35	2.36	3.2675E-02	1.1106E-02	8.4421E+07	9.5202E-02	2.7584E+06	9.2224E-02	54	3.5830E+07		-43.10	0.22		-43.15	0.22		-0.16	0.40		Standard

Table A2 Continued.

SIMS ANALYSES																					
Mount: BR6					Standard: UNIL-Q1 (Paine)					Analyse: δ^{30}Si				Value= -0.13±0.02 (NBS-28, 2σ)						Date: 03.09.2015	
	Beam	H'2/L'2 (30Si/28Si)		L'2 (30Si/Coeff)		H'2 (28Si/Coeff)		Time	Yield	mean	Measurements		mean	Drift correction		Calibration				Comment	
	nA	CPS	2SD	CPS	2SD	CPS	2SD		CPS/nA	2SD	$\delta^{30}Si$	2SD int	2SD	$\delta^{30}Si$	2SD		$\delta^{30}Si_{NBS28}$	2SD			
d30Si_020915_BR6_Paine@1	2.85	3.2600E-02	1.0308E-02	9.8177E+07	8.3010E-02	3.2019E+06	7.4661E-02	15:10	3.4493E+07	3.4162E+07	-45.29	0.21	-45.10							Setting: Standard	
d30Si_020915_BR6_Paine@2	2.85	3.2608E-02	8.4777E-03	9.8585E+07	1.3462E-01	3.2148E+06	1.3181E-01	15:13	3.4531E+07	1.5657E+06	-45.05	0.17	0.24							Setting: Standard	
d30Si_020915_BR6_Paine@3	2.86	3.2611E-02	1.1375E-02	9.6759E+07	9.7800E-02	3.1569E+06	9.1071E-02	15:17	3.3884E+07		-44.97	0.23								Setting: Standard	
d30Si_020915_BR6_Paine@4	2.86	3.2603E-02	9.7271E-03	9.8461E+07	7.8345E-02	3.2103E+06	7.9922E-02	15:20	3.4484E+07		-45.21	0.19								Setting: Standard	
d30Si_020915_BR6_Paine@5	2.86	3.2609E-02	1.1222E-02	9.9675E+07	1.9120E-01	3.2501E+06	1.9022E-01	15:23	3.4875E+07		-45.04	0.22								Setting: Standard	
d30Si_020915_BR6_Paine@6	2.86	3.2608E-02	7.9083E-03	9.3462E+07	3.1953E-01	3.0474E+06	3.1779E-01	15:26	3.2703E+07		-45.06	0.16								Setting: Standard	
d30Si_020915_BR6_Paine@9	2.85	3.2598E-02	9.7991E-03	9.3629E+07	1.8584E-01	3.0549E+06	1.6920E-01	15:48	3.2819E+07	3.3782E+07	-45.36	0.20	-45.25	-45.34	0.20	-45.23	-0.10	0.34	0.01	Standard	
d30Si_020915_BR6_Paine@9	duplicate							15:48		1.9693E+06			0.25			0.21			0.22	Standard	duplicate
d30Si_020915_BR6_Paine@10	2.86	3.2606E-02	1.0866E-02	9.6410E+07	1.3948E-01	3.1457E+06	1.2793E-01	15:51	3.3690E+07		-45.11	0.22		-45.09	0.22		0.15	0.34		Standard	
d30Si_020915_BR6_Paine@11	2.86	3.2600E-02	1.1102E-02	1.0067E+08	1.5093E-01	3.2838E+06	1.3535E-01	15:54	3.5151E+07		-45.29	0.22		-45.27	0.22		-0.03	0.34		Standard	
d30Si_020915_BR6_Paine@12	2.86	3.2600E-02	1.3121E-02	9.5810E+07	1.2286E-01	3.1253E+06	1.1224E-01	15:58	3.3468E+07		-45.29	0.26		-45.27	0.26		-0.04	0.35		Standard	
d30Si_020915_BR6_Paine@13	2.87	3.2592E-02	9.9742E-03	9.9673E+07	2.0366E-01	3.2516E+06	1.9003E-01	16:21	3.4778E+07	3.4004E+07	-45.52	0.20	-45.34	-45.50	0.20	-45.33	-0.28	0.34	-0.10	Standard	
d30Si_020915_BR6_Paine@14	2.87	3.2602E-02	9.6423E-03	9.7008E+07	1.2312E-01	3.1624E+06	1.2123E-01	16:24	3.3824E+07	1.0669E+06	-45.24	0.19	0.33	-45.22	0.19	0.29	0.02	0.34	0.30	Standard	
d30Si_020915_BR6_Paine@15	2.87	3.2595E-02	1.0272E-02	9.7065E+07	1.3454E-01	3.1640E+06	1.3189E-01	16:27	3.3856E+07		-45.45	0.21		-45.43	0.21		-0.20	0.34		Standard	
d30Si_020915_BR6_Paine@16	2.87	3.2604E-02	6.4968E-03	9.6249E+07	1.1832E-01	3.1381E+06	1.1709E-01	16:30	3.3557E+07		-45.17	0.13		-45.16	0.13		0.09	0.33		Standard	
d30Si_020915_Ki48_rad@1	2.87	3.2654E-02	1.0835E-02	9.1341E+07	7.4821E-02	2.9829E+06	7.3635E-02	16:34	3.1866E+07	2.4983E+07	-43.71	0.22	-44.19	-43.69	0.22		1.62	0.34		Ki48	
d30Si_020915_Ki48_rad@2	2.87	3.2624E-02	7.7468E-03	9.1638E+07	1.8806E-01	2.9898E+06	1.8353E-01	16:37	3.1974E+07	2.8041E+07	-44.58	0.15	0.73	-44.57	0.15		0.70	0.33		Ki48	
d30Si_020915_Ki48_rad@3	2.87	3.2639E-02	1.6026E-02	9.1689E+07	1.4856E-01	2.9926E+06	1.4161E-01	16:40	3.1989E+07		-44.15	0.32		-44.13	0.32		1.15	0.36		Ki48	
d30Si_020915_Ki48_rad@4	2.87	3.2634E-02	7.9662E-03	8.3345E+07	5.4489E-02	2.7198E+06	5.3755E-02	16:43	2.9085E+07		-44.31	0.16		-44.29	0.16		0.99	0.33		Ki48	
d30Si_020915_Ki48_rad@5	2.87	-2.9223E-01		4.9264E+02		-7.6538E+03	4.1698E-02	16:47	1.7166E+02		-9558.22									Ki48	Yield
d30Si_020915_BR6_Paine@17	2.87	3.2597E-02	9.3871E-03	9.8864E+07	1.9022E-01	3.2258E+06	1.7664E-01	16:50	3.4495E+07	3.4504E+07	-45.38	0.19	-45.38	-45.37	0.19	-45.37	-0.14	0.34	-0.13	Standard	
d30Si_020915_BR6_Paine@18	2.87	3.2579E-02	1.1024E-02	1.0322E+08	2.2235E-01	3.3632E+06	2.1936E-01	16:53	3.5976E+07	2.1273E+06	-45.91	0.22	0.77	-45.90	0.22	0.66	-0.69	0.34	0.70	Standard	
d30Si_020915_BR6_Paine@19	2.87	3.2609E-02	1.1687E-02	9.6092E+07	9.7992E-02	3.1335E+06	9.3768E-02	16:57	3.3491E+07		-45.02	0.23		-45.01	0.23		0.24	0.34		Standard	
d30Si_020915_BR6_Paine@20	2.87	3.2603E-02	9.7614E-03	9.7703E+07	9.6057E-02	3.1853E+06	9.2870E-02	17:00	3.4055E+07		-45.20	0.20		-45.19	0.20		0.05	0.34		Standard	
d30Si_020915_BR6_Paine@21	2.87	3.2609E-02	1.4716E-02	9.6472E+07	1.1339E-01	3.1459E+06	1.0780E-01	17:26	3.3601E+07	3.3866E+07	-45.04	0.29	-45.41	-45.03	0.29	-45.40	0.21	0.36	-0.17	Standard	
d30Si_020915_BR6_Paine@22	2.87	3.2587E-02	1.1020E-02	1.0016E+08	1.6617E-01	3.2639E+06	1.6556E-01	17:29	3.4868E+07	1.3777E+06	-45.66	0.22	0.56	-45.65	0.22	0.49	-0.43	0.34	0.51	Standard	
d30Si_020915_BR6_Paine@23	2.87	3.2589E-02	9.7018E-03	9.5567E+07	1.1007E-01	3.1163E+06	9.9105E-02	17:33	3.3299E+07		-45.60	0.19		-45.59	0.19		-0.37	0.34		Standard	
d30Si_020915_BR6_Paine@24	2.87	3.2598E-02	1.4101E-02	9.6797E+07	1.1054E-01	3.1554E+06	1.0929E-01	17:36	3.3697E+07		-45.34	0.28		-45.34	0.28		-0.11	0.35		Standard	
d30Si_020915_Ki43_rad@1	2.87	3.2631E-02	1.1986E-02	9.1151E+07	1.9092E-01	2.9743E+06	1.8759E-01	17:39	3.1737E+07	3.1679E+07	-44.40	0.24	-44.02	-44.39	0.24		0.89	0.35		Ki43	
d30Si_020915_Ki43_rad@2	2.87	3.2637E-02	8.4439E-03	9.5318E+07	1.2148E-01	3.1111E+06	1.1630E-01	17:42	3.3169E+07	2.0334E+06	-44.19	0.17	0.49	-44.19	0.17		1.10	0.34		Ki43	
d30Si_020915_Ki43_rad@3	2.87	3.2642E-02	1.2908E-02	9.0341E+07	1.5164E-01	2.9489E+06	1.4815E-01	17:46	3.1432E+07		-44.06	0.26		-44.06	0.26		1.24	0.35		Ki43	
d30Si_020915_Ki43_rad@4	2.87	3.2653E-02	1.1564E-02	8.6235E+07	1.8871E-01	2.8158E+06	1.8712E-01	17:49	3.0004E+07		-43.73	0.23		-43.73	0.23		1.58	0.34		Ki43	
d30Si_020915_Ki43_rad@5	2.88	3.2647E-02	1.3404E-02	9.1568E+07	4.9230E-02	2.9897E+06	4.5444E-02	17:54	3.1802E+07		-43.91	0.27		-43.91	0.27		1.39	0.35		Ki43	
d30Si_020915_Ki43_rad@6	2.88	3.2650E-02	1.0058E-02	9.1817E+07	1.2289E-01	2.9997E+06	1.2973E-01	17:57	3.1930E+07		-43.84	0.20		-43.83	0.20		1.47	0.34		Ki43	
d30Si_020915_BR6_Paine@25	2.87	3.2616E-02	1.1356E-02	9.0220E+07	1.6610E-01	2.9426E+06	1.6369E-01	18:00	3.1410E+07	3.2103E+07	-44.83	0.23	-45.41	-44.83	0.23	-45.41	0.43	0.34	-0.18	Standard	
d30Si_020915_BR6_Paine@26	2.88	3.2564E-02	1.1604E-02	8.8765E+07	3.3713E-01	2.8908E+06	3.3163E-01	18:04	3.0869E+07	2.3901E+06	-46.33	0.23	1.35	-46.33	0.23	1.17	-1.15	0.34	1.22	Standard	
d30Si_020915_BR6_Paine@27	2.87	3.2610E-02	1.1234E-02	9.6270E+07	1.1286E-01	3.1395E+06	1.0608E-01	18:07	3.3527E+07		-45.00	0.22		-44.99	0.22		0.25	0.34		Standard	
d30Si_020915_BR6_Paine@28	2.87	3.2594E-02	1.6649E-02	9.3602E+07	3.2507E-01	3.0508E+06	3.1861E-01	18:10	3.2607E+07		-45.48	0.33		-45.48	0.33		-0.25	0.36		Standard	
d30Si_020915_Ki20C_rad@1	2.87	3.2702E-02	1.5311E-02	7.2862E+07	1.1359E-01	2.3846E+06	1.3011E-01	18:14	2.5376E+07		-42.31	0.31		-42.31	0.31		3.07	0.36		Ki20	
d30Si_020915_Ki20C_rad@2	2.87	3.2674E-02	1.3194E-02	7.5096E+07	9.7037E-02	2.4536E+06	9.7677E-02	18:17	2.6136E+07		-43.14	0.26		-43.14	0.26		2.20	0.35		Ki20	
d30Si_020915_Ki20C_rad@3	2.87	3.2686E-02	1.3627E-02	6.8071E+07	1.0142E-01	2.2250E+06	1.0136E-01	18:20	2.3702E+07		-42.77	0.27		-42.77	0.27		2.59	0.35		Ki20	
d30Si_020915_Ki20C_rad@4	2.88	3.2642E-02	8.6278E-03	8.4333E+07	1.7955E-01	2.7526E+06	1.8100E-01	18:23	2.9319E+07		-44.07	0.17		-44.07	0.17		1.22	0.34		Ki20	
d30Si_020915_Ki20C_rad@5	2.87	3.2655E-02	9.5962E-03	7.9734E+07	1.5535E-01	2.6037E+06	1.5697E-01	18:27	2.7745E+07		-43.69	0.19		-43.69	0.19		1.62	0.34		Ki20	
d30Si_020915_BR6_Paine@29	2.87	3.2601E-02	1.0628E-02	1.0025E+08	1.3549E-01	3.2686E+06	1.3637E-01	18:30	3.4895E+07	3.5215E+07	-45.26	0.21	-45.54	-45.27	0.21	-45.54	-0.03	0.34	-0.32	Standard	
d30Si_020915_BR6_Paine@30	2.88	3.2590E-02	8.2813E-03	9.9192E+07	1.8276E-01	3.2328E+06	1.8266E-01	18:33	3.4498E+07	2.3817E+06	-45.59	0.17	0.80	-45.59	0.17	0.69	-0.37	0.33	0.72	Standard	
d30Si_020915_BR6_Paine@31	2.87	3.2573E-02	9.0740E-03	1.0625E+08	1.6989E-01	3.4634E+06	1.6183E-01	18:36	3.6978E+07		-46.08	0.18		-46.08	0.18		-0.89	0.34		Standard	
d30Si_020915_BR6_Paine@32	2.87	3.2603E-02	1.0416E-02	9.9135E+07	1.2055E-01	3.2339E+06	1.1218E-01	18:40	3.4488E+07		-45.21	0.21		-45.22	0.21		0.02	0.34		Standard	
d30Si_020915_BR6_Paine@33	2.87	3.2604E-02	1.0537E-02	9.9222E+07	1.3592E-01	3.2372E+06	1.2450E-01	19:03	3.4537E+07	3.4917E+07	-45.17	0.21	-45.38	-45.18	0.21	-45.39	0.06	0.34	-0.16	Standard	
d30Si_020915_BR6_Paine@34	2.88	3.2605E-02	1.0568E-02	9.8211E+07	9.2263E-02	3.2024E+06	8.9789E-02	19:06	3.4146E+07	2.1810E+06	-45.15	0.21	0.55	-45.16	0.21	0.47	0.08	0.34	0.50	Standard	
d30Si_020915_BR6_Paine@35	2.87	3.2585E-02	8.6040E-03	1.0499E+08	1.3089E-01	3.4232E+06	1.2243E-01	19:09	3.6533E+07		-45.73	0.17		-45.74	0.17		-0.53	0.34		Standard	
d30Si_020915_BR6_Paine@36	2.87	3.2594E-02	1.0620E-02	9.9013E+07	3.7047E-01	3.2274E+06	3.7127E-01	19:12	3.4451E+07		-45.46	0.21		-45.47	0.21		-0.25	0.34		Standard	
d30Si_020915_BR6_Paine@37	2.88	3.2595E-02	7.1932E-03	9.7245E+07	3.1926E-01	3.1697E+06	3.1870E-01	19:35	3.3816E+07	3.4381E+07	-45.44	0.14	-45.44	-45.45	0.14	-45.46	-0.23	0.33	-0.23	Standard	
d30Si_020915_BR6_Paine@38	2.88	3.2567E-02	1.2160E-02	1.0084E+08	3.1313E-01	3.2843E+06	3.1290E-01	19:38	3.5037E+07	1.0468E+06	-46.26	0.24	1.16	-46.28	0.24	1.00	-1.09	0.35	1.05	Standard	
d30Si_020915_BR6_Paine@39	2.88	3.2610E-02	1.1544E-02	9.8269E+07	5.8766E-02	3.2045E+06	5.2910E-02	19:42	3.4151E+07		-45.01	0.23		-45.02	0.23		0.22	0.34		Standard	
d30Si_020915_BR6_Paine@40	2.87	3.2608E-02	7.0475E-03	9.9229E+07	6.1553E-02	3.2357E+06	6.0752E-02	19:45	3.4522E+07		-45.06	0.14		-45.07	0.14		0.17	0.33		Standard	
d30Si_020915_BR6_Paine@41	2.88	3.2603E-02	8.5709E-03	9.9529E+07	8.6408E-02	3.2449E+06	8.6704E-02	20:08	3.4612E+07	3.4870E+07	-45.22	0.17	-45.27	-45.23	0.17	-45.28	0.01	0.34	-0.05	Standard	
d30Si_020915_BR6_Paine@42	2.88	3.2598E-02	1.4648E-02	9.7471E+07	1.5305E-01	3.1774E+06	1.5411E-01	20:11	3.3868E+07	1.5840E+06	-45.34	0.29	0.24	-45.35	0.29	0.21	-0.12	0.36	0.22	Standard	
d30Si_020915_BR6_Paine@43	2.88	3.2596E-02	9.4263E-03	1.0251E+08	1.0588E-01	3.3430E+06	9.7777E-02	20:14	3.5583E+07		-45.40	0.19		-45.41	0.19		-0.19	0.34		Standard	
d30Si_020915_BR6_Paine@44	2.88	3.2606E-02	1.1674E-02	1.0199E+08	7.4907E-02	3.3270E+06	6.6900E-02	20:17	3.5420E+07		-45.12	0.23		-45.14	0.23		0.10	0.34		Standard	
d30Si_020915_BR6_Paine@45	2.88	3.2602E-02	8.0255E-03	1.0007E+08	1.0896E-01	3.2640E+06	1.0119E-01	20:40	3.4734E+07	3.4243E+07	-45.24	0.16	-45.21	-45.26	0.16	-45.23	-0.03	0.33	0.01	Standard	
d30Si_020915_BR6_Paine@46	2.88	3.2598E-02	7.9395E-03	1.0098E+08	8.9550E-02	3.2919E+06	8.5410E-02	20:44	3.5064E+07	1.6072E+06	-45.34	0.16	0.32	-45.36	0.16	0.28	-0.13	0.33	0.29	Standard	
d30Si_020915_BR6_Paine@47	2.88	3.2611E-02	1.1262E-02	9.7611E+07	2.7802E-01	3.1829E+06	2.8087E-01	20:47	3.3876E+07		-44.97	0.23		-45.00	0.23		0.25	0.34		Standard	
d30Si_020915_BR6_Paine@48	2.88	3.2600E-02	8.7302E-03	9.6003E+07	5.6955E-02	3.1295E+06	5.2194E-02	20:50	3.3300E+07		-45.28	0.17		-45.30	0.17		-0.07	0.34		Standard	

Table A2 Continued.

SIMS ANALYSES								Mount: BR7	Standard: UNIL-Q1 (Paine)		Analyse: δ^{30}Si					Value= -0.13±0.02 (NBS-28, 2σ)				Date: 03.09.2015
	Beam	H'2/L'2 (30Si/28Si)		L'2 (30Si/Coeff)		H'2 (28Si/Coeff)		Time	Yield	mean	Measurements		mean	Drift correction			Calibration			Comment
	nA	CPS	2SD	CPS	2SD	CPS	2SD		CPS/nA	2SD	$\delta^{30}Si$	2SD int	2SD	$\delta^{30}Si$	2SD		$\delta^{30}Si_{NBS-28}$	2SD		
d30Si_040915_BR7_Paine_test@1	2.35	3.2698E-02	8.2542E-03	7.8392E+07	1.8327E-01	2.5630E+06	1.8224E-01	13:49	3.3338E+07	3.3096E+07	-42.42	0.17	-42.55							Setting: Standard
d30Si_040915_BR7_Paine_test@2	2.36	3.2695E-02	8.3876E-03	8.0136E+07	1.2329E-01	2.6203E+06	1.2045E-01	13:53	3.3979E+07	2.3352E+06	-42.50	0.17	0.47							Setting: Standard
d30Si_040915_BR7_Paine_test@3	2.36	3.2697E-02	1.5089E-02	7.8788E+07	1.3377E-01	2.5780E+06	1.2222E-01	13:56	3.3396E+07		-42.45	0.30								Setting: Standard
d30Si_040915_BR7_Paine_test@4	2.36	3.2695E-02	1.1602E-02	8.0159E+07	1.2819E-01	2.6208E+06	1.2989E-01	13:59	3.3978E+07		-42.51	0.23								Setting: Standard
d30Si_040915_BR7_Paine_test@5	2.36	3.2699E-02	1.0142E-02	7.8873E+07	1.2755E-01	2.5804E+06	1.1404E-01	14:03	3.3394E+07		-42.38	0.20								Setting: Standard
d30Si_040915_BR7_Paine_test@6	2.36	3.2686E-02	9.6415E-03	8.0167E+07	1.2827E-01	2.6205E+06	1.2985E-01	14:06	3.3940E+07		-42.78	0.19								Setting: Standard
d30Si_040915_BR7_Paine_test@7	2.36	3.2702E-02	1.0227E-02	7.2379E+07	3.9660E-01	2.3665E+06	3.9300E-01	14:09	3.0636E+07		-42.30	0.20								Setting: Standard
d30Si_040915_BR7_Paine_test@8	2.36	3.2678E-02	1.1543E-02	7.5878E+07	2.7898E-01	2.4797E+06	2.7848E-01	14:13	3.2104E+07		-43.01	0.23								Setting: Standard
d30Si_040915_BR7_Paine@1	2.36	3.2700E-02	1.6150E-02	7.7564E+07	1.7097E-01	2.5364E+06	1.6831E-01	14:17	3.2867E+07	3.3035E+07	-42.35	0.32	-42.37	-42.43	0.32	-42.45	-0.13	0.24	-0.15	Standard
d30Si_040915_BR7_Paine@02	2.37	3.2700E-02	7.3254E-03	7.9038E+07	1.5356E-01	2.5865E+06	1.4316E-01	14:20	3.3411E+07	5.1591E+05	-42.38	0.15	0.04	-42.46	0.15	0.03	-0.15	0.19	0.03	Standard
d30Si_040915_BR7_Paine@03	2.36	3.2700E-02	1.3863E-02	7.7696E+07	1.4544E-01	2.5388E+06	1.5577E-01	14:23	3.2865E+07		-42.37	0.28		-42.45	0.28		-0.14	0.22		Standard
d30Si_040915_BR7_Paine@04	2.36	3.2699E-02	1.1811E-02	7.8019E+07	1.4630E-01	2.5511E+06	1.4873E-01	14:27	3.2997E+07		-42.40	0.24		-42.47	0.24		-0.17	0.21		Standard
d30Si_040915_Ki57_rad@1	2.36	3.2726E-02	9.7275E-03	7.7400E+07	1.3478E-01	2.5330E+06	1.3156E-01	14:30	3.2735E+07	3.1285E+07	-41.61	0.19	-41.14	-41.68	0.19		0.65	0.20		Ki57
d30Si_040915_Ki57_rad@2	2.36	3.2752E-02	1.3111E-02	6.9962E+07	1.7990E-01	2.2916E+06	1.7616E-01	14:33	2.9602E+07	2.1509E+06	-40.83	0.26	1.28	-40.91	0.26		1.46	0.22		Ki57
d30Si_040915_Ki57_rad@3	2.36	3.2744E-02	1.2240E-02	7.4255E+07	1.3508E-01	2.4315E+06	1.3284E-01	14:37	3.1399E+07		-41.06	0.24		-41.13	0.24		1.23	0.21		Ki57
d30Si_040915_Ki57_rad@4	2.37	3.2726E-02	1.2459E-02	7.5864E+07	1.5457E-01	2.4845E+06	1.4234E-01	14:40	3.2057E+07		-41.60	0.25		-41.68	0.25		0.66	0.21		Ki57
d30Si_040915_Ki57_rad@5	2.37	3.2755E-02	1.0355E-02	7.3148E+07	1.8908E-01	2.3959E+06	1.8647E-01	14:43	3.0922E+07		-40.76	0.21		-40.83	0.21		1.54	0.20		Ki57
d30Si_040915_Ki57_rad@6	2.37	3.2738E-02	1.1352E-02	7.3339E+07	1.6555E-01	2.4013E+06	1.6167E-01	14:47	3.0989E+07		-41.24	0.23		-41.31	0.23		1.04	0.21		Ki57
d30Si_040915_Ki57_rad@7	2.36	3.2719E-02	1.3351E-02	7.6744E+07	1.2646E-01	2.5109E+06	1.2384E-01	14:50	3.2468E+07		-41.81	0.27		-41.88	0.27		0.45	0.22		Ki57
d30Si_040915_Ki57_rad@8	2.37	3.2726E-02	1.1628E-02	7.5207E+07	9.0513E-02	2.4612E+06	9.3291E-02	14:53	3.1789E+07		-41.60	0.23		-41.66	0.23		0.67	0.21		Ki57
d30Si_040915_Ki57_rad@9	2.37	3.2793E-02	1.3895E-02	6.9961E+07	1.0132E-01	2.2956E+06	7.9234E-02	14:56	2.9555E+07		-39.63	0.28								Ki57 yield
d30Si_040915_Ki57_rad@10	2.37	3.2736E-02	1.4276E-02	7.4133E+07	2.5698E-01	2.4299E+06	2.3483E-01	15:00	3.1336E+07		-41.31	0.29		-41.38	0.29		0.98	0.23		Ki57
d30Si_040915_Ki3c_rad@1	2.37	3.2714E-02	1.2811E-02	7.7656E+07	1.5262E-01	2.5403E+06	1.4815E-01	15:03	3.2821E+07		-41.95	0.26		-42.01	0.26		0.31	0.22		Ki03C
d30Si_040915_BR7_Paine@05	2.36	3.2701E-02	1.1867E-02	7.9516E+07	1.3463E-01	2.6004E+06	1.3081E-01	15:07	3.3631E+07	3.3415E+07	-42.33	0.24	-42.33	-42.39	0.24	-42.39	-0.09	0.21	-0.08	Standard
d30Si_040915_BR7_Paine@06	2.37	3.2702E-02	1.0781E-02	7.7973E+07	1.3932E-01	2.5497E+06	1.3343E-01	15:10	3.2949E+07	6.2761E+05	-42.29	0.22	0.17	-42.35	0.22	0.14	-0.05	0.20	0.15	Standard
d30Si_040915_BR7_Paine@07	2.37	3.2704E-02	1.2501E-02	7.9432E+07	1.5085E-01	2.5977E+06	1.4955E-01	15:13	3.3556E+07		-42.24	0.25		-42.31	0.25		0.01	0.21		Standard
d30Si_040915_BR7_Paine@08	2.37	3.2697E-02	1.2610E-02	7.9350E+07	1.5563E-01	2.5947E+06	1.5621E-01	15:16	3.3526E+07		-42.44	0.25		-42.50	0.25		-0.20	0.22		Standard
d30Si_040915_Ki3c_rad@2	2.37	3.2709E-02	1.4099E-02	7.8436E+07	1.6892E-01	2.5658E+06	1.6788E-01	15:20	3.3137E+07	3.2645E+07	-42.09	0.28	-42.01	-42.15	0.28		0.17	0.22		Ki03C
d30Si_040915_Ki3c_rad@3	2.37	3.2727E-02	1.3517E-02	7.3853E+07	2.5015E-01	2.4170E+06	2.4799E-01	15:23	3.1199E+07	1.4913E+06	-41.56	0.27	1.06	-41.61	0.27		0.73	0.22		Ki03C
d30Si_040915_Ki3c_rad@4	2.37	3.2731E-02	1.6375E-02	7.4904E+07	1.0126E-01	2.4519E+06	9.9863E-02	15:26	3.1633E+07		-41.45	0.33		-41.50	0.33		0.84	0.24		Ki03C
d30Si_040915_Ki3c_rad@5	2.37	3.2706E-02	8.2757E-03	7.8671E+07	1.3618E-01	2.5732E+06	1.3386E-01	15:30	3.3225E+07		-42.18	0.17		-42.23	0.17		0.08	0.19		Ki03C
d30Si_040915_Ki3c_rad@6	2.37	3.2696E-02	9.1298E-03	7.9000E+07	1.5135E-01	2.5833E+06	1.4940E-01	15:33	3.3381E+07		-42.47	0.18		-42.53	0.18		-0.23	0.20		Ki03C
d30Si_040915_Ki3c_rad@7	2.37	3.2727E-02	1.3385E-02	7.6718E+07	1.4830E-01	2.5108E+06	1.4374E-01	15:36	3.2405E+07		-41.56	0.27		-41.61	0.27		0.73	0.22		Ki03C
d30Si_040915_Ki3c_rad@8	2.37	3.2718E-02	1.7101E-02	7.7635E+07	1.3033E-01	2.5416E+06	1.1748E-01	15:40	3.2795E+07		-41.82	0.34		-41.87	0.34		0.46	0.24		Ki03C
d30Si_040915_Ki3c_rad@9	2.37	3.2717E-02	8.9040E-03	7.6749E+07	1.5763E-01	2.5127E+06	1.4171E-01	15:43	3.2430E+07		-41.85	0.18		-41.90	0.18		0.43	0.20		Ki03C
d30Si_040915_Ki3c_rad@10	2.37	3.2671E-02	1.0620E-02	7.9130E+07	1.4139E-01	2.5854E+06	1.3634E-01	15:46	3.3427E+07		-43.22	0.21		-43.27	0.21		-1.00	0.20		Ki03C
d30Si_040915_Ki42_rad@1	2.37	3.2752E-02	1.4032E-02	7.2386E+07	2.0918E-01	2.3730E+06	1.9782E-01	15:50	3.0594E+07		-40.85	0.28		-40.90	0.28		1.47	0.22		Ki42
d30Si_040915_BR7_Paine@09	2.37	3.2696E-02	1.1891E-02	8.0320E+07	1.3071E-01	2.6276E+06	1.1872E-01	15:53	3.3926E+07	3.3536E+07	-42.48	0.24	-42.60	-42.53	0.24	-42.64	-0.22	0.21	-0.34	Standard
d30Si_040915_BR7_Paine@10	2.37	3.2693E-02	1.3240E-02	7.9106E+07	1.3460E-01	2.5862E+06	1.3099E-01	15:56	3.3397E+07	7.0590E+05	-42.56	0.26	0.21	-42.61	0.26	0.18	-0.31	0.22	0.19	Standard
d30Si_040915_BR7_Paine@11	2.37	3.2687E-02	1.0073E-02	7.9791E+07	1.3410E-01	2.6083E+06	1.3452E-01	16:00	3.3703E+07		-42.73	0.20		-42.78	0.20		-0.49	0.20		Standard
d30Si_040915_BR7_Paine@12	2.37	3.2691E-02	1.1246E-02	7.8429E+07	1.3907E-01	2.5642E+06	1.3735E-01	16:03	3.3118E+07		-42.61	0.22		-42.65	0.22		-0.36	0.21		Standard
d30Si_040915_Ki42_rad@2	2.37	3.2755E-02	1.4653E-02	7.2759E+07	1.1304E-01	2.3845E+06	1.0210E-01	16:06	3.0726E+07	3.1870E+07	-40.75	0.29	-40.92	-40.79	0.29		1.59	0.23		Ki42
d30Si_040915_Ki42_rad@3	2.37	3.2748E-02	1.2128E-02	7.3407E+07	1.4083E-01	2.4040E+06	1.3832E-01	16:10	3.0995E+07	1.7750E+06	-40.95	0.24	0.48	-40.99	0.24		1.38	0.21		Ki42
d30Si_040915_Ki42_rad@4	2.37	3.2748E-02	9.4508E-03	7.6768E+07	1.5635E-01	2.5157E+06	1.4288E-01	16:13	3.2390E+07		-40.96	0.19		-41.00	0.19		1.37	0.20		Ki42
d30Si_040915_Ki42_rad@5	2.37	3.2728E-02	1.0159E-02	7.8410E+07	1.4340E-01	2.5684E+06	1.2855E-01	16:16	3.3094E+07		-41.54	0.20		-41.58	0.20		0.76	0.20		Ki42
d30Si_040915_Ki42_rad@6	2.37	3.2748E-02	1.2327E-02	7.7803E+07	1.4448E-01	2.5496E+06	1.3323E-01	16:20	3.2843E+07		-40.95	0.25		-40.99	0.25		1.38	0.21		Ki42
d30Si_040915_Ki42_rad@7	2.37	3.2754E-02	1.2484E-02	7.4738E+07	1.5139E-01	2.4478E+06	1.4943E-01	16:23	3.1534E+07		-40.78	0.25		-40.81	0.25		1.56	0.21		Ki42
d30Si_040915_Ki42_rad@8	2.37	3.2754E-02	1.7647E-02	7.5432E+07	8.3375E-02	2.4708E+06	7.7791E-02	16:26	3.1834E+07		-40.79	0.35		-40.82	0.35		1.56	0.25		Ki42
d30Si_040915_Ki42_rad@9	2.37	3.2757E-02	1.0388E-02	7.6180E+07	1.0354E-01	2.4955E+06	9.7220E-02	16:30	3.2121E+07		-40.68	0.21		-40.71	0.21		1.67	0.20		Ki42
d30Si_040915_Ki42_rad@10	2.37	3.2747E-02	1.1595E-02	7.7232E+07	1.0593E-01	2.5293E+06	9.9794E-02	16:33	3.2573E+07		-40.97	0.23		-41.00	0.23		1.36	0.21		Ki42
d30Si_040915_Ki8C_rad@1	2.37	3.2712E-02	1.1604E-02	7.7547E+07	1.5599E-01	2.5386E+06	1.4424E-01	16:36	3.2724E+07		-42.02	0.23		-42.05	0.23		0.27	0.21		Ki08C
d30Si_040915_BR7_Paine@13	2.37	3.2700E-02	1.3691E-02	8.0261E+07	1.2938E-01	2.6245E+06	1.3295E-01	16:40	3.3839E+07	3.3527E+07	-42.37	0.27	-42.36	-42.40	0.27	-42.39	-0.09	0.22	-0.08	Standard
d30Si_040915_BR7_Paine@14	2.37	3.2702E-02	8.3553E-03	7.8908E+07	1.3886E-01	2.5803E+06	1.3841E-01	16:43	3.3280E+07	7.2116E+05	-42.32	0.17	0.18	-42.34	0.17	0.16	-0.03	0.19	0.16	Standard
d30Si_040915_BR7_Paine@15	2.37	3.2703E-02	7.6391E-03	8.0293E+07	1.3009E-01	2.6259E+06	1.2846E-01	16:46	3.3832E+07		-42.28	0.15		-42.30	0.15		0.01	0.19		Standard
d30Si_040915_BR7_Paine@16	2.37	3.2696E-02	1.2995E-02	7.8639E+07	1.4622E-01	2.5714E+06	1.4354E-01	16:50	3.3155E+07		-42.49	0.26		-42.51	0.26		-0.21	0.22		Standard
d30Si_040915_Ki8C_rad@2	2.39	3.2707E-02	1.0117E-02	7.9204E+07	1.3837E-01	2.5904E+06	1.4382E-01	16:53	3.3126E+07	3.3048E+07	-42.15	0.20	-42.48	-42.17	0.20		0.15	0.20		Ki08C
d30Si_040915_Ki8C_rad@3	2.38	3.2702E-02	1.1450E-02	7.8792E+07	9.7952E-02	2.5765E+06	9.7218E-02	16:56	3.3103E+07	5.9433E+05	-42.31	0.23	0.60	-42.34	0.23		-0.03	0.21		Ki08C
d30Si_040915_Ki8C_rad@4	2.38	3.2702E-02	9.7923E-03	7.8952E+07	1.5730E-01	2.5821E+06	1.5384E-01	17:00	3.3200E+07		-42.29	0.20		-42.31	0.20		0.00	0.20		Ki08C
d30Si_040915_Ki8C_rad@5	2.38	3.2680E-02	9.0114E-03	7.8552E+07	1.4236E-01	2.5691E+06	1.3202E-01	17:03	3.3033E+07		-42.95	0.18		-42.97	0.18		-0.69	0.20		Ki08C
d30Si_040915_Ki8C_rad@6	2.38	3.2697E-02	1.3315E-02	7.9130E+07	1.4645E-01	2.5894E+06	1.3265E-01	17:06	3.3272E+07		-42.45	0.27		-42.47	0.27		-0.17	0.22		Ki08C
d30Si_040915_Ki8C_rad@7	2.38	3.2691E-02	1.3943E-02	7.9173E+07	1.3667E-01	2.5883E+06	1.3841E-01	17:09	3.3306E+07		-42.62	0.28		-42.64	0.28		-0.34	0.22		Ki08C
d30Si_040915_Ki8C_rad@8	2.38	3.2695E-02	1.5903E-02	7.7481E+07	1.4995E-01	2.5332E+06	1.4558E-01	17:13	3.2583E+07		-42.50	0.32		-42.52	0.32		-0.21	0.24		Ki08C
d30Si_040915_Ki8C_rad@9	2.38	3.2693E-02	1.2909E-02	7.7631E+07	1.5343E-01	2.5382E+06	1.5118E-01	17:16	3.2665E+07		-42.57	0.26		-42.59	0.26		-0.29	0.22		Ki08C
d30Si_040915_Ki8C_rad@10	2.38	3.2681E-02	9.9828E-03	7.9547E+07	1.3007E-01	2.5997E+06	1.2859E-01	17:19	3.3470E+07		-42.91	0.20		-42.92	0.20		-0.64	0.20		Ki08C
d30Si_040915_Ki4c_rad@1	2.38	3.2683E-02	1.0581E-02	7.8571E+07	1.4618E-01	2.5697E+06	1.2978E-01	17:23	3.3075E+07		-42.85	0.21		-42.86	0.21		-0.57	0.20		Ki04C
d30Si_040915_BR7_Paine@17	2.37	3.2698E-02	1.1616E-02	7.9776E+07	1.5064E-01	2.6085E+06	1.5216E-01	17:26	3.3599E+07	3.3439E+07	-42.41	0.23	-42.49	-42.42	0.23	-42.50	-0.11	0.21	-0.20	Standard
d30Si_040915_BR7_Paine@18	2.38	3.2700E-02	9.2503E-03	7.8698E+07	1.3669E-01	2.5735E+06	1.3640E-01	17:29	3.3105E+07	5.6407E+05	-42.37	0.19	0.29	-42.37	0.19	0.25	-0.07	0.20	0.26	Standard
d30Si_040915_BR7_Paine@19	2.38	3.2689E-02	1.2761E-02	8.0168E+07	1.2207E-01	2.6208E+06	1.2007E-01	17:33	3.3733E+07		-42.70	0.26		-42.70	0.26		-0.41	0.22		Standard
d30Si_040915_BR7_Paine@20	2.38	3.2696E-02	8.3351E-03	7.9140E+07	1.1313E-01	2.5875E+06	1.1307E-01	17:36	3.3318E+07		-42.49	0.17		-42.50	0.17		-0.20	0.19		Standard

Table A2 Continued.

SIMS ANALYSES						Mount: BR7			Standard: UNIL-Q1 (Paine)		Analyse: δ^{30}Si			Value= -0.13±0.02 (NBS-28, 2σ)						Date: 03.09.2015
	Beam	H'2/L'2 (30Si/28Si)		L'2 (30Si/Coeff)		H'2 (28Si/Coeff)		Time	Yield	mean	Measurements		mean	Drift correction			Calibration			Comment
	nA	*CPS*	*2SD*	*CPS*	*2SD*	*CPS*	*2SD*		CPS/nA	*2SD*	$\delta^{30}Si$	*2SD int*	*2SD*	$\delta^{30}Si$	*2SD*		$\delta^{30}Si_{NBS-28}$	*2SD*		
d30Si_040915_Ki4c_rad@2	2.37	3.2729E-02	1.2325E-02	7.6127E+07	1.9181E-01	2.4913E+06	1.8649E-01	17:39	3.2063E+07	3.2878E+07	-41.52	0.25	-42.56	-41.52	0.25		0.83	0.21		Ki04C
d30Si_040915_Ki4c_rad@3	2.37	3.2667E-02	1.0837E-02	7.8304E+07	1.3228E-01	2.5580E+06	1.2756E-01	17:43	3.2974E+07	6.9141E+05	-43.33	0.22	1.06	-43.33	0.22		-1.06	0.21		Ki04C
d30Si_040915_Ki4c_rad@4	2.37	3.2681E-02	1.3559E-02	7.8335E+07	1.4863E-01	2.5601E+06	1.4785E-01	17:46	3.3005E+07		-42.91	0.27		-42.91	0.27		-0.62	0.22		Ki04C
d30Si_040915_Ki4c_rad@5	2.37	3.2701E-02	1.3728E-02	7.8715E+07	1.3996E-01	2.5743E+06	1.3648E-01	17:49	3.3148E+07		-42.32	0.27		-42.32	0.27		-0.01	0.22		Ki04C
d30Si_040915_Ki4c_rad@6	2.37	3.2694E-02	9.7254E-03	7.9001E+07	1.4777E-01	2.5827E+06	1.4588E-01	17:53	3.3264E+07		-42.54	0.19		-42.54	0.19		-0.24	0.20		Ki04C
d30Si_040915_Ki4c_rad@7	2.38	3.2701E-02	1.0231E-02	7.7888E+07	1.5143E-01	2.5472E+06	1.5421E-01	17:56	3.2794E+07		-42.34	0.20		-42.33	0.20		-0.02	0.20		Ki04C
d30Si_040915_Ki4c_rad@8	2.38	3.2703E-02	1.2546E-02	7.7486E+07	1.7084E-01	2.5342E+06	1.6635E-01	17:59	3.2620E+07		-42.26	0.25		-42.26	0.25		0.05	0.21		Ki04C
d30Si_040915_Ki4c_rad@9	2.37	3.2701E-02	1.2891E-02	7.7773E+07	1.4372E-01	2.5436E+06	1.3778E-01	18:03	3.2766E+07		-42.32	0.26		-42.32	0.26		-0.01	0.22		Ki04C
d30Si_040915_Ki4c_rad@10	2.38	3.2672E-02	9.7734E-03	7.8574E+07	1.4518E-01	2.5670E+06	1.4134E-01	18:06	3.3075E+07		-43.18	0.20		-43.17	0.20		-0.90	0.20		Ki04C
d30Si_040915_Ki1R_rad@1	2.38	3.2722E-02	1.3647E-02	7.4896E+07	9.0437E-02	2.4499E+06	8.1294E-02	18:09	3.1531E+07		-41.71	0.27		-41.71	0.27		0.63	0.22		Ki01
d30Si_040915_BR7_Paine@21	2.37	3.2709E-02	1.0353E-02	7.8733E+07	1.4037E-01	2.5751E+06	1.3639E-01	18:13	3.3166E+07	3.3423E+07	-42.10	0.21	-42.33	-42.09	0.21	-42.32	0.23	0.20	-0.01	Standard
d30Si_040915_BR7_Paine@22	2.38	3.2703E-02	1.5345E-02	7.9892E+07	1.3314E-01	2.6127E+06	1.3371E-01	18:16	3.3631E+07	6.0414E+05	-42.28	0.31	0.39	-42.27	0.31	0.33	0.05	0.23	0.35	Standard
d30Si_040915_BR7_Paine@23	2.38	3.2699E-02	1.0750E-02	7.8776E+07	1.3540E-01	2.5759E+06	1.3198E-01	18:19	3.3162E+07		-42.39	0.22		-42.37	0.22		-0.07	0.20		Standard
d30Si_040915_BR7_Paine@24	2.38	3.2693E-02	9.0273E-03	8.0209E+07	1.2220E-01	2.6225E+06	1.2037E-01	18:23	3.3733E+07		-42.56	0.18		-42.55	0.18		-0.25	0.20		Standard
d30Si_040915_Ki1R_rad@2	2.38	3.2727E-02	6.6060E-03	7.1271E+07	8.3266E-02	2.3325E+06	7.9401E-02	18:26	3.0004E+07	3.2318E+07	-41.57	0.13	-42.03	-41.56	0.13		0.79	0.19		Ki01
d30Si_040915_Ki1R_rad@3	2.38	3.2725E-02	9.5079E-03	7.6277E+07	1.4698E-01	2.4963E+06	1.4784E-01	18:29	3.2094E+07	2.1061E+06	-41.64	0.19	0.90	-41.63	0.19		0.71	0.20		Ki01
d30Si_040915_Ki1R_rad@4	2.38	3.2716E-02	1.0750E-02	7.6057E+07	1.3781E-01	2.4881E+06	1.3567E-01	18:33	3.1998E+07		-41.90	0.22		-41.89	0.22		0.44	0.20		Ki01
d30Si_040915_Ki1R_rad@5	2.38	3.2692E-02	1.5202E-02	7.8438E+07	1.5438E-01	2.5664E+06	1.3945E-01	18:36	3.3025E+07		-42.59	0.30		-42.57	0.30		-0.27	0.23		Ki01
d30Si_040915_Ki1R_rad@6	2.38	3.2726E-02	1.0371E-02	7.5802E+07	1.6710E-01	2.4807E+06	1.6308E-01	18:39	3.1874E+07		-41.59	0.21		-41.57	0.21		0.77	0.20		Ki01
d30Si_040915_Ki1R_rad@7	2.38	3.2718E-02	9.4345E-03	7.8006E+07	8.1243E-02	2.5522E+06	8.3504E-02	18:43	3.2817E+07		-41.84	0.19		-41.82	0.19		0.51	0.20		Ki01
d30Si_040915_Ki1R_rad@8	2.38	3.2685E-02	8.1087E-03	7.9685E+07	1.2523E-01	2.6047E+06	1.2536E-01	18:46	3.3523E+07		-42.79	0.16		-42.77	0.16		-0.48	0.19		Ki01
d30Si_040915_Ki1R_rad@9	2.38	3.2705E-02	9.2173E-03	7.8350E+07	1.4268E-01	2.5623E+06	1.4096E-01	18:49	3.2982E+07		-42.21	0.18		-42.19	0.18		0.12	0.20		Ki01
d30Si_040915_Ki1R_rad@10	2.38	3.2696E-02	1.5368E-02	7.9151E+07	1.4851E-01	2.5900E+06	1.4061E-01	18:53	3.3326E+07		-42.47	0.31		-42.44	0.31		-0.14	0.23		Ki01
d30Si_040915_Ki32_rad@1	2.38	3.2746E-02	9.9746E-03	7.6427E+07	1.5956E-01	2.5029E+06	1.5584E-01	18:56	3.2177E+07		-41.03	0.20		-41.00	0.20		1.37	0.20		Ki32
d30Si_040915_BR7_Paine@25	2.37	3.2705E-02	1.0661E-02	8.0291E+07	1.4897E-01	2.6256E+06	1.4693E-01	18:59	3.3811E+07	3.3515E+07	-42.22	0.21	-42.34	-42.19	0.21	-42.32	0.12	0.20	0.00	Standard
d30Si_040915_BR7_Paine@26	2.38	3.2698E-02	1.1091E-02	7.8955E+07	1.4315E-01	2.5815E+06	1.4135E-01	19:03	3.3211E+07	5.7907E+05	-42.42	0.22	0.21	-42.39	0.22	0.18	-0.08	0.21	0.19	Standard
d30Si_040915_BR7_Paine@27	2.38	3.2697E-02	1.2416E-02	8.0114E+07	1.3865E-01	2.6211E+06	1.2694E-01	19:06	3.3707E+07		-42.44	0.25		-42.41	0.25		-0.11	0.21		Standard
d30Si_040915_BR7_Paine@28	2.38	3.2702E-02	1.3578E-02	7.9193E+07	1.4346E-01	2.5915E+06	1.3255E-01	19:09	3.3331E+07		-42.30	0.27		-42.27	0.27		0.04	0.22		Standard
d30Si_040915_Ki32_rad@2	2.38	3.2763E-02	1.4155E-02	7.2852E+07	8.8968E-02	2.3856E+06	8.0526E-02	19:13	3.0657E+07	3.0895E+07	-40.50	0.28	-40.46	-40.47	0.28		1.92	0.23		Ki32
d30Si_040915_Ki32_rad@3	2.38	3.2758E-02	8.1320E-03	7.4174E+07	1.8626E-01	2.4297E+06	1.8332E-01	19:16	3.1221E+07	1.9450E+06	-40.67	0.16	0.75	-40.64	0.16		1.74	0.19		Ki32
d30Si_040915_Ki32_rad@4	2.38	3.2767E-02	1.2007E-02	7.4106E+07	1.9446E-01	2.4280E+06	1.9182E-01	19:19	3.1175E+07		-40.41	0.24		-40.38	0.24		2.02	0.21		Ki32
d30Si_040915_Ki32_rad@5	2.38	3.2760E-02	9.4522E-03	7.1487E+07	1.8862E-01	2.3420E+06	1.8708E-01	19:23	3.0072E+07		-40.60	0.19		-40.57	0.19		1.82	0.20		Ki32
d30Si_040915_Ki32_rad@6	2.38	3.2772E-02	1.6343E-02	7.1276E+07	2.0414E-01	2.3359E+06	1.9883E-01	19:26	2.9999E+07		-40.25	0.33		-40.21	0.33		2.19	0.24		Ki32
d30Si_040915_Ki32_rad@7	2.38	3.2774E-02	1.1828E-02	6.9365E+07	2.1179E-01	2.2734E+06	2.0952E-01	19:29	2.9184E+07		-40.19	0.24		-40.15	0.24		2.25	0.21		Ki32
d30Si_040915_Ki32_rad@8	2.38	3.2793E-02	1.1851E-02	7.2993E+07	2.2250E-01	2.3937E+06	2.2439E-01	19:33	3.0718E+07		-39.63	0.24		-39.59	0.24		2.84	0.21		Ki32
d30Si_040915_Ki32_rad@9	2.38	3.2757E-02	1.1189E-02	7.4943E+07	1.0623E-01	2.4551E+06	1.0541E-01	19:36	3.1515E+07		-40.69	0.22		-40.65	0.22		1.73	0.21		Ki32
d30Si_040915_Ki32_rad@10	2.38	3.2761E-02	1.0789E-02	7.6603E+07	1.6177E-01	2.5097E+06	1.5683E-01	19:39	3.2237E+07		-40.58	0.22		-40.53	0.22		1.86	0.21		Ki32
d30Si_040915_BR7_Paine@29	2.38	3.2699E-02	1.0052E-02	7.8953E+07	1.2690E-01	2.5832E+06	1.1595E-01	19:46	3.3243E+07	3.3342E+07	-42.39	0.20	-42.44	-42.34	0.20	-42.39	-0.03	0.20	-0.09	Standard
d30Si_040915_BR7_Paine@30	2.38	3.2705E-02	1.0667E-02	8.0284E+07	1.3436E-01	2.6270E+06	1.2416E-01	19:49	3.3775E+07	7.9618E+05	-42.21	0.21	0.36	-42.16	0.21	0.31	0.16	0.20	0.32	Standard
d30Si_040915_BR7_Paine@31	2.38	3.2692E-02	1.1636E-02	7.9674E+07	1.5080E-01	2.6064E+06	1.3727E-01	19:53	3.3509E+07		-42.58	0.23		-42.54	0.23		-0.24	0.21		Standard
d30Si_040915_BR7_Paine@32	2.38	3.2693E-02	1.4567E-02	7.8079E+07	1.4935E-01	2.5544E+06	1.3539E-01	19:56	3.2842E+07		-42.58	0.29		-42.53	0.29		-0.23	0.23		Standard
d30Si_040915_Ki34S_rad@1	2.38	3.2718E-02	1.4395E-02	7.2962E+07	3.7414E-01	2.3870E+06	3.7193E-01	20:29	3.0681E+07		-41.82	0.29		-41.76	0.29		0.58	0.23		Ki34
d30Si_040915_BR7_Paine@33	2.38	3.2699E-02	1.1880E-02	7.9544E+07	1.5090E-01	2.6009E+06	1.4877E-01	20:33	3.3431E+07	3.3038E+07	-42.38	0.24	-42.43	-42.32	0.24	-42.36	-0.01	0.21	-0.06	Standard
d30Si_040915_BR7_Paine@34	2.38	3.2697E-02	1.1580E-02	7.7549E+07	1.5769E-01	2.5358E+06	1.5553E-01	20:36	3.2582E+07	1.7158E+06	-42.45	0.23	0.07	-42.39	0.23	0.06	-0.08	0.21	0.06	Standard
d30Si_040915_BR7_Paine@35	2.38	3.2697E-02	1.0881E-02	8.0952E+07	1.1373E-01	2.6487E+06	1.0839E-01	20:39	3.4029E+07		-42.45	0.22		-42.39	0.22		-0.08	0.21		Standard
d30Si_040915_BR7_Paine@36	2.38	3.2698E-02	1.4187E-02	7.6419E+07	1.8788E-01	2.4985E+06	1.8414E-01	20:43	3.2109E+07		-42.43	0.28		-42.36	0.28		-0.05	0.22		Standard
d30Si_040915_Ki34S_rad@2	2.38	3.2740E-02	1.0332E-02	7.8865E+07	1.3088E-01	2.5821E+06	1.3295E-01	20:46	3.3192E+07	3.3004E+07	-41.18	0.21	-41.40	-41.12	0.21		1.25	0.20		Ki34
d30Si_040915_Ki34S_rad@3	2.38	3.2742E-02	1.2278E-02	7.9581E+07	1.4501E-01	2.6054E+06	1.4147E-01	20:49	3.3440E+07	1.8242E+06	-41.13	0.25	0.53	-41.06	0.25		1.30	0.21		Ki34
d30Si_040915_Ki34S_rad@4	2.38	3.2727E-02	1.3991E-02	7.7557E+07	1.5705E-01	2.5402E+06	1.4536E-01	20:53	3.2598E+07		-41.56	0.28		-41.49	0.28		0.85	0.22		Ki34
d30Si_040915_Ki34S_rad@5	2.38	3.2738E-02	1.1103E-02	7.9996E+07	1.3153E-01	2.6190E+06	1.2928E-01	20:56	3.3603E+07		-41.25	0.22		-41.18	0.22		1.18	0.21		Ki34
d30Si_040915_Ki34S_rad@6	2.38	3.2732E-02	1.3780E-02	7.8167E+07	1.6674E-01	2.5587E+06	1.6541E-01	20:59	3.2824E+07		-41.44	0.28		-41.37	0.28		0.99	0.22		Ki34
d30Si_040915_Ki34S_rad@7	2.38	3.2738E-02	1.1524E-02	7.9965E+07	1.7029E-01	2.6177E+06	1.6526E-01	21:03	3.3614E+07		-41.24	0.23		-41.17	0.23		1.19	0.21		Ki34
d30Si_040915_Ki34S_rad@8	2.38	3.2744E-02	1.0931E-02	7.8033E+07	1.4801E-01	2.5567E+06	1.3571E-01	21:06	3.2790E+07		-41.08	0.22		-41.01	0.22		1.36	0.21		Ki34
d30Si_040915_Ki34S_rad@9	2.38	3.2719E-02	1.2330E-02	8.0386E+07	1.5851E-01	2.6299E+06	1.5703E-01	21:09	3.3815E+07		-41.81	0.25		-41.73	0.25		0.60	0.21		Ki34
d30Si_040915_Ki34S_rad@10	2.38	3.2731E-02	1.4680E-02	7.9626E+07	1.6714E-01	2.6061E+06	1.6125E-01	21:13	3.3488E+07		-41.44	0.29		-41.36	0.29		0.99	0.23		Ki34
d30Si_040915_BR7_Paine@37	2.37	3.2695E-02	1.4404E-02	7.5378E+07	2.1280E-01	2.4668E+06	1.9983E-01	21:16	3.1741E+07	3.4492E+07	-42.51	0.29	-42.71	-42.43	0.29	-42.63	-0.12	0.23	-0.34	Standard
d30Si_040915_BR7_Paine@38	2.38	3.2695E-02	9.7545E-03	8.2600E+07	1.0324E-01	2.7006E+06	9.9784E-02	21:19	3.4748E+07	4.3771E+06	-42.50	0.20	0.50	-42.42	0.20	0.43	-0.12	0.20	0.45	Standard
d30Si_040915_BR7_Paine@39	2.38	3.2683E-02	1.2191E-02	8.1758E+07	2.0009E-01	2.6719E+06	1.9608E-01	21:23	3.4393E+07		-42.85	0.24		-42.77	0.24		-0.48	0.21		Standard
d30Si_040915_BR7_Paine@40	2.38	3.2678E-02	1.0592E-02	8.8088E+07	1.4745E-01	2.8764E+06	1.6072E-01	21:26	3.7085E+07		-43.00	0.21		-42.92	0.21		-0.63	0.20		Standard

Table A2 Continued.

	SIMS ANALYSES						Mount: BR1		Standard: UNIL-Q1 (Paine)		Analyse: δ^{30}Si			Value= -0.13±0.02 (NBS-28, 2σ)						Date: 03.09.2015
	Beam	H'2/L'2 (30Si/28Si)		L'2 (30Si/Coeff)		H'2 (28Si/Coeff)		Time	Yield	mean	Measurements		mean	Drift correction			Calibration			Comment
	nA	*CPS*	*2SD*	*CPS*	*2SD*	*CPS*	*2SD*		CPS/nA	*2SD*	$\delta^{30}Si$	*2SD int*	*2SD*	$\delta^{30}Si$	*2SD*		$\delta^{30}Si_{NBS-28}$	*2SD*		
d30Si_030316_Paine@1	2.41	3.2711E-02	1.0759E-02	8.9319E+07	1.0787E-01	2.9214E+06	1.0921E-01	9:33	3.7112E+07	3.7091E+07	-42.03	0.22	-41.96							Setting: Standard
d30Si_030316_Paine@2	2.41	3.2713E-02	1.0975E-02	8.9839E+07	9.2660E-02	2.9392E+06	9.2405E-02	9:37	3.7203E+07	1.3945E+05	-41.97	0.22	0.16							Setting: Standard
d30Si_030316_Paine@3	2.42	3.2713E-02	1.3642E-02	8.9735E+07	8.8443E-02	2.9358E+06	9.1665E-02	9:40	3.7140E+07		-41.97	0.27								Setting: Standard
d30Si_030316_Paine@4	2.42	3.2715E-02	1.6678E-02	8.9320E+07	8.2644E-02	2.9218E+06	9.3164E-02	9:43	3.6965E+07		-41.91	0.33								Setting: Standard
d30Si_030316_Paine@5	2.41	3.2715E-02	2.0306E-02	8.9446E+07	9.7514E-02	2.9263E+06	1.0197E-01	9:46	3.7068E+07		-41.94	0.41								Setting: Standard
d30Si_030316_Paine@6	2.42	3.2718E-02	1.5530E-02	8.9677E+07	9.6322E-02	2.9346E+06	1.0047E-01	9:50	3.7077E+07		-41.82	0.31								Setting: Standard
d30Si_030316_Paine@7	2.42	3.2709E-02	2.0341E-02	8.9911E+07	9.0500E-02	2.9411E+06	9.6693E-02	9:53	3.7110E+07		-42.09	0.41								Setting: Standard
d30Si_030316_Paine@8	2.42	3.2714E-02	1.0389E-02	8.9782E+07	9.1614E-02	2.9380E+06	9.6711E-02	9:56	3.7050E+07		-41.94	0.21								Setting: Standard
d30Si_030316_Paine1@1	2.39	3.2737E-02	2.4704E-02	8.7680E+07	1.4409E-01	2.8709E+06	1.4169E-01	10:47	3.6690E+07	3.6679E+07	-41.29	0.49	-41.50			-41.71			-0.08	Standard internal variation
d30Si_030316_Paine1@02	2.40	3.2725E-02	1.2921E-02	8.7934E+07	1.3623E-01	2.8785E+06	1.3639E-01	10:51	3.6678E+07	9.3305E+04	-41.63	0.26	0.39	-41.76	0.26	0.27	-0.13	0.18	0.28	Standard
d30Si_030316_Paine1@03	2.41	3.2733E-02	1.5435E-02	8.8164E+07	1.1103E-01	2.8859E+06	1.1988E-01	10:54	3.6617E+07		-41.39	0.31		-41.52	0.31		0.11	0.20		Standard
d30Si_030316_Paine1@04	2.41	3.2722E-02	1.2299E-02	8.8485E+07	1.1525E-01	2.8957E+06	1.1686E-01	10:57	3.6730E+07		-41.71	0.25		-41.84	0.25		-0.21	0.18		Standard
d30Si_030316_KI10@1	2.40	3.2717E-02	1.3073E-02	8.7666E+07	1.2726E-01	2.8685E+06	1.2708E-01	11:00	3.6459E+07	3.6069E+07	-41.87	0.26	-41.71	-41.99	0.26		-0.38	0.18		Ki10
d30Si_030316_KI10@2	2.41	3.2715E-02	1.2622E-02	8.7628E+07	1.1817E-01	2.8670E+06	1.2151E-01	11:04	3.6379E+07	1.5050E+06	-41.91	0.25	0.60	-42.03	0.25		-0.42	0.18		Ki10
d30Si_030316_KI10@3	2.41	3.2728E-02	1.2585E-02	8.7514E+07	1.2743E-01	2.8643E+06	1.2805E-01	11:07	3.6247E+07		-41.53	0.25		-41.65	0.25		-0.02	0.18		Ki10
d30Si_030316_KI10@4	2.42	3.2712E-02	1.4220E-02	8.8558E+07	9.9412E-02	2.8971E+06	1.0848E-01	11:10	3.6538E+07		-42.02	0.28		-42.13	0.28		-0.52	0.19		Ki10
d30Si_030316_KI10@5	2.42	3.2740E-02	2.0834E-02	8.3629E+07	1.2022E-01	2.7363E+06	1.3343E-01	11:13	3.4552E+07		-41.20	0.42		-41.31	0.42		0.34	0.24		Ki10
d30Si_030316_KI10@6	2.42	3.2722E-02	1.4942E-02	8.7734E+07	9.5698E-02	2.8703E+06	9.7849E-02	11:17	3.6238E+07		-41.72	0.30		-41.82	0.30		-0.20	0.20		Ki10
d30Si_030316_KI5C@1	2.42	3.2725E-02	2.4343E-02	8.8286E+07	9.8969E-02	2.8898E+06	1.0265E-01	11:20	3.6409E+07	3.6454E+07	-41.62	0.49	-41.77	-41.72	0.49		-0.09	0.27		Ki05C
d30Si_030316_KI5C@2	2.43	3.2716E-02	1.5099E-02	8.8658E+07	8.9288E-02	2.9010E+06	9.8341E-02	11:23	3.6538E+07	2.3928E+05	-41.89	0.30	0.37	-41.99	0.30		-0.37	0.20		Ki05C
d30Si_030316_KI5C@3	2.42	3.2713E-02	1.2623E-02	8.8169E+07	1.0078E-01	2.8844E+06	1.0301E-01	11:26	3.6405E+07		-41.98	0.25		-42.07	0.25		-0.46	0.18		Ki05C
d30Si_030316_KI5C@4	2.42	3.2729E-02	1.2654E-02	8.7773E+07	1.0371E-01	2.8725E+06	1.0607E-01	11:30	3.6265E+07		-41.53	0.25		-41.62	0.25		0.01	0.18		Ki05C
d30Si_030316_KI5C@5	2.42	3.2715E-02	1.1420E-02	8.8240E+07	9.8707E-02	2.8869E+06	9.9694E-02	11:33	3.6511E+07		-41.92	0.23		-42.01	0.23		-0.39	0.17		Ki05C
d30Si_030316_KI5C@6	2.42	3.2723E-02	1.6568E-02	8.8408E+07	1.0311E-01	2.8930E+06	1.0044E-01	11:36	3.6599E+07		-41.68	0.33		-41.76	0.33		-0.14	0.21		Ki05C
d30Si_030316_Paine1@05	2.51	3.2727E-02	2.2749E-02	8.9040E+07	1.1418E-01	2.9136E+06	1.2071E-01	11:39	3.5493E+07	3.6463E+07	-41.56	0.45	-41.73	-41.64	0.45	-41.81	-0.01	0.26	-0.18	Standard
d30Si_030316_Paine1@06	2.42	3.2713E-02	2.2219E-02	8.9003E+07	1.2129E-01	2.9116E+06	1.2608E-01	11:43	3.6782E+07	1.2978E+06	-41.97	0.44	0.35	-42.05	0.44	0.30	-0.43	0.26	0.31	Standard
d30Si_030316_Paine1@07	2.42	3.2723E-02	2.2491E-02	8.9000E+07	1.0947E-01	2.9125E+06	1.1177E-01	11:46	3.6721E+07		-41.68	0.45		-41.75	0.45		-0.13	0.26		Standard
d30Si_030316_Paine1@08	2.42	3.2722E-02	1.8381E-02	8.9223E+07	1.0292E-01	2.9197E+06	1.0827E-01	11:49	3.6856E+07		-41.72	0.37		-41.79	0.37		-0.16	0.22		Standard
d30Si_030316_KI27@1	2.42	3.2739E-02	1.2491E-02	8.6257E+07	9.2205E-02	2.8248E+06	9.9921E-02	11:52	3.5704E+07	3.5900E+07	-41.21	0.25	-41.12	-41.28	0.25		0.37	0.18		Ki27
d30Si_030316_KI27@2	2.41	3.2765E-02	1.1935E-02	8.4843E+07	9.0573E-02	2.7799E+06	9.6118E-02	11:56	3.5177E+07	1.4009E+06	-40.45	0.24	1.08	-40.52	0.24		1.16	0.17		Ki27
d30Si_030316_KI27@3	2.41	3.2758E-02	1.0698E-02	8.4489E+07	1.0628E-01	2.7681E+06	1.0827E-01	11:59	3.5044E+07		-40.65	0.21		-40.71	0.21		0.96	0.17		Ki27
d30Si_030316_KI27@4	2.42	3.2733E-02	9.3970E-03	8.8642E+07	9.4396E-02	2.9021E+06	9.9339E-02	12:02	3.6656E+07		-41.39	0.19		-41.45	0.19		0.19	0.16		Ki27
d30Si_030316_KI27@5	2.42	3.2714E-02	1.6537E-02	8.8413E+07	1.0798E-01	2.8933E+06	9.4731E-02	12:05	3.6594E+07		-41.96	0.33		-42.01	0.33		-0.39	0.21		Ki27
d30Si_030316_KI27@6	2.41	3.2745E-02	2.3863E-02	8.7409E+07	1.1510E-01	2.8623E+06	1.1974E-01	12:09	3.6226E+07		-41.05	0.48		-41.10	0.48		0.56	0.27		Ki27
d30Si_030316_Paine1@09	2.41	3.2723E-02	1.4878E-02	8.9375E+07	9.3278E-02	2.9244E+06	9.5865E-02	12:31	3.7053E+07	3.7010E+07	-41.68	0.30	-41.85	-41.70	0.30	-41.87	-0.07	0.20	-0.25	Standard
d30Si_030316_Paine1@10	2.41	3.2723E-02	9.7175E-03	8.9112E+07	8.3263E-02	2.9160E+06	8.3455E-02	12:35	3.6925E+07	1.7022E+05	-41.68	0.19	0.39	-41.70	0.19	0.33	-0.07	0.16	0.35	Standard
d30Si_030316_Paine1@11	2.41	3.2712E-02	2.0510E-02	8.8989E+07	9.0197E-02	2.9113E+06	9.1713E-02	12:38	3.6953E+07		-42.01	0.41		-42.03	0.41		-0.42	0.24		Standard
d30Si_030316_Paine1@12	2.41	3.2712E-02	2.4919E-02	8.9316E+07	1.0257E-01	2.9223E+06	1.0884E-01	12:41	3.7107E+07		-42.02	0.50		-42.03	0.50		-0.42	0.28		Standard
d30Si_030316_KI54@1	2.41	3.2721E-02	1.1635E-02	8.9080E+07	1.3214E-01	2.9155E+06	1.3217E-01	12:45	3.6955E+07	3.6623E+07	-41.74	0.23	-41.60	-41.75	0.23		-0.12	0.17		Ki54
d30Si_030316_KI54@2	2.41	3.2730E-02	1.6300E-02	8.8868E+07	1.1907E-01	2.9080E+06	1.2089E-01	12:48	3.6843E+07	1.0533E+06	-41.48	0.33	0.91	-41.49	0.33		0.15	0.21		Ki54
d30Si_030316_KI54@3	2.41	3.2703E-02	1.2153E-02	8.8962E+07	1.2166E-01	2.9094E+06	1.2365E-01	12:51	3.6853E+07		-42.27	0.24		-42.27	0.24		-0.67	0.18		Ki54
d30Si_030316_KI54@4	2.41	3.2750E-02	1.0544E-02	8.5753E+07	1.1821E-01	2.8084E+06	1.1738E-01	12:54	3.5584E+07		-40.91	0.21		-40.91	0.21		0.75	0.16		Ki54
d30Si_030316_KI54@5	2.40	3.2733E-02	1.3503E-02	8.7922E+07	1.3833E-01	2.8781E+06	1.4030E-01	12:57	3.6573E+07		-41.39	0.27		-41.39	0.27		0.25	0.19		Ki54
d30Si_030316_KI54@6	2.40	3.2720E-02	8.5859E-03	8.8770E+07	1.4404E-01	2.9045E+06	1.4309E-01	13:01	3.6928E+07		-41.79	0.17		-41.78	0.17		-0.16	0.15		Ki54
d30Si_030316_Paine1@13	2.41	3.2727E-02	1.2941E-02	8.9585E+07	6.1890E-02	2.9314E+06	6.4085E-02	13:24	3.7236E+07	3.7082E+07	-41.58	0.26	-41.77	-41.55	0.26	-41.73	0.08	0.18	-0.11	Standard
d30Si_030316_Paine1@14	2.41	3.2716E-02	1.3135E-02	8.9363E+07	1.0831E-01	2.9241E+06	1.1719E-01	13:27	3.7109E+07	2.5074E+05	-41.88	0.26	0.29	-41.85	0.26	0.25	-0.23	0.18	0.26	Standard
d30Si_030316_Paine1@15	2.41	3.2716E-02	1.7074E-02	8.9123E+07	9.0650E-02	2.9162E+06	9.4825E-02	13:30	3.6935E+07		-41.89	0.34		-41.85	0.34		-0.23	0.21		Standard
d30Si_030316_Paine1@16	2.41	3.2722E-02	1.9889E-02	8.9360E+07	8.8332E-02	2.9246E+06	9.1550E-02	13:33	3.7050E+07		-41.73	0.40		-41.69	0.40		-0.06	0.24		Standard
d30Si_030316_Paine1@17	2.41	3.2717E-02	2.0220E-02	8.9435E+07	9.7479E-02	2.9261E+06	9.9900E-02	14:06	3.7148E+07	3.7218E+07	-41.86	0.40	-41.85	-41.78	0.40	-41.77	-0.16	0.24	-0.15	Standard
d30Si_030316_Paine1@18	2.41	3.2714E-02	1.0900E-02	8.9699E+07	8.5840E-02	2.9343E+06	8.7235E-02	14:09	3.7229E+07	9.8011E+04	-41.95	0.22	0.21	-41.87	0.22	0.18	-0.25	0.17	0.19	Standard
d30Si_030316_Paine1@19	2.41	3.2722E-02	1.6915E-02	8.9744E+07	1.0809E-01	2.9369E+06	1.1677E-01	14:13	3.7263E+07		-41.71	0.34		-41.62	0.34		0.01	0.21		Standard
d30Si_030316_Paine1@20	2.41	3.2716E-02	1.1862E-02	8.9669E+07	8.8921E-02	2.9336E+06	9.5004E-02	14:16	3.7231E+07		-41.90	0.24		-41.81	0.24		-0.19	0.17		Standard
d30Si_030316_Paine1@21	2.39	3.2721E-02	1.0923E-02	8.9023E+07	8.3748E-02	2.9129E+06	8.6352E-02	14:48	3.7243E+07	3.7281E+07	-41.76	0.22	-41.84	-41.63	0.22	-41.71	0.00	0.17	-0.08	Standard
d30Si_030316_Paine1@22	2.39	3.2716E-02	1.1678E-02	8.9116E+07	9.3004E-02	2.9160E+06	9.4926E-02	14:52	3.7296E+07	1.0114E+05	-41.89	0.23	0.21	-41.76	0.23	0.18	-0.14	0.17	0.19	Standard
d30Si_030316_Paine1@23	2.39	3.2714E-02	8.4705E-03	8.9145E+07	1.0339E-01	2.9162E+06	1.0703E-01	14:55	3.7346E+07		-41.96	0.17		-41.83	0.17		-0.20	0.15		Standard
d30Si_030316_Paine1@24	2.39	3.2721E-02	1.4403E-02	8.9111E+07	8.4870E-02	2.9159E+06	9.3423E-02	14:58	3.7238E+07		-41.74	0.29		-41.61	0.29		0.03	0.19		Standard

Table A2 Continued.

	SIMS ANALYSES							Mount: BR5	Standard: UNIL-Q1 (Paine)		Analyse: δ^{30}Si			Value= -0.13±0.02 (NBS-28, 2σ)						Date: 03.09.2015
	Beam	H'2/L'2 (30Si/28Si)		L'2 (30Si/Coeff)		H'2 (28Si/Coeff)		Time	Yield	mean	Measurements		mean	Drift correction		Calibration				Comment
	nA	CPS	2SD	CPS	2SD	CPS	2SD		CPS/nA	2SD	$\delta^{30}Si$	2SD int	2SD	$\delta^{30}Si$	2SD		$\delta^{30}Si_{NBS-28}$	2SD		
d30Si_030316_PaineBR5@1	2.39	3.2730E-02	1.2599E-02	8.9573E+07	1.0093E-01	2.9319E+06	1.0717E-01	16:17	3.7465E+07	3.7413E+07	-41.50	0.25	-41.84	-41.50	0.25	-41.85	0.18	0.23	-0.18	Setting: Standard
d30Si_030316_PaineBR5@02	2.39	3.2721E-02	1.0458E-02	8.9823E+07	1.0913E-01	2.9390E+06	1.0732E-01	16:21	3.7539E+07	2.3644E+05	-41.76	0.21	0.40	-41.76	0.21	0.37	-0.09	0.22	0.39	Setting: Standard
d30Si_030316_PaineBR5@03	2.39	3.2725E-02	1.2325E-02	8.9977E+07	1.0489E-01	2.9438E+06	1.0862E-01	16:24	3.7605E+07		-41.62	0.25		-41.63	0.25		0.05	0.23		Setting: Standard
d30Si_030316_PaineBR5@04	2.39	3.2711E-02	2.1218E-02	8.9126E+07	9.7604E-02	2.9159E+06	9.8091E-02	16:27	3.7230E+07		-42.03	0.42		-42.04	0.42		-0.38	0.29		Setting: Standard
d30Si_030316_PaineBR5@05	2.39	3.2716E-02	2.1827E-02	8.9233E+07	1.1680E-01	2.9191E+06	1.1611E-01	16:30	3.7355E+07		-41.90	0.44		-41.91	0.44		-0.24	0.29		Setting: Standard
d30Si_030316_PaineBR5@06	2.40	3.2712E-02	1.3882E-02	8.9614E+07	9.7443E-02	2.9324E+06	1.0325E-01	16:34	3.7386E+07		-42.02	0.28		-42.03	0.28		-0.37	0.24		Setting: Standard
d30Si_030316_PaineBR5@07	2.40	3.2715E-02	1.4699E-02	8.9665E+07	9.7678E-02	2.9335E+06	9.8519E-02	16:37	3.7371E+07		-41.92	0.29		-41.93	0.29		-0.26	0.24		Setting: Standard
d30Si_030316_PaineBR5@08	2.40	3.2712E-02	9.9247E-03	8.9736E+07	1.1275E-01	2.9354E+06	1.1201E-01	16:40	3.7355E+07		-42.00	0.20		-42.01	0.20		-0.34	0.22		Setting: Standard
d30Si_030316_PaineBR5@09	2.40	3.2722E-02	1.1383E-02	8.9731E+07	9.3143E-02	2.9363E+06	9.5543E-02	17:32	3.7343E+07	3.7437E+07	-41.72	0.23	-41.79	-41.73	0.23	-41.79	-0.06	0.22	-0.12	Standard
d30Si_030316_PaineBR5@10	2.40	3.2707E-02	1.6588E-02	9.0586E+07	1.0616E-01	2.9632E+06	1.0919E-01	17:35	3.7812E+07	5.0357E+05	-42.15	0.33	0.49	-42.15	0.33	0.42	-0.50	0.25	0.44	Standard
d30Si_030316_PaineBR5@11	2.39	3.2726E-02	1.1308E-02	8.9312E+07	8.5992E-02	2.9228E+06	8.8626E-02	17:39	3.7316E+07		-41.60	0.23		-41.60	0.23		0.08	0.22		Standard
d30Si_030316_PaineBR5@12	2.39	3.2723E-02	1.1822E-02	8.8908E+07	9.9542E-02	2.9094E+06	1.0273E-01	17:42	3.7276E+07		-41.68	0.24		-41.69	0.24		-0.01	0.23		Standard
d30Si_030316_KI38@1	2.38	3.2767E-02	9.6572E-03	8.7401E+07	1.1483E-01	2.8638E+06	1.1743E-01	17:45	3.6678E+07	3.6738E+07	-40.40	0.19	-41.03	-40.40	0.19		1.33	0.22		Ki38
d30Si_030316_KI38@2	2.39	3.2745E-02	1.6468E-02	8.8321E+07	1.0313E-01	2.8895E+06	1.1617E-01	17:48	3.7001E+07	4.6645E+05	-41.04	0.33	0.69	-41.04	0.33		0.66	0.25		Ki38
d30Si_030316_KI38@3	2.39	3.2749E-02	1.6855E-02	8.7888E+07	1.2609E-01	2.8783E+06	1.2716E-01	17:52	3.6789E+07		-40.92	0.34		-40.93	0.34		0.78	0.26		Ki38
d30Si_030316_KI38@4	2.39	3.2759E-02	1.4869E-02	8.6769E+07	9.4572E-02	2.8429E+06	9.8309E-02	17:55	3.6235E+07		-40.63	0.30		-40.64	0.30		1.08	0.24		Ki38
d30Si_030316_KI38@5	2.40	3.2742E-02	1.5259E-02	8.7890E+07	9.5538E-02	2.8782E+06	1.0338E-01	17:58	3.6660E+07		-41.12	0.31		-41.13	0.31		0.57	0.25		Ki38
d30Si_030316_KI38@6	2.39	3.2743E-02	8.3122E-03	8.8221E+07	1.2460E-01	2.8887E+06	1.2989E-01	18:01	3.6855E+07		-41.12	0.17		-41.12	0.17		0.58	0.21		Ki38
d30Si_030316_KI38@7	2.39	3.2746E-02	1.2357E-02	8.7202E+07	1.1260E-01	2.8553E+06	1.1156E-01	18:05	3.6523E+07		-41.02	0.25		-41.02	0.25		0.69	0.23		Ki38
d30Si_030316_KI38@8	2.39	3.2738E-02	1.0977E-02	8.8044E+07	1.1828E-01	2.8824E+06	1.2185E-01	18:08	3.6892E+07		-41.26	0.22		-41.26	0.22		0.43	0.22		Ki38
d30Si_030316_KI38@9	2.39	3.2723E-02	1.8451E-02	8.8567E+07	1.0884E-01	2.8986E+06	1.1093E-01	18:11	3.7007E+07		-41.68	0.37		-41.69	0.37		-0.01	0.27		Ki38
d30Si_030316_KI38@10	2.40	3.2742E-02	1.8200E-02	8.8034E+07	1.0554E-01	2.8807E+06	1.1634E-01	18:14	3.6744E+07		-41.13	0.36		-41.13	0.36		0.57	0.27		Ki38
d30Si_030316_PaineBR5@13	2.39	3.2723E-02	2.5206E-02	8.9681E+07	8.3345E-02	2.9349E+06	8.0731E-02	18:18	3.7470E+07	3.7493E+07	-41.69	0.50	-41.92	-41.70	0.50	-41.92	-0.02	0.32	-0.26	Standard
d30Si_030316_PaineBR5@14	2.39	3.2709E-02	9.5730E-03	8.9554E+07	9.9818E-02	2.9297E+06	1.0143E-01	18:21	3.7506E+07	1.4107E+05	-42.09	0.19	0.35	-42.10	0.19	0.30	-0.44	0.22	0.32	Standard
d30Si_030316_PaineBR5@15	2.39	3.2712E-02	1.6328E-02	8.9727E+07	1.0251E-01	2.9355E+06	1.0840E-01	18:24	3.7582E+07		-42.01	0.33		-42.01	0.33		-0.35	0.25		Standard
d30Si_030316_PaineBR5@16	2.40	3.2717E-02	1.4308E-02	8.9624E+07	8.3673E-02	2.9329E+06	8.7202E-02	18:27	3.7414E+07		-41.87	0.29		-41.88	0.29		-0.21	0.24		Standard
d30Si_030316_PaineBR5@17	2.39	3.2714E-02	2.0163E-02	8.9743E+07	8.7382E-02	2.9369E+06	8.7169E-02	19:10	3.7581E+07	3.7565E+07	-41.96	0.40	-41.68	-41.96	0.40	-41.68	-0.29	0.28	-0.01	Standard
d30Si_030316_PaineBR5@18	2.39	3.2733E-02	1.3335E-02	8.9291E+07	9.2416E-02	2.9227E+06	9.7886E-02	19:13	3.7429E+07	2.1225E+05	-41.39	0.27	0.47	-41.39	0.27	0.41	0.30	0.24	0.42	Standard
d30Si_030316_PaineBR5@19	2.38	3.2721E-02	9.5349E-03	8.9482E+07	1.0740E-01	2.9281E+06	1.1118E-01	19:16	3.7562E+07		-41.74	0.19		-41.75	0.19		-0.07	0.22		Standard
d30Si_030316_PaineBR5@20	2.39	3.2725E-02	1.0092E-02	8.9967E+07	9.9850E-02	2.9442E+06	1.0295E-01	19:19	3.7688E+07		-41.64	0.20		-41.64	0.20		0.04	0.22		Standard
d30Si_030316_PaineBR5@21	2.38	3.2713E-02	8.0536E-03	8.9526E+07	1.0469E-01	2.9286E+06	1.0780E-01	20:12	3.7688E+07	3.7556E+07	-41.99	0.16	-41.74	-41.99	0.16	-41.74	-0.33	0.21	-0.06	Standard
d30Si_030316_PaineBR5@22	2.38	3.2719E-02	1.0759E-02	8.9650E+07	1.0102E-01	2.9334E+06	1.0200E-01	20:15	3.7641E+07	2.6451E+05	-41.80	0.22	0.56	-41.80	0.22	0.49	-0.13	0.22	0.51	Standard
d30Si_030316_PaineBR5@23	2.39	3.2735E-02	1.8993E-02	8.9235E+07	8.2768E-02	2.9202E+06	8.7244E-02	20:18	3.7402E+07		-41.34	0.38		-41.34	0.38		0.35	0.27		Standard
d30Si_030316_PaineBR5@24	2.38	3.2719E-02	1.8026E-02	8.9227E+07	8.9843E-02	2.9197E+06	9.5974E-02	20:21	3.7493E+07		-41.82	0.36		-41.82	0.36		-0.15	0.26		Standard
d30Si_030316_PaineBR5@25	2.37	3.2725E-02	9.4497E-03	8.9020E+07	9.3873E-02	2.9132E+06	9.4630E-02	20:57	3.7497E+07	3.7523E+07	-41.62	0.19	-41.68	-41.62	0.19	-41.68	0.05	0.22	0.00	Standard
d30Si_030316_PaineBR5@26	2.37	3.2714E-02	9.4758E-03	8.9036E+07	1.2596E-01	2.9128E+06	1.2561E-01	21:00	3.7552E+07	6.1096E+04	-41.94	0.19	0.40	-41.94	0.19	0.34	-0.28	0.22	0.36	Standard
d30Si_030316_PaineBR5@27	2.38	3.2724E-02	1.1021E-02	8.9323E+07	9.4406E-02	2.9231E+06	9.7635E-02	21:04	3.7547E+07		-41.67	0.22		-41.67	0.22		0.01	0.22		Standard
d30Si_030316_PaineBR5@28	2.38	3.2731E-02	2.3450E-02	8.9223E+07	8.0472E-02	2.9228E+06	8.5623E-02	21:07	3.7496E+07		-41.47	0.47		-41.47	0.47		0.22	0.30		Standard
d30Si_030316_PaineBR5@29	2.38	3.2722E-02	1.7666E-02	8.9386E+07	1.0125E-01	2.9250E+06	1.0752E-01	21:59	3.7602E+07	3.7442E+07	-41.71	0.35	-41.73	-41.71	0.35	-41.73	-0.03	0.26	-0.06	Standard
d30Si_030316_PaineBR5@30	2.39	3.2717E-02	1.7077E-02	8.9014E+07	7.6190E-02	2.9124E+06	7.6389E-02	22:02	3.7318E+07	2.3680E+05	-41.86	0.34	0.22	-41.86	0.34	0.19	-0.19	0.26	0.20	Standard
d30Si_030316_PaineBR5@31	2.38	3.2720E-02	2.1973E-02	8.9071E+07	8.3952E-02	2.9145E+06	8.9301E-02	22:05	3.7436E+07		-41.77	0.44		-41.76	0.44		-0.09	0.29		Standard
d30Si_030316_PaineBR5@32	2.37	3.2726E-02	1.5505E-02	8.8837E+07	8.3440E-02	2.9078E+06	8.6051E-02	22:09	3.7411E+07		-41.59	0.31		-41.59	0.31		0.09	0.25		Standard
d30Si_030316_PaineBR5@33	2.38	3.2721E-02	1.3838E-02	8.9275E+07	2.0890E-01	2.9211E+06	2.1479E-01	23:01	3.7505E+07	3.7453E+07	-41.76	0.28	-41.84	-41.75	0.28	-41.84	-0.08	0.24	-0.17	Standard
d30Si_030316_PaineBR5@34	2.39	3.2725E-02	9.0185E-03	8.9135E+07	8.3633E-02	2.9171E+06	8.6517E-02	23:04	3.7365E+07	2.1759E+05	-41.63	0.18	0.40	-41.63	0.18	0.34	0.05	0.21	0.36	Standard
d30Si_030316_PaineBR5@35	2.38	3.2709E-02	1.0680E-02	8.9046E+07	7.4305E-02	2.9131E+06	7.8298E-02	23:07	3.7359E+07		-42.10	0.21		-42.09	0.21		-0.44	0.22		Standard
d30Si_030316_PaineBR5@36	2.38	3.2717E-02	1.4468E-02	8.9289E+07	1.1296E-01	2.9197E+06	1.2456E-01	23:11	3.7581E+07		-41.87	0.29		-41.87	0.29		-0.20	0.24		Standard
d30Si_030316_KI6CS@1	2.38	3.2722E-02	1.9406E-02	8.7653E+07	1.1806E-01	2.8679E+06	1.1871E-01	23:14	3.6853E+07	3.6480E+07	-41.71	0.39	-41.79	-41.71	0.39		-0.03	0.27		Ki06cs
d30Si_030316_KI6CS@02	2.38	3.2724E-02	1.5753E-02	8.7284E+07	1.2918E-01	2.8560E+06	1.3197E-01	23:17	3.6609E+07	3.7636E+05	-41.66	0.32	0.68	-41.66	0.32		0.02	0.25		Ki06cs
d30Si_030316_KI6CS@03	2.39	3.2729E-02	1.1059E-02	8.7634E+07	1.0250E-01	2.8686E+06	1.0664E-01	23:20	3.6684E+07		-41.53	0.22		-41.52	0.22		0.16	0.22		Ki06cs
d30Si_030316_KI6CS@04	2.38	3.2717E-02	1.0195E-02	8.6466E+07	1.1364E-01	2.8289E+06	1.1619E-01	23:24	3.6270E+07		-41.86	0.20		-41.85	0.20		-0.19	0.22		Ki06cs
d30Si_030316_KI6CS@05	2.38	3.2727E-02	1.2670E-02	8.6605E+07	1.2435E-01	2.8346E+06	1.2345E-01	23:27	3.6401E+07		-41.57	0.25		-41.57	0.25		0.11	0.23		Ki06cs
d30Si_030316_KI6CS@06	2.38	3.2731E-02	1.2047E-02	8.6069E+07	1.3062E-01	2.8174E+06	1.3209E-01	23:30	3.6140E+07		-41.45	0.24		-41.44	0.24		0.24	0.23		Ki06cs
d30Si_030316_KI6CS@07	2.39	3.2715E-02	2.0194E-02	8.6460E+07	7.6094E-02	2.8291E+06	8.9311E-02	23:33	3.6238E+07		-41.91	0.40		-41.91	0.40		-0.24	0.28		Ki06cs
d30Si_030316_KI6CS@08	2.38	3.2730E-02	2.3637E-02	8.7172E+07	1.0617E-01	2.8539E+06	1.1325E-01	23:37	3.6559E+07		-41.47	0.47		-41.47	0.47		0.22	0.31		Ki06cs
d30Si_030316_KI6CS@09	2.38	3.2716E-02	2.1692E-02	8.6667E+07	1.2336E-01	2.8359E+06	1.2215E-01	23:40	3.6440E+07		-41.90	0.43		-41.90	0.43		-0.23	0.29		Ki06cs
d30Si_030316_KI6CS@10	2.38	3.2728E-02	1.8277E-02	8.6594E+07	1.0120E-01	2.8339E+06	1.0515E-01	23:43	3.6394E+07		-41.54	0.37		-41.54	0.37		0.15	0.27		Ki06cs
d30Si_030316_KI6CS@11	2.38	3.2702E-02	9.8627E-03	8.7268E+07	1.0338E-01	2.8539E+06	1.0495E-01	23:46	3.6597E+07		-42.30	0.20		-42.29	0.20		-0.64	0.22		Ki06cs
d30Si_030316_KI6CS@12	2.39	3.2689E-02	9.9951E-03	8.7275E+07	7.8217E-02	2.8530E+06	7.9221E-02	23:50	3.6579E+07		-42.69	0.20		-42.68	0.20		-1.05	0.22		Ki06cs
d30Si_030316_KI6CS@13	2.38	3.2721E-02	1.1297E-02	8.6792E+07	1.3359E-01	2.8398E+06	1.3558E-01	23:53	3.6487E+07		-41.76	0.23		-41.75	0.23		-0.08	0.22		Ki06cs
d30Si_030316_KI6CS@14	2.38	3.2722E-02	1.4451E-02	8.6860E+07	1.1513E-01	2.8422E+06	1.2289E-01	23:56	3.6475E+07		-41.71	0.29		-41.70	0.29		-0.03	0.24		Ki06cs
d30Si_030316_PaineBR5@37	2.39	3.2729E-02	1.7262E-02	8.9669E+07	9.5199E-02	2.9330E+06	1.0826E-01	23:59	3.7575E+07	3.7601E+07	-41.50	0.35	-41.76	-41.49	0.35	-41.75	0.19	0.26	-0.08	Standard
d30Si_030316_PaineBR5@38	2.40	3.2716E-02	9.9543E-03	9.0157E+07	1.1405E-01	2.9500E+06	1.1168E-01	0:03	3.7643E+07	2.6371E+05	-41.90	0.20	0.36	-41.89	0.20	0.31	-0.22	0.22	0.32	Standard
d30Si_030316_PaineBR5@39	2.40	3.2720E-02	1.3629E-02	9.0501E+07	9.3523E-02	2.9616E+06	9.3058E-02	0:06	3.7750E+07		-41.79	0.27		-41.78	0.27		-0.11	0.24		Standard
d30Si_030316_PaineBR5@40	2.40	3.2718E-02	1.0085E-02	8.9845E+07	9.4685E-02	2.9395E+06	9.5942E-02	0:09	3.7435E+07		-41.85	0.20		-41.84	0.20		-0.17	0.22		Standard
d30Si_030316_PaineBR5@41	2.40	3.2719E-02	1.2431E-02	8.9440E+07	1.0284E-01	2.9266E+06	1.0764E-01	1:01	3.7325E+07	3.7387E+07	-41.80	0.25	-41.88	-41.79	0.25	-41.87	-0.12	0.23	-0.20	Standard
d30Si_030316_PaineBR5@42	2.39	3.2715E-02	1.7413E-02	8.9710E+07	8.6706E-02	2.9354E+06	9.4042E-02	1:04	3.7473E+07	2.6215E+05	-41.93	0.35	0.30	-41.92	0.35	0.26	-0.25	0.26	0.27	Standard
d30Si_030316_PaineBR5@43	2.39	3.2710E-02	1.7304E-02	8.9676E+07	8.7877E-02	2.9342E+06	9.4081E-02	1:08	3.7517E+07		-42.07	0.35		-42.06	0.35		-0.40	0.26		Standard
d30Si_030316_PaineBR5@44	2.39	3.2722E-02	2.1597E-02	8.9067E+07	9.5382E-02	2.9147E+06	1.0388E-01	1:11	3.7234E+07		-41.73	0.43		-41.72	0.43		-0.04	0.29		Standard

二次イオン質量分析法（SIMS）を用いた 中部日本犬山地域中生代層状チャート中の放散虫殻 Si 同位体分析

Maximilien BÔLE・池田　昌之・Peter O. BAUMGARTNER・
堀　利栄・Anne-Sophie BOUVIER

要　旨

全球シリカ循環は長期的気候システムの重要な要素だが，その制御要因は古環境指標の制約に乏しいため，不確実性が大きい．本論では，二次イオン質量分析計（SIMS）によって測定された犬山地域の中生代チャートに含まれる放散虫化石のシリカ変動（δ^{30}Si）を報告する．測定の結果，放散虫殻 δ^{30}Si は -0.3 〜 2 ‰で，現在及び新生代の放散虫殻の値と調和的であった．さらに，予察的な δ^{30}Si 変動は低解像度にもかかわらず，1,000 万年スケールでは生物起源シリカ（BSi）埋没速度と逆相関し，従来の古生産性プロキシとしての δ^{30}Si の解釈に矛盾する結果となった．この時間スケールでは BSi 埋没速度は風化速度に依存するため，風化しやすく低 δ^{30}Si の苦鉄質岩の風化速度変化によって，この逆相関は説明されるかもしれない．さらに高解像度で δ^{30}Si 記録を測定することで，過去のシリカ循環をより深く理解できると期待される．